BONUS BIO-C3

Biodiversity changes: causes, consequences and management implications

Deliverable No: 3.4		Workpackage number and leader: 3, Helén Andersson, P12	
Date:	30.04.2016	Delivery due date: 30.04.2017	Month 40
Title:	Report on dynamics of benthic and pelagic habitats in space and time under different driver forcing, including identification of vulnerable habitats.		
Lead partner for deliverable:		Helén Andersson, (P12), Swedish Meteorological and Hydrological Institute (SMHI)	
Other contributing partners		P2, P6, P9, P8, P11, P12	
Authors		Helén C. Andersson, Elin Almroth Rosell, Robinson Hordoir, Jonne Kotta, Paul Kotterba, Brian R. MacKenzie, Lena von Nordheim, Daniel Oesterwind, Andrius Siaulys, Henrik Skov, Irene Wåhlström, Anastasija Zaiko	
Andersson, H.C., Almroth Rosell, E., Hordoir, R., Kotta, J., Kotterba, P., MacKenzie, B.R., von Nordheim, L., Oesterwind, D., Siaulys, A., Skov, H., Wåhlström, I., and Zaiko, A. (2017): *Report on dynamics of benthic and pelagic habitats in space and time under different driver forcing, including identification of vulnerable habitats*. BIO-C3 Deliverable, D3.4. EU BONUS BIO-C3, DOI: 10.3289/BIO-C3_D3.4, 30 pp + Appendices			
Dissemination level (PU=public, PP=Restricted, CO=confidential)			PU
Nature of the Deliverable (RE=Report, OT=Other)			RE

Acknowledgements

The research leading to these results is part of the BIO-C3 project and has received funding from BONUS, the joint Baltic Sea research and development programme (Art 185), funded jointly from the European Union's Seventh Programme for research, technological development and demonstration and from national funding institutions.

BIO-C3 overview

The importance of biodiversity for ecosystems on land has long been acknowledged. In contrast, its role for marine ecosystems has gained less research attention. The overarching aim of BIO-C3 is to address biodiversity changes, their causes, consequences and possible management implications for the Baltic Sea. Scientists from 7 European countries and 13 partner institutes are involved. Project coordinator is the GEOMAR Helmholtz Centre for Ocean Research Kiel, Germany, assisted by DTU Aqua, National Institute of Aquatic Resources, Technical University of Denmark.

Why is Biodiversity important?

An estimated 130 animal and plant species go extinct every day. In 1992 the United Nations tried countering this process with the "Biodiversity Convention". It labeled biodiversity as worthy of preservation – at land as well as at sea. Biological variety should not only be preserved for ethical reasons: It also fulfils key ecosystem functions and provides ecosystem services. In the sea this includes healthy fish stocks, clear water without algal blooms but also the absorption of nutrients from agriculture.

Biodiversity and BIO-C3

To assess the role of biodiversity in marine ecosystems, BIO-C3 uses a natural laboratory: the Baltic Sea. The Baltic is perfectly suited since its species composition is very young, with current salt level persisting for only a few thousand years. It is also relatively species poor, and extinctions of residents or invasions of new species is therefore expected to have a more dramatic effect compared to species rich and presumably more stable ecosystems.

Moreover, human impacts on the Baltic ecosystem are larger than in most other sea regions, as this marginal sea is surrounded by densely populated areas. A further BIO-C3 focus is to predict and assess future anthropogenic impacts such as fishing and eutrophication, as well as changes related to global (climate) change using a suite of models.

If talking about biological variety, it is important to consider genetic diversity as well, a largely neglected issue. A central question is whether important organisms such as zooplankton and fish can cope or even adapt on contemporary time scales to changed environmental conditions anticipated under different global change scenarios.

BIO-C3 aims to increase understanding of both temporal changes in biodiversity - on all levels from genetic diversity to ecosystem composition - and of the environmental and anthropogenic pressures driving this change. For this purpose, we are able to exploit numerous long term data sets available from the project partners, including on fish stocks, plankton and benthos organisms as well as abiotic environmental conditions. Data series are extended and expanded through a network of Baltic cruises with the research vessels linked to the consortium, and complemented by extensive experimental, laboratory, and modeling work.

From science to management

The ultimate BIO-C3 goal is to use understanding of what happened in the past to predict what will happen in the future, under different climate projections and management scenarios: essential information for resource managers and politicians to decide on the course of actions to maintain and improve the biodiversity status of the Baltic Sea for future generations.

Table of Contents

I. Executive Summary

The Baltic Sea is a dynamic environment that responds to various drivers that operate at different temporal and spatial scales. Changes in the drivers will influence the marine environment and change the prerequisites of the current ecosystem. The Baltic Sea is one of the world´s largest estuaries and has a unique setting with its brackish water environment where relatively few species have had the ability to adapt. At the same time the Baltic Sea is exposed to many anthropogenic stressors. The catchment area covers about 20% of the European continent and some 90 million people lives there. Pollution of different sorts is brought to the sea by diffusive flow, point sources and with the rivers. The ship traffic is among the heaviest in the world, and can potentially increase both biological (e. g., introduction of non-native species) and chemical pollution. The water exchange with adjacent seas is very limited. All together this has made the Baltic Sea a much polluted in-land sea with huge problems with eutrophication and consequential harmful algal blooms and large hypoxic areas. Climate change will further put pressure on this already stressed marine environment. Regional projections of global IPCC climate scenarios indicate that there will be significant changes in water temperature, surface and bottom salinity, ice coverage, oxygen levels and acidification. The nutrient loads from land might increase due to increased precipitation and river runoff and biogeochemical processes will be affected. As a consequence the marine habitats may change in a number of ways, which will have different implications on the different life stages of the inhabitant species. The changes could also give habitat advantages to non-native species, which also will impact the current ecosystem structure and functioning.

The task 3.4 '*Dynamics of habitats in space and time under driver forcing*' in BONUS BIO-C3 aimed to investigate the dynamics of current habitats of the Baltic Sea by examining historical data on marine physics, chemistry, geology, and socio-economic development. Further, the task developed models to represent spatio-temporal variation of drivers. This was done in order to improve the process-based and mechanistic understanding of environmental habitats in the Baltic Sea ecosystem. By applying future projections of regional climate change up to the year 2100 for different scenarios of emission outlets of greenhouse gases and nutrients, we aimed to assess possible future changes and the consequences these might have on the present species. The task was central within BIO-C3 as it interlinked with all other WP's, e.g. using tolerance and threshold knowledge generated under WP1 and 2 and feeding into hind- and forecasting under WP3 and 4 as well as indicators under WP5.

Specifically, we investigated spatial patterns and temporal dynamics of benthic and pelagic habitats at a fine-scale resolution in coastal and offshore areas. It was based on empirical data from national surveys and monitoring activities and predictors processed from the benthic ecosystem models. Area and volume of vulnerable habitats were identified, using overlay mapping of drivers and essential habitats as well as combining mapping technologies, such as hyperspectral remote sensing and habitat identification from video analysis, with probability mapping and machine learning. Further, we investigated climate-

related changes of deep-water stagnation periods, salinity and temperature in order to derive indicators relating the environmental pressures to habitat impacts.

The results show that eutrophication causes oxygen levels to decline in many benthic areas in the Baltic so that there is an increased risk of frequent periods with hypoxia or anoxia. Both direct and indirect effects from climate change can further enhance deoxygenation processes. It is evident that this will cause a decline in the size and extent of benthic habitats, and may have contributed to the decline of e.g. the Western Baltic Spring Spawning Herring due to lower oxygen levels in preferred spawning areas (Core Activity 1). However, other studies within task 3.4 also suggest that many species could benefit from expected environmental changes; for example, climate-change related warming could give enhanced biomasses of some species through the positive relation between temperature and growth (Core Activity 4). A larger threat to native species can be the impact of invasive species, as seen on the rapid decline of blue mussels at the Lithuanian coast (Core Activity 2).

Benthic species display patchiness in their distribution. This is described in task 3.4 and it was concluded that this gives important implications for the requirement of high-resolution model data, in order to establish status and trends of benthic habitats (Core Activity 2). However, the task has also investigated the possibility to create high-resolution biodiversity maps from special predictive modelling, biodiversity data and georeferenced environmental data layers. The results were encouraging, with high correlation between observations and models in studied areas (Core Activity 5).

Many of the Baltic Sea habitats are conditioned by the larger scale circulation. Here the frequencies and magnitudes of the major Baltic inflows (MBIs) are a prominent feature. They have for instance an impact on the oxygen levels and nutrient concentrations in the Baltic. A study within this task revealed that the influence of the recent MBIs and the consequential re-oxygenation of Baltic proper deep water had a large impact on benthic nutrient fluxes (Core Activity 6). There was an observed increase in the DIN:DIP relation in the water column, showing the significant influence of MBIs on the eutrophication status. The future evolution of MBI occurrences is still uncertain. A model study in the task reveals that there are indications of a decreasing overturning circulation under climate change (Core Activity 7). The different IPCC climate scenarios analyzed show the importance of mitigation of greenhouse-gas concentrations and that the future marine changes in salinity, temperature, nutrients etc. will be more drastic in the higher emission scenarios (Core Activity 7 and 8). Furthermore, to combat eutrophication a successful implementation of the HELCOM Baltic Sea Action Plan will be of even more importance in a warmer world (Core Activity 8).

II. Introduction

Global climate model results indicate that significant environmental changes can be a reality before the end of the 21st century (IPCC 2013). Changes in the physical and biogeochemical marine environment can potentially have wide-ranging effects on biodiversity. Altered diversity patterns and latitudinal and altitudinal shifts in species distribution has been shown to stem from the change in suitable habitats (e.g. Doney et al., 2012, Hiddink et al., 2015).

The Baltic Sea is the largest brackish water body on the planet and is experiencing one of the highest rates of warming in the world (Belkin, 2009). The drainage area is populated by some 90 million people and subject to multiple stressors such as fisheries, shipping, tourism and constructions. Climate change is predicted to increase warming, freshening and the extent of hypoxia/anoxia (BACC, 2008, Meier et al., 2011). Large-scale patterns emerging from the climate change are evident, including changes in primary production (Bopp et al., 2013), eutrophication patterns (Meier et al., 2012) and patterns of harmful algal blooms (Wells et al., 2015). It is increasingly important to understand the forthcoming environmental change in the Baltic Sea basin and coastal waters and the impact on the habitats. Modeling studies about the climate change effects on the Baltic marine ecosystem indicates that regional management is likely to play a major role in determining the future of the Baltic Sea ecosystem (Niiranen et al, 2013).

Within WP 3.4 we aimed to investigate habitats on a small spatial scale and with high temporal resolution to pin-point some main environmental divers and both positive and negative feedbacks on biodiversity and biomass. Specific studies were conducted in Greifswald Bay on the German coast of the Southern Baltic Sea, the Lithuanian coastal reefs, the Gulf of Riga, Irbe Strait, and the easternmost parts of the Gulf of Finland. Mesoscale features were investigated in the Estonian coastal sea, and through studies of the Baltic proper sediment fluxes. Through a 3D physical ocean model and a 3D coupled physical-biogeochemical model, large scale properties of the Baltic marine environment was analysed. Time scales of the studies ranges from seasonal to decadal.

The overall objective of the task 3.4 was to understand the dynamics of current habitats in the Baltic Sea and how environmental changes, from e.g. eutrophication and climate change, will change the habitats in different parts, and on different temporal and spatial scales. This will aid the understanding on how resilient the system is to change, identify trends and predict future changes in biodiversity. The outcomes of the task are essential for e.g. WP4, where BONUS BIO-C3 wants to assess the impacts of changing biodiversity on ecosystem functioning. It is also feeding into WP5 through input to the understanding on how management of e.g. pollution and non-indigenous species can influence biodiversity, and through input on relevant indicators of biodiversity and environmental change.

The WP 3.4 produced many different studies and many extensive datasets, both observational and from models. The main results are highlighted in the section III Core Activities, while more detailed descriptions are provided as appendices.

1. References

BACC, 2008. Assessment of climate change for the Baltic Sea Basin. Springer, Heidelberg, 474

Belkin, 2009. Rapid warming of Large Marine Ecosystems, Progress in Oceanography 81, 207–213

Bopp et al. 2013, Multiple stressors of ocean ecosystems in the 21st century: projections with CMIP5 models Biogeosciences 10, 6225–6245

Doney, S.C., Ruckelshaus, M., Duffy, J.E., Barry, J.P., Chan, F., English, C.A., Galindo, H.M., Grebmeier, J.M., Hollowed, A.B., Knowlton, N., Polovina, J., Rabalais, N.N., Sydeman, W.J., Talley, L.D., 2012. Climate change impacts on marine ecosystems. Annu. Rev. Mar. Sci. 4, 11e37.

Hiddink, J.G., Burrows, M.T., García Molinos, J., 2015. Temperature tracking by North Sea benthic invertebrates in response to climate change. Glob. Change Biol. 21, 117e129.

IPCC, 2013. Climate Change 2013: The Physical Science Basis. Working Group I contribution to the Intergovernmental Panel on Climate Change, <http:// ipcc.ch/report/ar5/wg1/>.

Meier et al., 2012, Comparing reconstructed past variations and future projections of the Baltic Seaecosystem—first results from multi-model ensemble simulations, Environ. Res. Lett. 7 034005

Meier, H.E.M., Andersson, H.C., Eilola, K., Gustafsson, B.G., Kuznetsov, I., Muller-Karulis, B., Neumann, T., Savchuk, O.P., 2011. Hypoxia in future climates: a model ensemble study for the Baltic Sea. Geophys. Res. Lett. 38, L24608. http://dx.doi.org/10.1029/2011GL049929.

Niiranen, S., Yletyinen, J., Tomczak, M.T., Blenckner, T., Hjerne, O., MacKenzie, B., Muller-Karulis, B., Neumann, T., Meier, H.E.M., 2013. Combined effects of global climate change and regional ecosystem drivers on an exploited marine food web. Global Change Biol. http://dx.doi.org/10.1111/gcb.12309.

Wells et al., 2015. Harmful algal blooms and climate change: Learning from the past and present to forecast the future, Harmful Algae 49 (2015) 68–93

III. Core Activity

1. Examining short-term changes in habitat characteristics in an inshore spawning ground of Baltic herring

Abstract: Greifswald Bay on the German coast of the Southern Baltic Sea is considered to be one of the most important spawning grounds of the Western Baltic Spring spawning herring. This species strongly depends on appropriate demersal spawning substrates since herring – in contrast to many other pelagic species - produce adhesive and stationary eggs that were preferably attached to submerged aquatic vegetation (SAV). A drastic decline in SAV has been observed in the study area during the 20th century which is mainly attributed to the general eutrophication of the system. Recent studies indicate that the reduction in substrate availability might have crucial consequences for herring reproduction particularly in combination with additional environmental changes such as climate regime shifts. By the means of video transect investigations we compared the SAV coverage and composition on known herring spawning beds in Greifswald Bay with observations and data from previous studies to examine short term temporal changes in the habitat characteristics. We found a decline in SAV coverage within the last five years and an increasing importance of filamentous algae (e.g. *Pylaiella littoralis*) which need to be examined in further studies particularly focussing on the possible consequences for the success of herring reproduction.

Progress: All work completed..

Deviations: No deviations from work plan.

Introduction: Greifswald Bay is considered to be a major spawning area for the Western Baltic Spring Spawning Herring (WBSSH). Since the 1970s, a continuous monitoring of the annual herring larvae production is conducted within this area by the Thünen institute of Baltic Sea Fisheries (and its predecessors, respectively). A larval index (N20) generated by this 'Rügen herring larvae survey' (RHLS) has been implemented in the stock assessment procedures in recent years. Good relations between the N20 index and later herring stages (1 year old juveniles) indicate Greifswald Bay being a representative reproduction area for this stock. For this reason, TI-OF conducted numerous case studies on early life stage ecology of herring within this lagoon including examinations of egg mortality caused by storm events, predation and spawning substrate characteristics. Since Baltic herring are litho-phytophilous spawners attaching adhesive eggs to demersal substrates, preferably submerged aquatic vegetation, SAV), the availability of appropriate spawning substrates might be crucial for a successful reproduction. In earlier studies (e.g. Kanstinger et al. 2016) a drastic reduction of available SAV in Greifswald Bay during the 20th century was described, with unknown consequences for herring spawning in the area. We performed a video transect monitoring on known spawning beds within Greifswald Bay to examine the habitat characteristics and their changes compared to earlier observations (e.g. aerial SAV coverage monitoring in spring 2009)

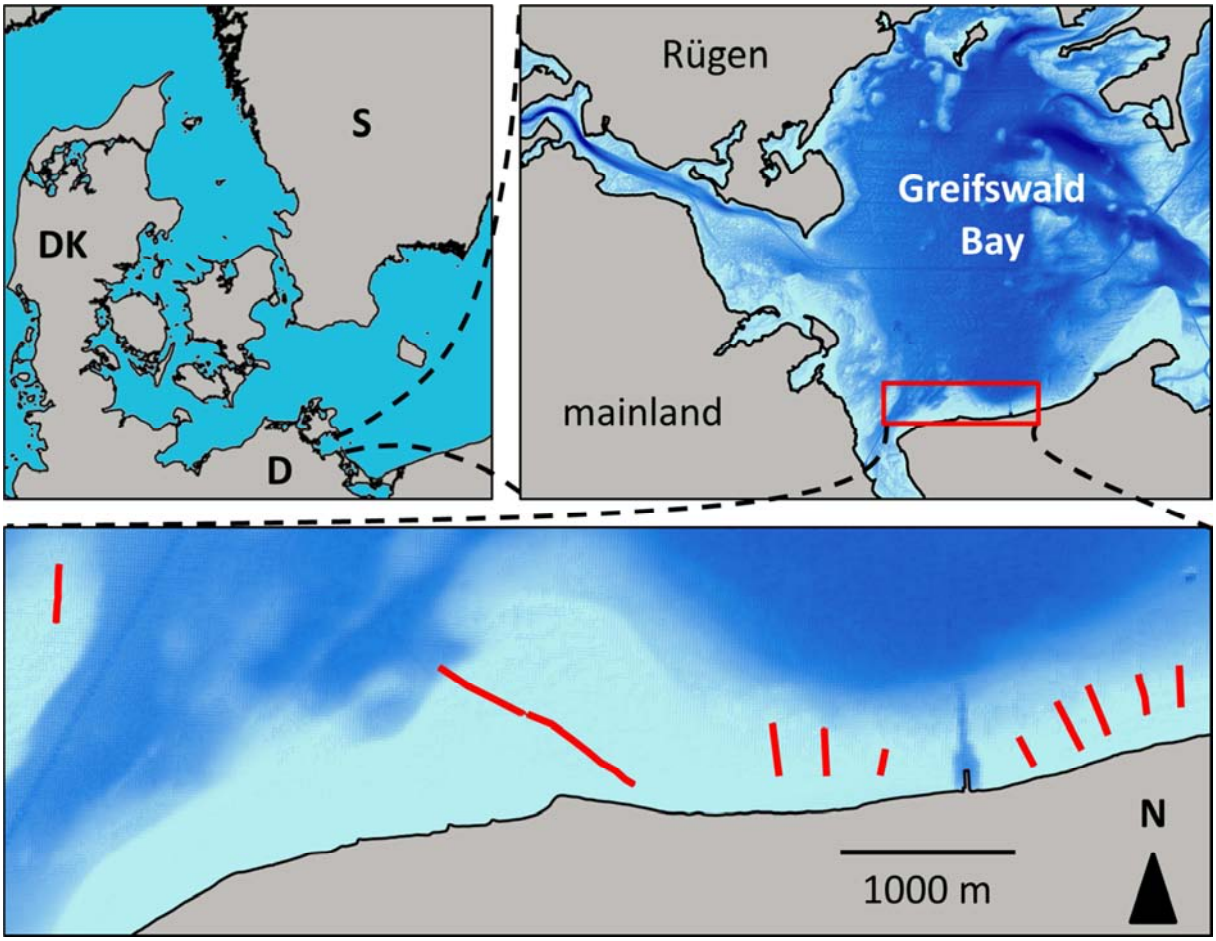

Figure 1. Video transect sampling at the southern coast of Greifswald Bay in the Western Baltic Sea. Video transects (red lines in the lower panel) were conducted at different locations in water depths between 0.5 and 4.5 m. Light blue areas in the maps of Greifswald Bay represent areas of less than 5.0 m water depth. Source of elevation data: Federal Maritime and Hydrographic Agency of Germany (BSH).

Methods and Results: During the early spring of 2016 (March, 17th) TI-OF conducted a video transect survey in Greifswald Bay, a major spawning ground of spring spawning Atlantic herring (*Clupea harengus*). We investigated the habitat characteristics at the southern coast of the bay which has in earlier studies been considered to be a major spawning bed for herring. Each transect was examined using a small video sledge equipped with a GoPro camera. The sledge was lowered from a research boat down to the sea floor and moved horizontally in a stepwise manner (lifted shortly and lowered again) while the boat was descending slowly from the starting point. Usually, the investigation of transects started in the shallow littoral and was oriented along a depth gradient (usually resulting in a movement vertical to the shoreline, *see* Figure 3.4.1). A continuous video sequence was recorded on each transect covering the whole range from the shallow starting point down to sublittoral areas below the maximum depth of macrophyte coverage. At each second during the recording, a hand held receiver (Garmin®GPSmap®62) for the Global Positioning System (GPS) automatically recorded the precise position of the boat. Additionally, start and end points of each transect were labelled with a waypoint.

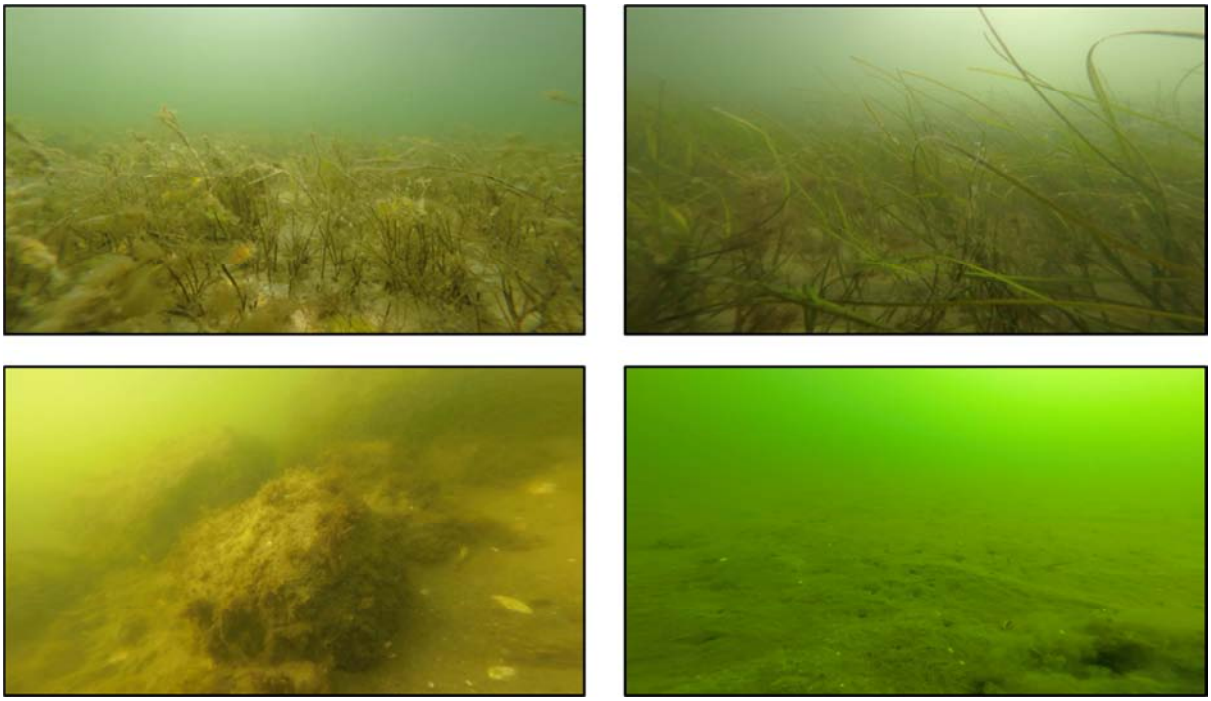

Figure 2. Freeze frames from different habitats captured during the Video transect investigations in early spring 2016. Upper left panel: Sandy bottom & pond weeds (Potamogetonaceae) with adherent brown and green algae in the upper littoral area. Upper right panel: Sandy bottom and sea grass (Zosteraceae) with adherent brown algae and herring eggs in deeper parts of the littoral zone (approximately 2 m water depth). Lower left panel: Sandy bottom and rocks with adherent small-sized brown and red algae found at a more exposed part of the shallow littoral. Lower right panel: muddy bottom with no vegetation at the sublittoral end of a transect (water depth of > 4 meter)

We used freeze frames of the videos to investigate specific sea floor characteristics (Figure 3.4.2). These include the type of sediment, the coverage of macrophytes, the composition of the macrophyte community, the number of stones/rocks, and – if possible – the amount of herring spawn. In a second step, these data were merged with the recorded GPS data and further analysed using special Geographic Information Systems (ArcGIS®). We compared our findings with results from aerial SAV monitoring investigations in 2009 to evaluate temporal shifts and changes in the small scale habitat characteristics. Despite an increased turbidity in the eutrophicated Greifswald Bay the video material was appropriate to evaluate the SAV coverage and the type of macrophyte. As expected, we found different types of macrophyte communities at different sites depending on the water depth, the sediment characteristics (presence of stones/rocks) and the exposure to hydrodynamic forces. As described in earlier studies (e.g. Kanstinger et al. 2016) the sheltered shallow littoral zone in the study site at the Southern coast of the bay was dominated by pondweeds (Potamogetonaceae) while deeper areas lacking any hard substrates were characterized by meadows of eelgrass (*Zostera marina*, Figure 3.4.2.). Shallow sites that were more exposed to hydrodynamics, i.e. wave action, were lacking SAV on the soft bottom in between stones and rocks while we observed small filamentous brown and red algae attached to these hard substrates.

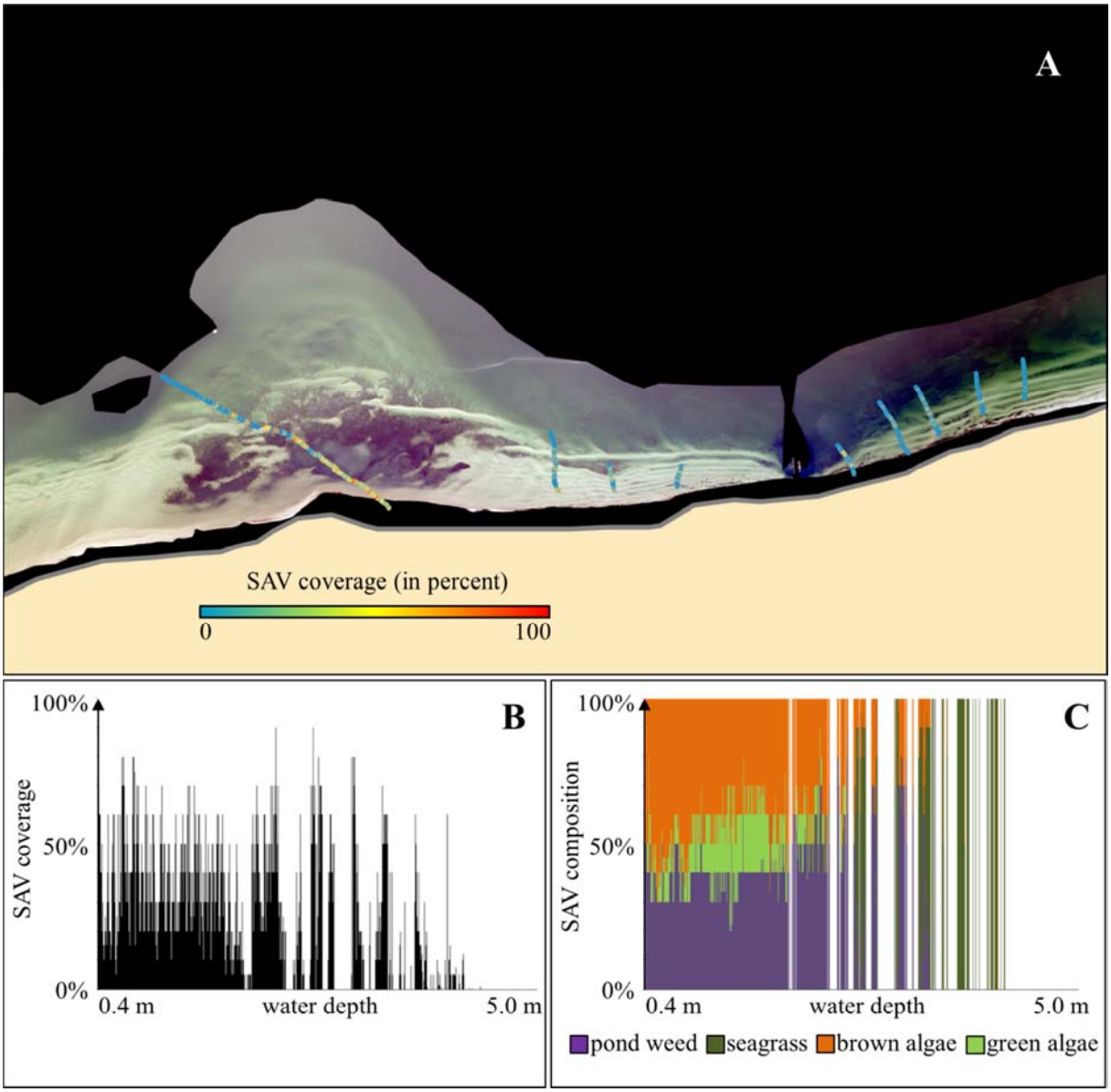

Figure 3. Results of the video transect investigations conducted in spring 2016. A) SAV coverage on the distinct transects represented in a color ramp underlayed with an aerial image taken in spring 2009, black areas represent areas too deep or too shallow for the automatic analysis of SAV coverage and were shaded. B) Exemplarily shown SAV coverage along the transect (from south-east, shallow to north-west, deeper) on the spawning bed at Gahlkow (leftmost transect in figure A)) and the corresponding relative SAV composition along the same transect.

Particularly for the long transect across the spawning bed at "Gahlkower Haken" (leftmost transect shown in Figure 3.4.3.A) we found changes in the SAV coverage and composition compared to earlier investigations. While Aerial images (taken in early spring in 2009) show a dense and homogenous SAV coverage especially in the shallower parts of the study site, we found less macrophytes in 2016 distributed in a more patchy way on the same area (Figure 3.4.3A and B). Furthermore, we found a high amount of filamentous brown algae, probably *Pylaiella littoralis*, covering meadows of pondweed in areas shallower than 2 m water depth (Figure 3.4.3.C). This is in good accordance with personal observations at the study site indicating exceptional high occurrences of these algae on the spawning grounds during the recent years. If this is caused by the combination of high nutrient loads and

extremely mild winters during the last years needs to be addressed in future research as well as the possible consequences for the resident SAV community which might be negatively affected by mass occurrences of *Pylaiella littoralis* and other fast growing filamentous algae.

Recommendations: Changes in the SAV composition might affect the reproduction success of Western Baltic spring spawning herring which depends on the availability of appropriate inshore spawning substrate. Effects of changing spawning substrates on the spawning behaviour and the egg development are subject to ongoing research activities at TI-OF and should be considered in future predictions on stock/population dynamics.

2. Assessment of the benthic habitat change/extension of the mussel beds based on the long-term video analysis

Abstract: The results of long term video analysis from Lithuanian coastal reefs were used to assess the major decline of blue mussel population in Lithuanian coastal area in recent years. An empirical model was created to predict the coverage of blue mussel before the decline, identify main factors shaping its distribution and to locate most degraded areas.

Progress: All work completed and we refer to the detailed report by Šiaulys et al. (2017) in the Appendix.

Deviations: No deviations from work plan.

Introduction: Blue mussel beds, together with red algae *Furcellaria lumbricalis*, are the main engineering species in Lithuanian coastal reefs, serving as an important food source for several fish species and wintering birds, providing habitats for associated macrofauna and fulfilling water filtration function. However, in the past decade a decline of coastal blue mussel population due to invasion of round goby was observed threatening to diminish ecosystem services provided by the most important habitat in Lithuanian marine waters. In this study, we use all available video data from Lithuanian coastal area to estimate the changes in blue mussel beds in the past 15 years.

Methods and Results: The present study uses 3 hours and 25 minutes video footage Lithuanian coastal reefs filmed between 2003 and 2014 with different equipment: ROV, drop-down camera and hand-held camera by SCUBA divers. Each video transect was divided into 30 s segments that served as a sample. In each sample several features were manually estimated: the percentage substrate types (boulders, cobble, pebble and sand) and the coverage (in percent) of blue mussel on each substrate type. Based on the 2003-2010 video and sampling data an empirical model was created in order to identify the main shaping factors and predict special distribution of blue mussel beds before the decline. Environmental and biological explanatory variables were depth, temperature, Secchi depth, salinity, wave generated orbital velocity, near-bottom current velocity and the biomass of red alga *Furcellaria lumbricalis*. The decline started to take place between 2010 and 2013, when the average coverage of blue mussel on the most favourable substrate (boulders) declined approx. two times – from 82.5 ± 28.8 % to 45.3 ± 30.8 %, while in 2014 the decline became more severe – from 45.3 ± 30.8 % to 1 ± 0.4 % (Fig. 1). Similar trend was observed

on less favourable substrate (cobble), where the average coverage declined from 43 ± 9 % in 2003-2010 to 0.2 ± 0.1 % in 2014. According to modelling results, two main factors were the most important for the distribution of blue mussel in Lithuanian coastal area: depth and wave generated orbital velocity. It is fair to notice, that predictions were made exclusively for hard bottom, so the importance of sediments was not estimated. The results have shown (Fig. 2) that the highest biomass of blue mussel was present in the northern part of Lithuanian coastal reefs at depths of 15-20 m, where the biomass reaching approx. 7.5 kg per square meter. In the southern part, the closest to the Klaipeda port, the biomass was lowest (< 1 kg per sq. meter) but still considerable. The coverage of blue mussel was more homogeneous with highest coverage of 60-80 % present throughout all coastal area.

Recommendations: The decline of the costal blue mussel population started between 2010 and 2013 and was extremely severe (from dense colonies to single individuals). In biotope scale, the entire biotope AA.A1E1 (Baltic photic rock and boulders dominated by Mytilidae) was replaced by AA.A2T (Baltic photic rock and boulders characterized by sparse epibenthic macrocommunity, mostly barnacles), according HELCOM HUB classification system. It is fair to assume that ecosystem services, once provided by mussels, are entirely lost in Lithuanian coastal area. Since we couldn't detect any significant changes in environmental factors, that are shaping the distribution of blue mussels, this supports other findings that the decline was caused by the invasive fish round goby.

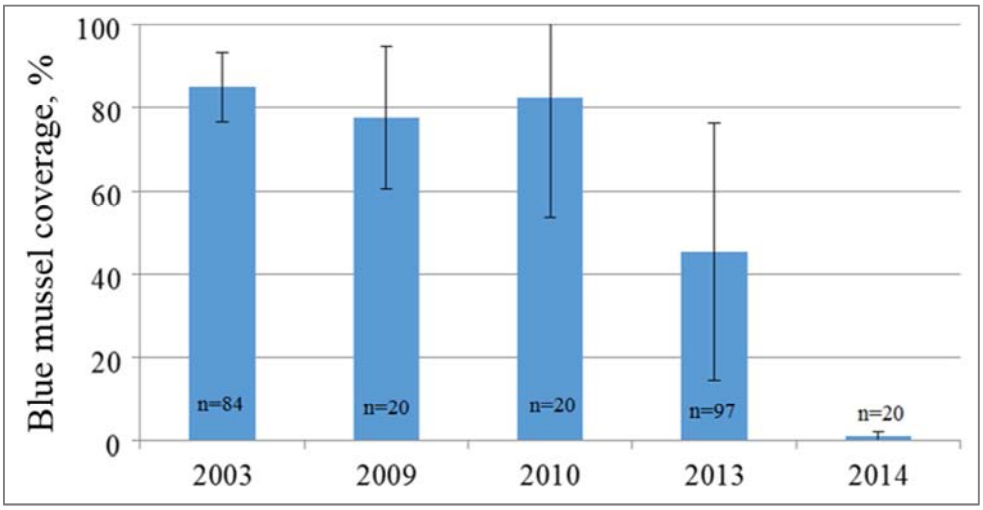

Figure 4. Average coverage (with standard deviations) of blue mussel on boulder substrate in the Lithuanian coastal area since 2003.

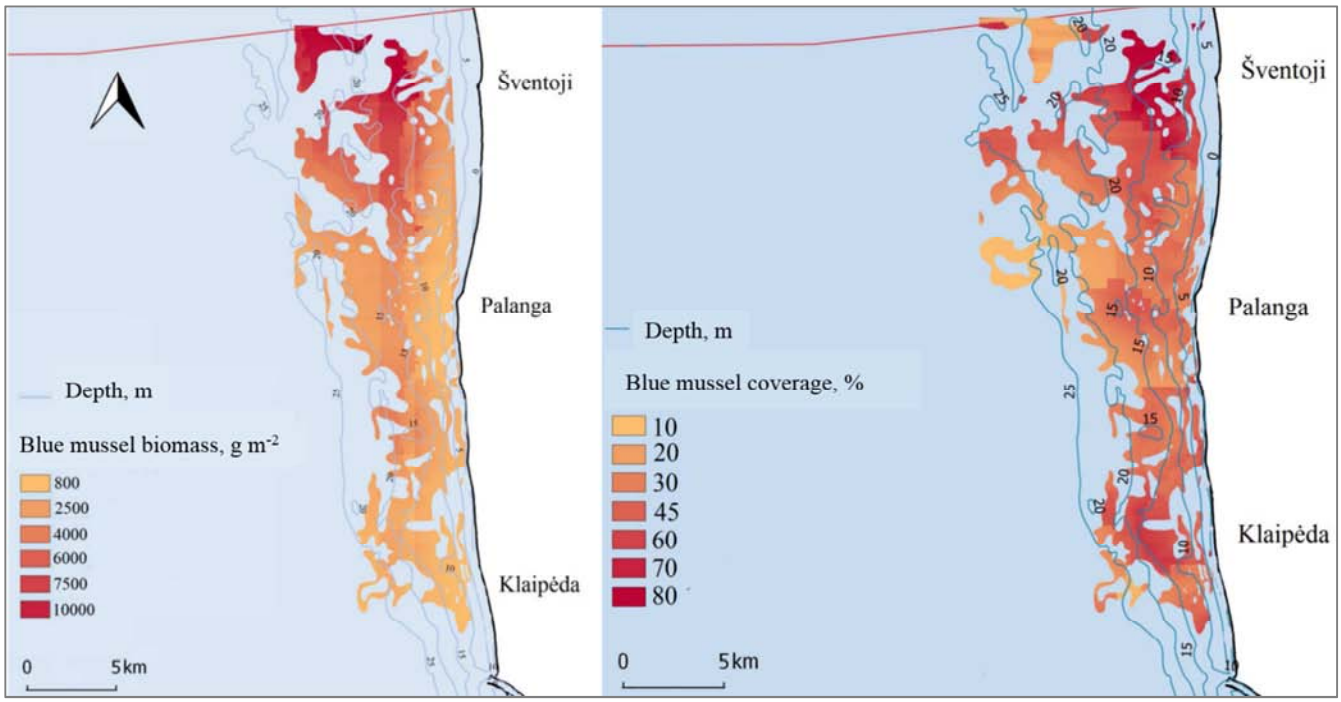

Figure 5. Modelled biomass (left) and coverage (right) of blue mussel in Lithuanian coastal area on hard substrates before the decline.

3. Small-scale metastability in a coastal ecosystem of the Baltic Sea

Abstract: A downscaled food-web model has been developed to study the dynamics of the small-scale spatial structure of the biomasses of two bivalve species (*Macoma balthica* and *Mytilus edulis*) in the Gulf of Riga and Irbe Strait between 1970 and 2003. Both local *Macoma* and *Mytilus* biomasses display high levels of patchiness superimposed on seasonal trends, with spatial gradients in the order of 10x and seasonal trends in the order of 3-4x background biomass levels. The distribution of the modelled biomass was extremely patchy for both species. Yet, despite the patchiness, the spatial gradients in the biomass showed remarkable stability and persistence over the 34 years. This is the case even for the recent development in *Mytilus*, which has declined since 1990, - a decline which has mainly affected the high density patches. The results have highlighted the occurrence of metastable small-scale distributions of biomasses of marine invertebrates in coastal areas of the Baltic Sea. The study further indicated challenges using large-scale ecosystem models to describe gradients and patchiness in productivity found in benthic habitats of coastal ecosystems of the Baltic Sea. The existence of metastability has important implications for the requirements for high-resolution model data needed to establish the status and trends of these habitats.

Progress: All work completed and we refer to the detailed report by Skov et al. (2017) in the Appendix.

Deviations from the work-plan: No deviations from work plan.

Introduction: Due to the paucity of detailed monitoring data from many coastal areas ecosystem models are often applied in order to quantify the available biomass of benthic

invertebrates over time. In the Baltic Sea ecosystem models have routinely been run covering large regions, and for sake of efficiency spatial resolution applied has typically been large (>10^{-1} km). With a spatial resolution, which is obviously larger than the scale of patchiness found in for instance mussels a strong assumption underlying large-scale ecosystem models has been that patchiness occurs mainly as a random process within large-scale units. The aim of the study was to investigate whether this assumption holds true for the coastal ecosystems of the Baltic Sea and use DHI's ecosystem model for the Gulf of Riga to throw light on the potential challenges to describe gradients and patchiness in benthic productivity found in these areas. At the same time, the model study aimed at describing small-scale stability and persistence of patches of benthic invertebrates (bivalves) in the area.

Methods and results: A high-resolution food-web model based on a coupled local biophysical and ecosystem model (MIKE 3 FM & ECOLAB) has been developed to study the dynamics of the small-scale spatial structure of the biomasses of two bivalve species (*Macoma balthica* and *Mytilus edulis*) in the Gulf of Riga and Irbe Strait between 1970 and 2003. Weekly estimates of biomass (g DW soft tissue/m^2) were extracted. As the biomasses of both bivalve species show seasonal trends superimposed on spatial gradients the derivation of long-term trends in spatial structure and biomass was undertaken by analysing temporal trends on deseasoned biomass values at the scale of each grid node (5 km). Deseasoning was undertaken by subtracting the long-term average from each weekly estimate and standardising the resulting value to anomaly *z*-scores by dividing by the standard deviation. The non-parametric Median Trend (Theil 1950, Sen, 1968, Hoaglin et al. 2000) test was used to compute the size and significance of the trend for each of the 3040 grid nodes, which subsequently could be visualised to identify zones with similar trends. This is a robust non-parametric trend operator, which is highly recommended for assessing the rate of change in noisy time series, as it is less sensitive than least-squares estimators because it is much less sensitive to outliers. It is calculated by determining the slope between every pairwise combination and then finding the median value. The Median Trend test was applied for the entire 34 year time series, as well as for each of the following three periods: 1970-1980, 1981-1990 and 1991-2003.

Both local *Macoma* and *Mytilus* biomasses displayed high levels of patchiness superimposed on seasonal trends, with spatial gradients at any one time frequently in the order of 10x and seasonal trends in the order of 3-4x background biomass levels (Figure 1, Figure 2). The distribution of the modelled biomass was extremely patchy for both species. Yet, despite the patchiness, the spatial gradients in the biomass showed remarkable stability and persistence over the 34 years. Patches of higher biomass of *Mytilus* defined by the 90 percentile of the modelled mean biomass during each decade covered only between 5.9% and 6.2% of the model area (Figure 1) and the mean distributions for *Mytilus* were highly correlated between decades (*r* 0.972-0.979, Pearson). For *Macoma* patches of higher biomass covered between 8.2% and 8.9% of the model area (Figure 2) and the mean distributions for *Macoma* were also highly correlated between decades (*r* 0.812-0.982, Pearson). The metastability was seen in *Mytilus* even during the period after 1990, when a population decline was observed in the Gulf, which mainly affected the patches of high biomass (Figure 3).

Recommendations: The results have highlighted the challenges using large-scale ecosystem models to describe gradients and patchiness in productivity found in benthic habitats of coastal ecosystems of the Baltic Sea. In spite of seasonal trends and a recent decline in the population of *Mytilus* in the studied region the spatial structure of the modelled biomass of both species clearly indicates the occurrence of pervasive patchiness and strong persistence in patterns of distribution. The existence of metastability of distribution patterns has important implications for the requirements for high-resolution model data needed to establish the status and trends of benthic habitats in coastal ecosystems. If metastability in the distribution of benthic biomasses persists over long periods of time assessments of ecosystem impacts of human activities could be biased, i.e. models will tend to overestimate impacts outside patches (type II error) and underestimate impacts inside patches (type I error).

‘

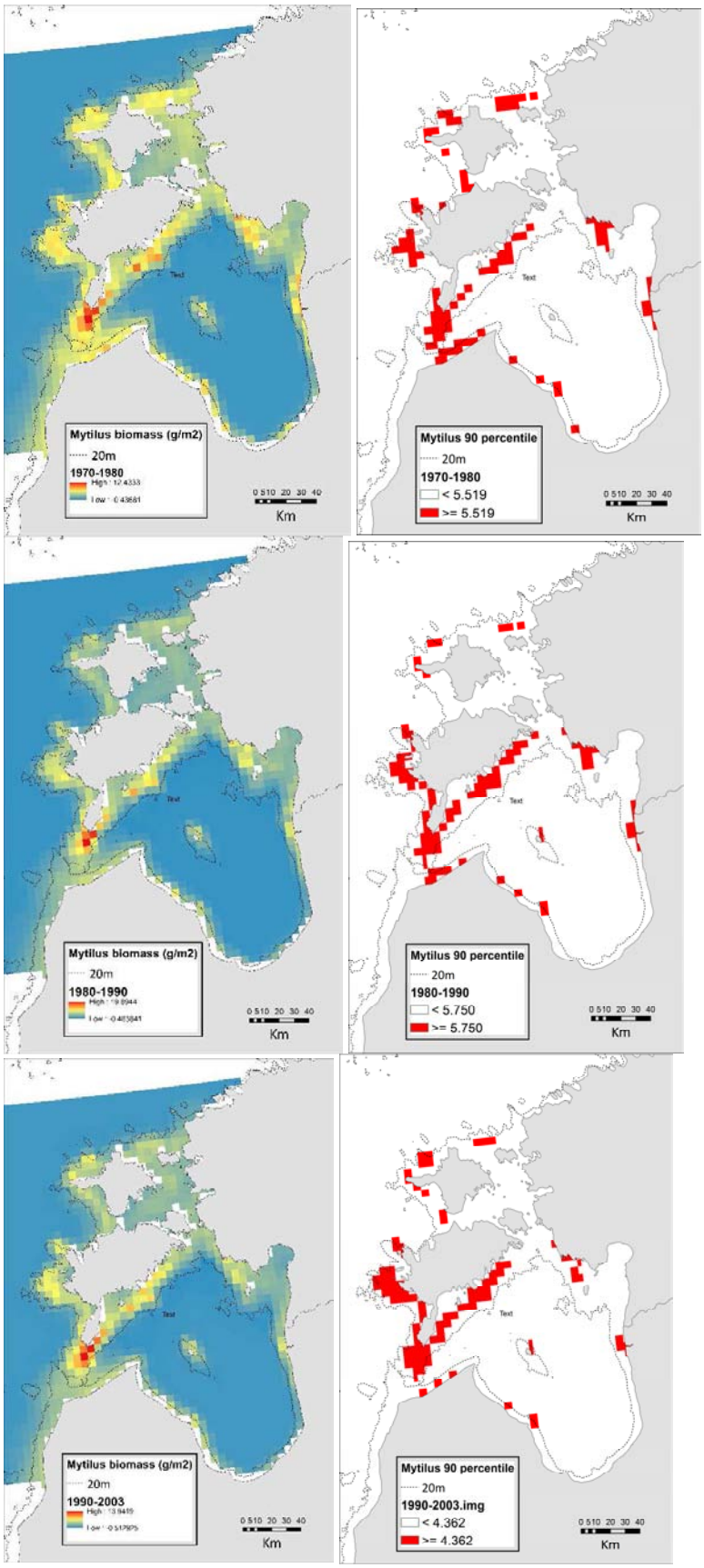

Figure 6. Modelled mean biomass of Mytilus edulis in the Gulf of Riga during 1970-1980, 1981-1990 and 1991-2003 (left panel) and patches defined by the 90 percentile of modelled mean biomass (right panel).

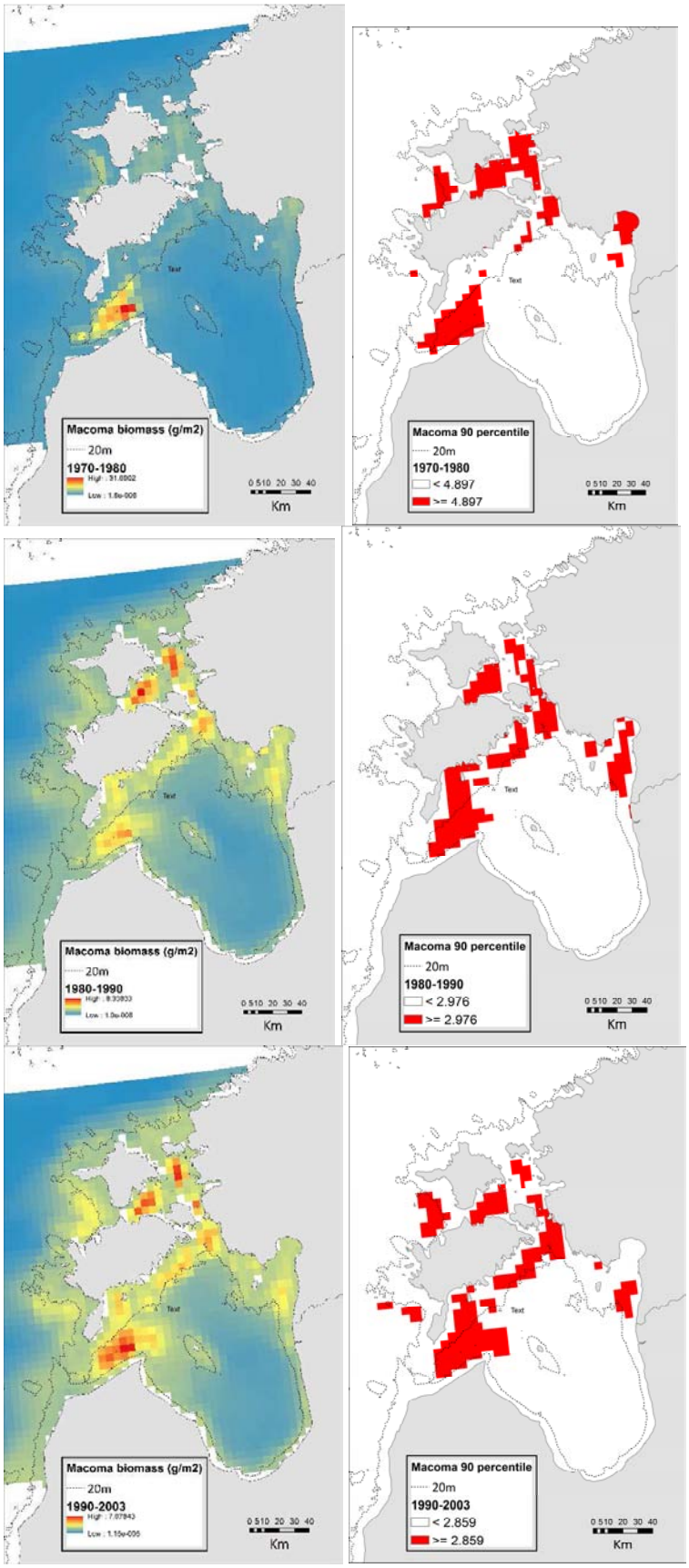

Page 19: Figure 7. Modelled mean biomass of Macoma balthica in the Gulf of Riga during 1970-1980, 1981-1990 and 1991-2003 (left panel and patches defined by the 90 percentile of modelled mean biomass (right panel).

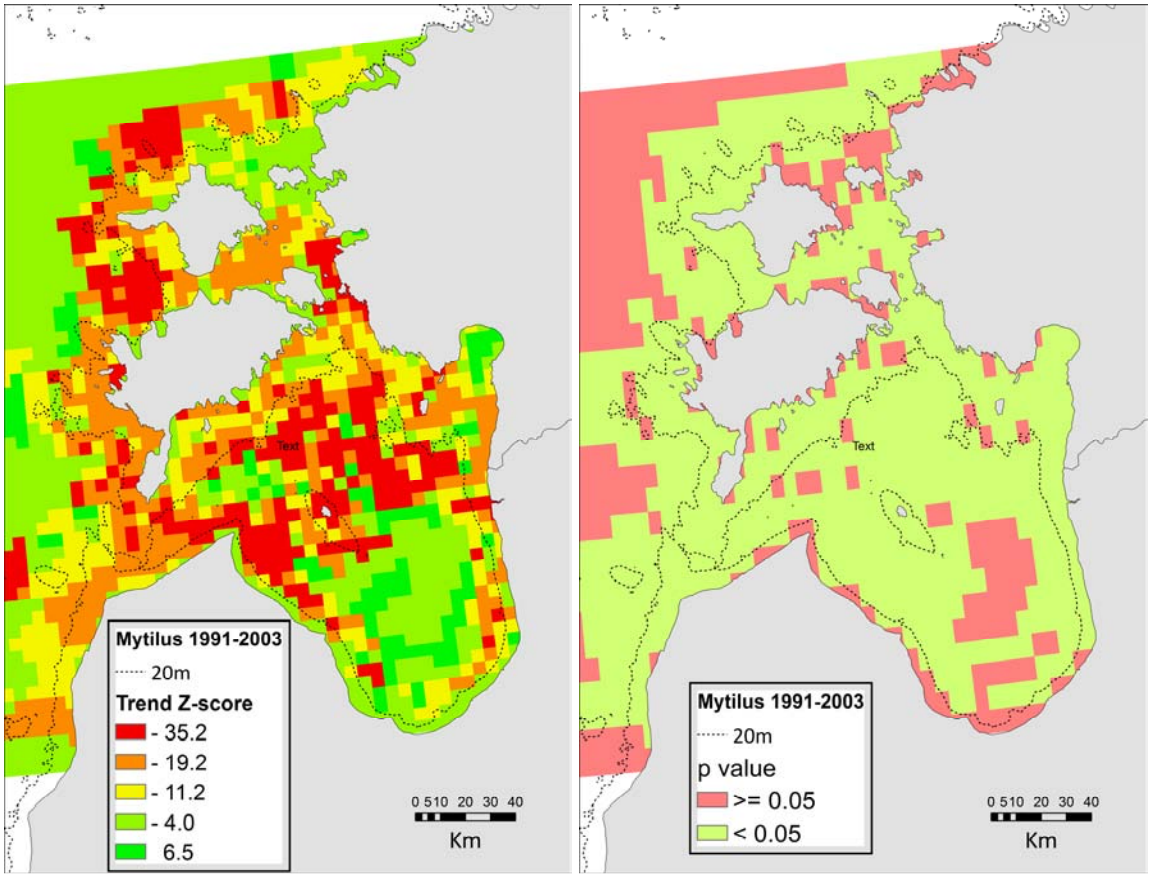

Figure 8. Spatial pattern of z-scores and p values of the Median Trend test for the biomass of Mytilus edulis for the period 1991-2003 when the population was declining.

4. Realized niche width of a brackish water submerged aquatic vegetation under current environmental conditions and projected influences of climate change

Abstract: Little is known about how organisms might respond to multiple climate stressors and this lack of knowledge limits our ability to manage coastal ecosystems under contemporary climate change. Ecological models provide managers and decision makers with greater certainty that the systems affected by their decisions are accurately represented. In this study Boosted Regression Trees modelling was used to relate the cover of submerged aquatic vegetation to the abiotic environment in the brackish Baltic Sea. The analyses showed that the majority of the studied submerged aquatic species are most sensitive to changes in water temperature, current velocity and winter ice scour. Surprisingly, water salinity, turbidity and eutrophication have little impact on the distributional pattern of the studied biota. Both small and large scale environmental variability contributes to the variability of submerged aquatic vegetation. When modelling species distribution under the projected influences of climate change, all of the studied submerged aquatic species appear to be very resilient to a broad range of environmental

perturbation and biomass gains are expected when seawater temperature increases. This is mainly because vegetation develops faster in spring and has a longer growing season under the projected climate change scenario.

Progress: All work completed and we refer to the published article by Kotta et al. (2014) in the appendix.

Deviations: No deviations from work plan.

Introduction: Seagrasses and other plants of higher order are unique by occupying the subtidal photic zone of soft sediments. They form extensive habitats in sheltered near coastal zones and are among the most productive habitats worldwide. Furthermore, they provide a range of ecological functions such as coastline protection, sediment stabilization, wave attenuation, land-derived nutrient filtration, and carbon fixation, just to name a few; thereby providing some of the most valuable ecosystem services on Earth. The submerged aquatic species are also important as food, shelter and space for many invertebrates and fish, many of which are socioeconomically important.

Human use of the coastal marine environment is increasing and diversifying worldwide. Given its multiple stresses, submerged aquatic species have gone through an unusually fast transition in terms of areal decline in habitat. Although large scale processes on the formation of biotic patterns is not well known, it is plausible that contemporary climate change, interacting with other anthropogenic stressors, accounts for a large part of the observed decline. Ecologists have typically interpreted the composition of communities as the outcome of local-scale processes.

Non-independent effects are common in nature and therefore it is expected that the combined effects of two or more variables cannot be predicted from the individual effect of each. However, anticipating the future consequences of the interacting pressures is a pre-requisite to sustainable management of coastal ecosystems under current environmental conditions and contemporary climate change. Due to the non-linear response of biota to the environment, even gradual changes in future climate may provoke sudden and perhaps unpredictable shifts in submerged aquatic plant communities as many are close to their physiological tolerance limit and different species have different response mechanisms.

Among physical disturbances changes in water temperature and wave induced current velocity are the key large-scale processes that are expected to alter species distributions. Specifically, elevated water temperatures favour plant growth and result in increased cover of submerged aquatic species. Elevated wave stress affects sediment characteristics and water turbidity, thereby favouring opportunistic species and disfavouring the pristine water species. The reduction of ice cover is also expected to have direct and indirect consequences. A direct consequence is the prolongation of the growth season and elevated macrophyte cover/biomass values. Currently, the co-existence of species is granted due to the presence of moderate ice disturbance that removes a significant amount of vegetation annually. In the absence of such disturbance, however, fast growing species are favoured over slow growing species. Finally, increased fresh water inputs favour higher order plants of fresh water origin over seagrasses. But increased riverine inputs may also elevate sedimentation rates that impact negatively on the whole macrophyte community. As species are shown to have strong individualistic responses to their environment we also expect large variability of responses among species.

The aims of this work are to (1) identify the most important environmental variables defining the cover of submerged aquatic vegetation, (2) specify the spatial scales where such relationships are the strongest and (3) predict changes in the distributional pattern of the submerged aquatic vegetation from the current to future climate. The modelling approach aims to identify possible critical tipping points of all these variables where regime shifts in species distribution may occur, to provide a better understanding of the ecological frames in which outbreaks or local extinction are more likely to occur.

Methods and Results: The contribution of different environmental variables on the coverages of submerged aquatic plant species was explored using the Boosted Regression Tree method (BRT) and the BRT models were also used to predict the species coverages for the whole study area given ambient and projected climate conditions.

The novel predictive modelling technique called Boosted Regression Trees (BRT) combines the strength of machine learning and statistical modelling. BRT has no need for prior data transformation or elimination of outliers and can fit complex non-linear relationships. The BRT method also avoids overfitting the data, thereby providing very robust estimates. What is most important from the ecological perspective is that it automatically handles interaction effects between predictors. Due to its strong predictive performance, the BRT method is increasingly being used in ecological studies.

The distributional range of the submerged plant species was similar and they inhabited practically the whole Estonian coastal range. In general the studied species were not found in the easternmost parts of the Gulf of Finland and *Z. marina* also tended to avoid the turbid and diluted Pärnu Bay area. Plants were recorded up to 8 km distance from the shore. Higher order plants prevailed mainly on soft and mixed substrates and were not recorded deeper than 7m. Similarly, the niche modelling indicated that there was a large overlap in niche space among all submerged plant species. In general, the majority of the studied species are sensitive to changes in water temperature, current velocity and winter ice scour. Surprisingly, water salinity, turbidity and trophic state have low impact on the biota.

When modelling species distribution under the projected influences of climate change, all of the studied submerged aquatic species seem to benefit from climate change with no indication of local extinction. In general there is an abrupt increase in the vegetation cover over a certain threshold value and such a tipping point varied among species.

Recommendations: The results suggests that (1) local and seascape-scale environmental variability affects the cover patterns of submerged aquatic species with local variability exceeding seascape-scale variability, (2) physical disturbance such as seawater warming, elevated wave-induced current velocity and reduced ice scour override the effects of salinity reduction, elevated turbidity and pelagic production and (3) finally, practically all of the studied submerged aquatic species benefit from the projected influences of climate change with no indication of local extinction.

5. Mapping benthic biodiversity using georeferenced environmental data and predictive modelling

Abstract: Biodiversity is critical for maintaining and stabilizing ecosystem processes. There is a need for high resolution biodiversity maps that cover large sea areas in order to address

ecological questions related to biodiversity-ecosystem functioning relationships and to provide data for marine environmental protection and management decisions. However, traditional sampling-point-wise field work is not suitable for covering extensive areas in high detail. Spatial predictive modelling using biodiversity data from sampling points and georeferenced environmental data layers covering the whole study area is a potential way to create biodiversity maps for large spatial extents. Random forest (RF), generalized additive models (GAM) and boosted regression trees (BRT) were used in this study to produce benthic (macroinvertebrates, macrophytes) biodiversity maps in the northern Baltic Sea. Environmental raster layers (wave exposure, salinity, temperature etc.) were used as independent variables in the models to predict the spatial distribution of species richness. A validation dataset containing data that was not included in model calibration was used to compare the prediction accuracy of the models. Each model was also evaluated visually to check for possible modelling artefacts that are not revealed by mathematical validation. All three models proved to have high predictive ability. RF and BRT predictions had higher correlations with validation data and lower mean absolute error than those of GAM. BRT showed less overfitting artefacts compared to RF and GAM based on visual assessment and was the most accurate in sampling points. Depth and sediments were the most influential abiotic variables in predicting the spatial patterns biodiversity.

Progress: All work completed and we refer to the submitted manuscript by Petersen and Herkül (2017) in the appendix.

Deviations: No deviations from work plan.

Introduction: Marine ecosystems are heavily impacted by human activities like resource overexploitation, eutrophication, pollution and species introductions. All these stressors affect biodiversity and ecosystem functioning by decreasing habitat quality and modifying community composition. Biodiversity enhances the efficiency by which ecological communities capture resources, produce biomass, maintain water properties, recycle nutrients and through time it increases the stability of ecosystem processes. Biodiversity is one of the most important maintainers of ecosystem integrity and sustainability. Therefore, the knowledge on spatial patterns of biodiversity and its relations to environmental variability is important in order to gain understanding of the relationships between biodiversity and ecosystem functioning. High resolution biodiversity maps can be used to follow and detect changes in ecological systems and for marine spatial planning including allocation of marine protected areas. Additionally to monitoring and management, biodiversity maps have a considerable potential in basic ecological science as they enable testing a multitude of hypotheses related to scale-specific spatial patterns of benthic biodiversity and their causes.

Methods and Results: Benthic biodiversity maps of the whole Estonian sea area were produced by using a multitude of georeferenced environmental layers and three different modelling algorithms. The abiotic environmental variables included different bathymetrical (depth, slope of seabed), hydrodynamic (wave exposure, currents), geological (seabed substrate), and physico-chemical (temperature, salinity, transparency, nutrients, ammonium, ice conditions) variables. For modelling algorithms random forest (RF), generalized additive models (GAM) and boosted regression trees (BRT) were used and the predictive performance of different models was assessed. Model with the highest prediction

accuracy was used to produce predictions of total benthic species richness, macrozoobenthos species richness, and macrophytobenthos species richness.

All three tested modelling algorithms proved to have high predictive ability. Based on mathematical and visual validation, BRT had the highest prediction accuracy. Depth and sediments were the most influential environmental variables in all three mathematical models. All other environmental variables were with relatively lower impact, especially in BRT model, where only depth and sediments clearly stood out from other environmental variables.

Recommendations: Marine subtidal benthic habitats are difficult to reach and therefore expensive and time-consuming to study and consequently have poor spatial and historical data coverage compared to terrestrial habitats. For that reason, modelling techniques and remote sensing applications are especially needful in marine environment to fill in data gaps in both space and time. Successful inclusion of temporal aspects and biotic interaction into species distribution modelling would enable addressing future challenges in the context of climate change and non-native species invasions.

6. The influence of re-oxygenation of the Baltic proper deep water on the recycling of nutrients and carbon

Abstract: At the end of 2014 a major Baltic inflow brought oxygenated, salty water into the Baltic proper. The oxygenated dense water reached the Eastern Gotland basin in March 2015 and the previously long-term anoxic deep water was then exchanged. The effects from the re-oxygenation on the benthic fluxes of inorganic phosphorus, nitrogen, silicon and carbon were measured *in* situ in EGB in July 2015 using an autonomous benthic lander. There was an increased retention of phosphorus in the sediment from the re-oxygenation compared to from the earlier anoxic conditions, while no significant effects were observed on the benthic fluxes of ammonium, silicate and dissolved inorganic carbon. However, the re-oxygenation contributed to an increased nitrate concentration in the bottom water and a flux of nitrate into the sediment.

Progress: All work is completed and we refer to the publication by Hall et al. (2017) in the Appendix.

Deviations from the work-plan: No deviations from work plan.

Introduction: Cyanobacteria blooms and high P concentrations in the Baltic proper have been explained by a combination of external load from land and internal load from the sediments. Roughly 0.5 million tons N is imported to the Baltic Sea annually through N_2 fixation by pelagic cyanobacteria. Nitrogen-fixing cyanobacteria are limited by P, and the blooms are triggered by low N:P ratios in the nutrient pool. The low N:P ratios are caused by removal of fixed nitrogen (denitrification and anammox) together with enhanced benthic P regeneration due to oxygen depletion in deep waters. An intrusion of oxygenated salty water into the Baltic proper started at the end of 2014. This inflow is the largest Major Baltic Inflow (MBI) since 1951, and the third largest since oceanographic measurements in the Baltic Sea began in 1880. The water from the MBI reached the EGB in March 2015 and gave

unique opportunity to repeat same type of measurements that had previously been performed at fully anoxic stations, but this time under oxygenated conditions.

Methods and results: Benthic fluxes of nutrients, DIC and oxygen were measured in situ using chambers of the autonomous big Gothenburg benthic lander in June 2015 at two stations in the Gotland deep (170 and 210 m depth). Sediment and overlying water were then incubated in the four enclosed chambers for about 20 h during which samples were taken autonomously with syringes. The lander was then recovered and water samples were collected from the syringes. Nutrient and DIC samples were filtered immediately after sampling before analyse and salinity, temperature, and oxygen were measured continuously in each chamber with sensors. Rates of denitrification and DNRA were determined, as well as the contribution of annamox to the total N2 production, by an isotopic ^{15}N technique. The bottom water oxygen concentration, measured in situ with O2 optodes mounted on the benthic lander, was about 30-45 µM at the two study sites. Ammonium fluxes were consistently directed out of the sediment, whereas nitrate fluxes consistently were directed into the sediment. The average phosphate as well as the silicate flux was directed out from the sediment. Since the bottom water was anoxic in 2008 and 2010, oxygen uptake rates could only be measured in 2015. The DIP flux was the only flux that showed a statistically significant ($p<0.05$) difference compared two previously measured fluxes during anoxic conditions. In 2015 the DIP flux was significantly lower compared to the earlier observations.

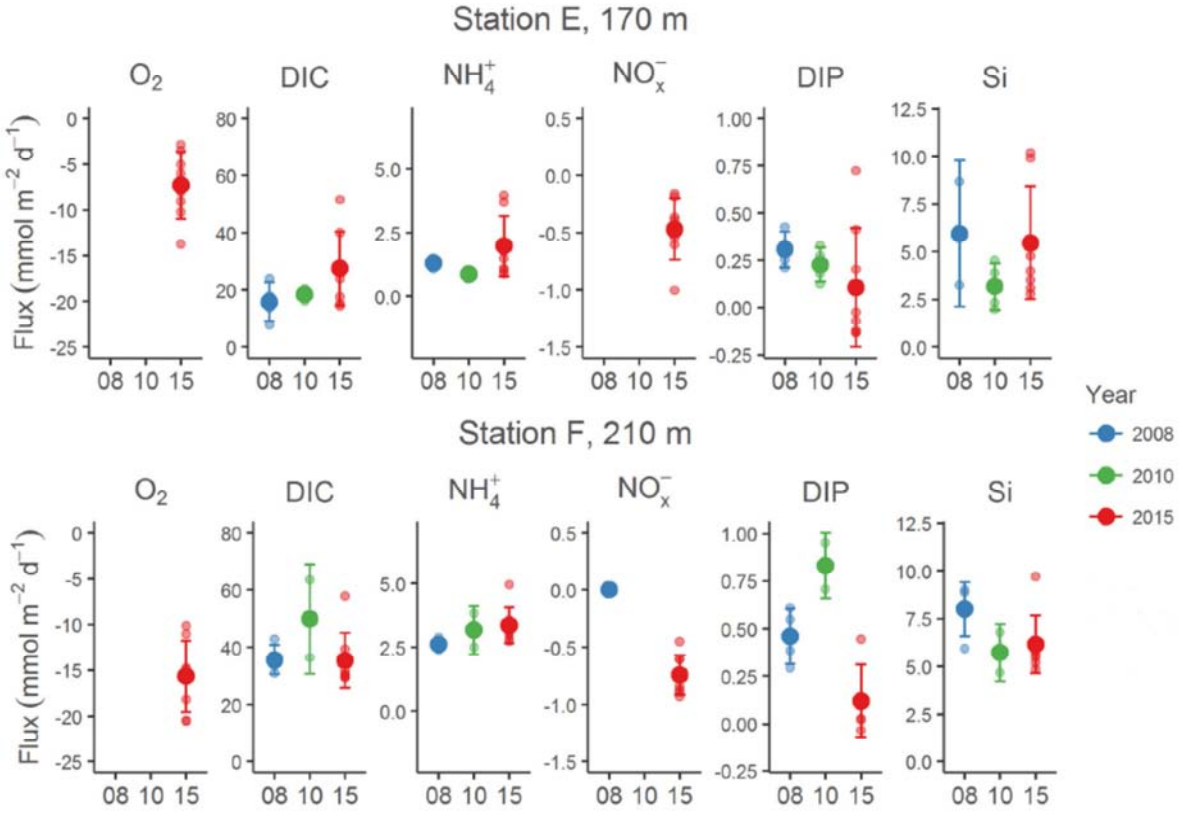

Figure 9. Benthic fluxes of O_2, DIC, NH_4^+, NO_x (NO_2^-+ NO_3^-), DIP and Si at stations E and F in 2008 (blue), 2010 (green), and 2015 (red). The years are given on the x-axis. The bottom water at these stations was anoxic in 2008 and 2010 (with essentially no NO_3^- present), but oxygenated in 2015 (this study). Each individual chamber flux is indicated with a small circle, the average flux with a big circle, and the standard deviation with a bar.

Recommendations: Due to the oxygenation of the bottom water the C:P and the N:P composition of the flux drastically changed. The molar ratio was much below the Redfield ratio under anoxia in 2008 and 2010 but increased for C:P to about 70 and for N:P to about 3–4. The very P rich (in relation to both C and N) benthic flux under anoxia thus turned into a P poor flux under oxygenated conditions due to sedimentary P retention. Oxygenation of the bottom water may thus increase the DIN:DIP ratio of nutrient pool in the water column, and thus indirectly influence eutrophication status, and the abundance and composition of phytoplankton and cyanobacteria communities in surface waters.

7. Sensitivity of the Overturning Circulation of the Baltic Sea to Climate Change. A Numerical Experiment

Abstract: Climate change is expected to impact the Baltic Sea marine environment in several ways, and hence impact both pelagic and benthic habitats. One prominent feature setting abiotic parameters such as salinity and oxygen levels in the Baltic is the overturning circulation. We have here used a number of different global climate scenarios to force a 3D physical ocean model covering the Baltic Sea area. The analysis showed that the Baltic overturning circulation, i.e. the amount of salty water masses that penetrate into the deepest parts of the estuary, decreased between the end of the 20th century and the end of the 21s century, and that the decrease is amplified in the case of the strongest greenhouse gas emission scenarios. The decrease in overturning circulation coincides with an increase of thermal stratification and is linked to a stronger and longer seasonal thermocline.

Progress: All work completed and we refer to the accepted paper by Hordoir et al. (2017) in the Appendix.

Deviations: No deviations from work plan.

Introduction: Many questions have arisen during the recent decades as the number of Major Baltic Inflows (MBIs) to the Baltic Sea has decreased. After a stagnation period from 1983 to 1993, several MBIs have occurred but their frequency has been lower than during the 1960s and 1970s. Then MBIs occurred during three consecutive years (2014, 2015 and 2016), but it is yet too early to say if this latest series is part of a longer trend. The future of Baltic inflows is a subject of importance, and several studies have tried to identify whether changes of wind patterns related with a changing climate could be responsible for their decrease. The Baltic Sea has a complex reaction to changes in atmospheric patterns, since they influence e.g. salinity, temperature and mixing which affects the baroclinic dynamics. The purpose of this study was to provide insight in possible future changes in Baltic Sea circulation processes. Of particular interest was to gain insight on the effect of changes in direct atmospheric forcing (wind forcing, temperature) on the Baltic Sea thermohaline structure and the baroclinic circulation.

Methods and Results: The study used the Nemo-Nordic ocean model for the Baltic Sea. Regional downscaled climate projections, based on two global climate models (EC-EARTH

and MPI) were used as atmospheric forcing for the control period (1961-2005), and for two emission scenarios (RCP 4.5 and RCP 8.5) for the period 2005-2100. Runoff changes can dramatically affect the haline structure of the Baltic Sea, but in this set of experiments we concentrated on the Baltic Sea response to changes in atmospheric forcing and therefore climatological runoff was used. A criteria relating the overturning circulation to a meridional transport function was defined. In the analyses it was shown that the overturning circulation of the Baltic Sea was decreased by up to 15% towards the end of the 21st century. The feature was identified for the main basin in the Baltic Sea, the Baltic Proper. It was also seen in the Bothnian Sea: although smaller in absolute value, this decrease was even higher in relative value (more than 20%). The decrease of the overturning circulation follows a trend which strengthens with the greenhouse gases scenarios and the temperature increase: a higher decrease in overturning circulation was observed when RCP 8.5 emission scenarios were used, regardless of the global climate model that provided the atmospheric forcing.

Recommendations: The analysis predicts that the increase of the thermal stratification in the Baltic Sea will decrease the overturning circulation. The approach provides a time integrated view of the problem and hence it is not clear how the strength and variability of the MBIs will be affected. Since the ecosystem is usually more sensitive to extreme values more than changes in mean values (lower salinity or oxygen extremes for example), this question should be approached in further investigations.

8. Potential habitat change in the Baltic Sea – implications of climate-change and nutrient-load scenarios on the future marine environment

Abstract: To investigate potential changes in benthic and pelagic habitats for marine organisms, a three-dimensional coupled physical and biogeochemical model is utilized to project changes in the water column and in the bottom waters in different parts of the Baltic Sea. The results suggest fresher water masses and warmer bottom water by the end of the 21st century. The results from the two more pessimistic nutrient load scenarios points to lower concentration of O_2 which in combination with changes in salinity might change the species ability to survive and reproduce in a future Baltic Sea. In addition, the results from the HELCOM core indicators with the more pessimistic nutrient load scenarios show a more eutrophic Baltic Sea. However, implementing the Baltic Sea Action Plan appears to improve the environment with lower concentrations of chl-a in the surface water in several basins and decreased O_2 debt in a future climate.

Progress: All work completed and a manuscript (Wåhlström et al. 2017) is in preparation (see Appendix).

Deviations: No deviations from work plan

Introduction: The brackish Baltic Sea is a vulnerable sea under high pressure from human induced activity. Due to the brackish water, many of the marine organisms are believed to live in areas and habitats close to the limit of their physiological tolerance as their origin is

from almost freshwater or marine environments. Thus, the ecosystem is sensitive to perturbations from eutrophication but also from global climate change affecting the physical conditions. Both eutrophication and climate change impacts the abiotic variables in the water column such as salinity, temperature as well as concentration of O_2 and nutrients. Availability of nutrients and O_2 are vital components for the marine production of organic matter and the energy transfer to higher trophic levels. However, strong eutrophication and O_2 consumption due to decomposition of organic matter can have severe negative effects on the ecosystem. Perturbations of these properties disturb the habitats and might change the species ability to survive and reproduce in a future Baltic Sea.
To investigate the combined effect from climate change and nutrient load on the habitat environment for both pelagic and benthic habitats in a future climate, a three-dimensional coupled physical-biogeochemical model for the Baltic Sea is utilized. The analyses include how volumes of water defined by a number of ranges with different combinations of salinity, temperature and O_2 might change by the end of the 21st century. We also investigate how these might change the cod reproductive volume (CRV). In addition, two of the HELCOM eutrophication core indicators, chl-a and O_2 debt, are investigated to study how climate change and nutrient loads might impact the eutrophication in a future climate.

Methods: In this study, transient scenario runs for the time period 1961-2099 are performed with a three-dimensional regional coupled ice-ocean model for the open Baltic Sea. The model is driven at the lateral boundary by four climate emission scenarios and is combined with three nutrient loads scenarios. Each of the nutrient load scenarios are calculated as ensemble average of the four climate emission scenarios for the future climate (2070-2099) and for present day (1970-1999). The three nutrient load are: current loads from rivers and current atmospheric deposition (REF); business as usual for loads from rivers assuming an exponential growth of agriculture in all Baltic Sea countries as projected in HELCOM (2007) and current atmospheric deposition (BAU); reduced river loads following HELCOM (2007) and 50% reduced atmospheric deposition (BSAP). The focus is on changes in salinity, temperature, O_2 and the cod reproductive volume (CRV) as well as two of the HELCOM eutrophication core indicators, chl-a and O_2 debt and the cod reproductive volume (CRV).

Results: The results in this study show a tendency towards generally fresher water masses by the end of the 21st century and warmer bottom water. The results in the two more pessimistic nutrient load scenarios (REF and BAU scenario) indicate decreased O_2 concentration in the entire water column and especially in the bottom water of the Gotland and NW Baltic Proper.
A concrete example of habitat modelling is the simulated CRV. In this study, a comparison between modelled and calculated CRV from observations of salinity and O_2 were executed and the performance of the modelled CRV was acceptable. The results from an investigation of the CRV in a future climate indicate a decreased CRV in all the basins and all nutrient scenarios and in the Gotland and NW Baltic Proper the CRV totally disappeared in a future climate.
The HELCOM eutrophication core indicators are tools used to follow up the progress to reach good environmental status in this area. In the REF and BAU scenario, concentrations of chl-a are enhanced in all basins by the end of the 21st century with the highest increase in the BAU scenario. However, in the more optimistic BSAP scenario, 4 out of 7 basins (Danish

Strait, Gotland Basin, Bothnian Sea and Gulf of Finland) showed reduced chl-a concentrations in future climate, indicating less phytoplankton blooms. In the results of the modelled O_2 debt in present climate there are large differences between basins with the largest undersaturation in the Gotland Basin and the least affected areas in the Arkona Basin and the Bothnian Bay. The results for the future basins reveal that the BAU scenario increases the O_2 debt in the Central Baltic Sea and the Bothnian Sea until the mid-21st century and then continue to be at the same undersaturated state to the end of the 21st century. However, implementing the Baltic Sea Action Plan reduces the O_2 debt to the 1970s level around the mid-21st century in the Gotland Basin, Golf of Finland, Bothnian Sea and Bay.

Recommendations: Eutrophication and climate change seems to impact the abiotic variables in the water column with fresher and less O_2 in the water column and especially in the bottom water where also warmer water are detected by the end of the 21st century. These results point potentially towards a harsher environment for species demanding oxygenated water and consequently, less area to live in and as a result possible translocation to other areas. However, implementing the Baltic Sea Action Plan, improved the O_2 conditions, increasing the species ability to survive and reproduce.
The two HELCOM eutrophication core indicators are negatively impacted from the eutrophication and climate change pointing towards increased eutrophication in a future Baltic Sea in the REF and BAU scenarios. However, if the nutrient loads were reduced (BSAP scenario) the chl-a concentration decreased in Danish Strait, Gotland Basin, Bothnian Sea and Gulf of Finland and the O_2 debt reached the 1970s level in the mid-21st century in the Gotland Basin, Golf of Finland, Bothnian Sea and Bay indicating less eutrophic water.

IV. Appendices

I. **Šiaulys, A., Stupelytė, A., Zaiko, A., 2017. Assessment of benthic habitat change o the mussel beds in Lithuanian coastal reefs (manuscript in preparation, under embargo until published)**

II. **Skov, H.., Kock Rasmussen, E., 2017. Small-scale metastability in a coastal ecosystem of the Baltic Sea. (manuscript in preparation, under embargo until published).**

III. **Kotta, J., Möller, T., Orav-Kotta, H., Pärnoja, M., 2014. Realized niche width of a brackish water submerged aquatic vegetation under current environmental conditions and projected influences of climate change. Marine Environmental Research, 102, 88-101.**

IV. **P Peterson, A., Herkül, K., 2017. Mapping benthic biodiversity using georeferenced environmental data and predictive modeling. (submitted manuscript, under embargo until published).**

V. **Hall, P.O., Almroth Rosell, E., Bonaglia, S., Dale, A.W., Hylén, A., Kononets, M., Nilsson, M., Sommer, S., vad de Velde, S., Viktorsson, L., 2017. Influence of Natural Oxygenation of Baltic Proper Deep Water on Benthic Recycling and Removal of Phosphorus, Nitrogen, Silicon and Carbon. Frontiers in Marine Science, doi: 10.3389/fmars.2017.00027.**

VI. **Hordoir, R., Höglund, A., Pemberton, P., Scimanke, S., 2017. Sensitivity of the Overturning Circulation of the Baltic Sea to Climate Change. A Numerical Experiment. Climate Dynamics, DOI 10.1007/s00382-017-3695-9**

VII. **Wåhlström, I., Andersson, H.C, Gröger, M., Höglund, A., Eilola, K., MacKenzie, B.R., Almroth Rosell, E., Plikshs, M., 2017. Potential habitat change in the Baltic Sea – implications of climate change and nutrient-load scenarios on the future marine environment. (manuscript in preparation, under embargo until published)**

Assessment of the benthic habitat change of the mussel beds in Lithuanian coastal reefs

Šiaulys, A., Stupelytė, A., Zaiko, A.

Embargoed until publication, for information please contact Anastasija Zaiko, email: anastasija.zaiko@jmtc.ku.lt

Small-scale metastability in a coastal ecosystem of the Baltic Sea *(Manuscript for Journal of Biogeography)*

Henrik Skov, Erik Kock Rasmussen

Embargoed until publication, for information contact Henrik Skov, email: hsk@dhigroup.com

Marine Environmental Research 102 (2014) 88–101

Contents lists available at ScienceDirect

Marine Environmental Research

journal homepage: www.elsevier.com/locate/marenvrev

Realized niche width of a brackish water submerged aquatic vegetation under current environmental conditions and projected influences of climate change

Jonne Kotta*, Tiia Möller, Helen Orav-Kotta, Merli Pärnoja

Estonian Marine Institute, University of Tartu, Mäealuse 14, 12618 Tallinn, Estonia

ARTICLE INFO

Article history:
Available online 20 May 2014

Keywords:
Species distribution
Baltic Sea
Submerged aquatic vegetation
Soft bottom
Climate change
Models

ABSTRACT

Little is known about how organisms might respond to multiple climate stressors and this lack of knowledge limits our ability to manage coastal ecosystems under contemporary climate change. Ecological models provide managers and decision makers with greater certainty that the systems affected by their decisions are accurately represented. In this study Boosted Regression Trees modelling was used to relate the cover of submerged aquatic vegetation to the abiotic environment in the brackish Baltic Sea. The analyses showed that the majority of the studied submerged aquatic species are most sensitive to changes in water temperature, current velocity and winter ice scour. Surprisingly, water salinity, turbidity and eutrophication have little impact on the distributional pattern of the studied biota. Both small and large scale environmental variability contributes to the variability of submerged aquatic vegetation. When modelling species distribution under the projected influences of climate change, all of the studied submerged aquatic species appear to be very resilient to a broad range of environmental perturbation and biomass gains are expected when seawater temperature increases. This is mainly because vegetation develops faster in spring and has a longer growing season under the projected climate change scenario.

1. Introduction

Seagrasses and other plants of higher order are unique by occupying the subtidal photic zone of soft sediments. They form extensive habitats in sheltered near coastal zones (Reusch et al., 2005; Larkum et al., 2006) and are among the most productive habitats worldwide (Duarte, 2002). Furthermore, they provide a range of ecological functions such as coastline protection, sediment stabilization, wave attenuation, land-derived nutrient filtration, and carbon fixation, just to name a few; thereby providing some of the most valuable ecosystem services on Earth (Costanza et al., 1997; Short et al., 2011). The submerged aquatic species are also important as food, shelter and space for many invertebrates and fish, many of which are socioeconomically important (Hemminga and Duarte, 2000).

Human use of the coastal marine environment is increasing and diversifying worldwide. Given its multiple stresses, submerged aquatic species have gone through an unusually fast transition in terms of areal decline in habitat (Orth et al., 2006; Waycott et al., 2009). Although large scale processes on the formation of biotic patterns is not well known, it is plausible that contemporary climate change, interacting with other anthropogenic stressors, accounts for a large part of the observed decline. Ecologists have typically interpreted the composition of communities as the outcome of local-scale processes. However, in recent decades this view has been challenged emphasizing the importance of large-scale processes, including climate change, that may result in dramatic shifts in species distribution patterns and thereby affect community species composition, diversity, structure and productivity (Hawkins et al., 2013). Concurrent with recent climate change effects, large-scale fluctuations in water temperature is considered likely to control the distribution of submerged aquatic vegetation because with increasing temperature the photosynthesis-to-respiration ratio steadily decreases (Glemarec et al., 1997; Marsh et al., 1986; Zimmerman et al., 1989). In addition, heavy storms may create physical disturbance capable of reducing seagrass cover and increasing fragmentation of seagrass beds (Fonseca and Bell, 1998; Fonseca et al., 2000). At northern latitudes, elevated ice scouring likewise destroys submerged aquatic vegetation (Robertson and Mann, 1984; Schneider and Mann, 1991) but

* Corresponding author.
E-mail address: jonne@sea.ee (J. Kotta).

http://dx.doi.org/10.1016/j.marenvres.2014.05.002
0141-1136/

contemporary climate change may release vegetation from such a disturbance.

Non-independent effects are common in nature (Hoffman et al., 2003; Reynaud et al., 2003) and therefore it is expected that the combined effects of two or more variables cannot be predicted from the individual effect of each. However, anticipating the future consequences of the interacting pressures is a pre-requisite to sustainable management of coastal ecosystems under current environmental conditions and contemporary climate change. In recent years large investments have been made towards modelling of ecological systems and predicting their future behaviour (e.g. Müller et al., 2009). However, many of these models perform poorly because very little is known about how organisms might respond to multiple climate stressors (e.g. temperature and wave induced currents) and it is difficult to deal with complex and non-linear systems, such as those seen in the marine environment (see Byrne and Przeslawski (2013) for an overview). Specifically, traditional statistical models tend to oversimplify the reality and/or statistical modelling itself may not be the most reliable way to disentangle the relationships between environmental variables and species distributional patterns because it begins by assuming an appropriate data model and the associated model parameters are estimated from the data. By contrast, machine learning avoids starting with a data model and rather uses an algorithm to discover the relationship between the response and its predictors (Hastie et al., 2009). The novel predictive modelling technique called Boosted Regression Trees (BRT) combines the strength of machine learning and statistical modelling. BRT has no need for prior data transformation or elimination of outliers and can fit complex non-linear relationships. The BRT method also avoids overfitting the data, thereby providing very robust estimates. What is most important from the ecological perspective is that it automatically handles interaction effects between predictors. Due to its strong predictive performance, the BRT method is increasingly being used in ecological studies (Elith et al., 2008).

The Baltic Sea hosts a mixture of submerged aquatic vegetation of marine, brackish or fresh water origin; each species characterized by its specific tolerance to environmental conditions (Snoeijs, 1999). Located at the margins of typical marine environments, the Baltic Sea is a vulnerable ecosystem and predicted dramatic climate change will challenge all the submerged aquatic species (Koch et al., 2013). Moreover, in the Northern Hemisphere high-latitude regions are expected to experience more severe warming compared to low-latitude regions (IPCC, 2013). In addition climate change is expected to prolong growing season, reduce ice cover as well as alter wind and precipitation patterns. Such changes are likely to have profound influences on water turbidity and salinity (Short and Neckles, 1999 and references therein). Due to the non-linear response of biota to the environment, even gradual changes in future climate may provoke sudden and perhaps unpredictable shifts in submerged aquatic plant communities as many are close to their physiological tolerance limit and different species have different response mechanisms. For example many submerged plant species are of fresh water origin but have a wide salinity tolerance and thus are often competitively superior over seagrasses under fluctuating salinity regimes (Stevenson, 1988; van den Berg et al., 1998).

Hydrodynamic conditions (Schanz and Asmus, 2003), nature of the substrate (Viaroli et al., 1997; De Boer, 2007), light (Peralta et al., 2002), temperature (Glemarec et al., 1997), salinity (Wortmann et al., 1997), water transparency (Krause-Jensen et al., 2008) and nutrient concentrations in the water column (Orth, 1977) are the key environmental variables affecting the distribution of submerged aquatic vegetation. In addition to this, ice conditions are also important in high-latitude regions (Robertson and Mann, 1984). Most of these variables are expected to change with changes in future climate; however, the strength of environment–biota relationships is likely a function of spatial scale. To date, the relationships between these environmental variables and the distributional patterns of aquatic vegetation have mostly been specified at one spatial scale but ignoring an infinite variety of other possibilities (Krause-Jensen et al., 2003; Appelgren and Mattila, 2005). In order to take into account these scale-specific effects, both small- and large-scale environmental variability should be incorporated into the models.

Seascape-scale (1–10 km) abiotic processes contribute to broadscale distributional patterns. Within these patterns smaller-scale processes (1–10 m) operate at a lower intensity to modify the distribution of species (Steele and Henderson, 1994). Among physical disturbances changes in water temperature and wave-induced current velocity are the key large-scale processes that are expected to alter species distributions. Specifically, elevated water temperatures favour plant growth and result in increased cover of submerged aquatic species (Xiao et al., 2010). Elevated wave stress affects sediment characteristics and water turbidity (Madsen et al., 2001), thereby favouring opportunistic species and disfavouring the pristine water species (Burkholder et al., 2007). The reduction of ice cover is also expected to have direct and indirect consequences. A direct consequence is the prolongation of the growth season and elevated macrophyte cover/biomass values. Currently, the co-existence of species is granted due to the presence of moderate ice disturbance that removes a significant amount of vegetation annually. In the absence of such disturbance, however, fast growing species are favoured over slow growing species. Finally, increased fresh water inputs favour higher order plants of fresh water origin over seagrasses (Touchette, 2007). But increased riverine inputs may also elevate sedimentation rates that impact negatively on the whole macrophyte community (Chambers et al., 1991). As species are shown to have strong individualistic responses to their environment we also expect large variability of responses among species (Bulleri et al., 2012).

The aims of this paper are to (1) identify the most important environmental variables defining the cover of submerged aquatic vegetation, (2) specify the spatial scales where such relationships are the strongest and (3) predict changes in the distributional pattern of the submerged aquatic vegetation from the current to future climate. The modelling approach aims to identify possible critical tipping points of all these variables where regime shifts in species distribution may occur, to provide a better understanding of the ecological frames in which outbreaks or local extinction are more likely to occur.

2. Material and methods

2.1. Study area

The study was carried out in the different sub-basins of the north-eastern Baltic Sea: the Baltic Proper, the Gulf of Riga, the West Estonian Archipelago Sea, and the Gulf of Finland (Fig. 1). The Baltic Sea is a geologically young semi-enclosed sea and one of the largest brackish water basins in the world. Due to short evolutionary history, low salinity and strong seasonality in temperature and light conditions, the number of submerged aquatic plant species is small, characterised by a mixture of marine, brackish or fresh water origin (Hällfors et al., 1981).

In the study area there is a strong permanent salinity gradient from west to east with western areas having higher salinity values. In coastal areas the dynamics of seawater temperatures is directly coupled with air temperatures. The average sea surface temperature is around 2 °C in winter and may rise up to 20 °C in August. The study area is characterized by a wide coastal zone with diverse bottom topography and underwater habitats (Kotta et al., 2008a; 2008b) (Table 1).

Fig. 1. Map of the sampling stations in the study area.

Table 1
List of environmental variables with their average, minima and maxima in different water bodies around the Estonian coastal sea given ambient and projected climate conditions. Water basins are denoted as follows: GOF – Gulf of Finland, WEAS – West Estonian Archipelago Sea, GOR – Gulf of Riga, BP – Baltic Proper. Environmental variables are as follows: Temperature – average water temperature, Salinity – average water salinity, Velocity – average current velocity, K_d – average water attenuation coefficient, Chlorophyll *a* – average chlorophyll *a* content in water, Slope – inclination of coastal slope, Soft sediment – percentage cover of soft sediment fractions, Ice cover – average ice cover over the study site.

Variable	Unit	Descriptive statistics	Current conditions				Projected climate conditions			
			GOF	WEAS	GOR	BP	GOF	WEAS	GOR	BP
Temperature	°C	Mean	12.9	14.2	13.4	12.8	16.9	18.2	17.4	16.8
		Minimum	10.3	11.4	10.2	11.0	14.3	15.4	14.2	14.9
		Maximum	17.3	19.1	18.5	18.1	21.3	23.1	22.5	22.1
Salinity	Unitless	Mean	5.3	7.0	5.5	7.3	3.9	5.2	4.1	5.5
		Minimum	3.3	6.0	3.4	6.4	2.5	4.5	2.6	4.8
		Maximum	7.5	7.3	6.8	7.8	5.6	5.5	5.1	5.9
Velocity	cm s^{-1}	Mean	1.9	5.5	2.8	4.0	1.9	5.5	2.8	4.0
		Minimum	0.1	0.1	0.2	0.1	0.1	0.1	0.2	0.1
		Maximum	5.2	11.7	7.4	9.7	5.2	11.7	7.4	9.7
K_d	Unitless	Mean	1.4	1.3	1.2	1.1	1.7	1.5	1.5	1.3
		Minimum	0.8	0.6	0.7	0.4	1.0	0.7	0.9	0.5
		Maximum	2.7	2.7	2.9	2.9	3.3	3.2	3.5	3.5
Chlorophyll *a*	mg m^{-3}	Mean	25.4	17.9	20.3	12.1	38.2	26.9	30.5	18.2
		Minimum	6.8	7.6	8.5	3.8	10.2	11.4	12.8	5.7
		Maximum	45.0	47.7	47.2	45.8	67.5	71.6	70.8	68.7
Slope	°C	Mean	0.5	0.1	0.1	0.2	0.5	0.1	0.1	0.2
		Minimum	0.0	0.0	0.0	0.0	0	0	0	0
		Maximum	22.9	5.1	5.9	11.1	22.9	5.1	5.9	11.1
Soft sediment	%	Mean	66.9	86.6	68.7	48.7	66.9	86.6	68.7	48.7
		Minimum	3.1	12.2	12.0	1.1	3.1	12.2	12.0	1.1
		Maximum	98.8	99.2	96.0	95.4	98.8	99.2	96.0	95.4
Ice cover	%	Mean	30.1	32.6	33.5	15.9	15.1	16.3	16.7	8.0
		Minimum	19.4	23.4	19.4	4.7	9.7	11.7	9.7	2.3
		Maximum	38.1	36.3	41.9	32.7	19.0	18.1	20.9	16.4
Depth	M	Mean	38.0	4.9	26.0	61.8	38.0	4.9	26.0	61.8
		Minimum	0.0	0.0	0.0	0.0	0.0	0.0	0.0	0.0
		Maximum	115.0	24.0	67.0	181.0	115.0	24.0	67.0	181.0

2.2. Predicted climate change

According to most climate change scenarios mean global surface temperatures will rise by 1.4–4.0 °C in the next 100 years, primarily depending on the amount of carbon dioxide emissions from anthropogenic sources (IPCC, 2013). However, in the Northern Hemisphere high-latitude regions are expected to experience even more dramatic warming estimated at up to 10 °C increases in air temperature (Heino et al., 2009; IPCC, 2013). Similarly, projected changes in future climate of the north-eastern Baltic Sea differ widely between various regional models. On average, oceanographic studies demonstrate that changes in temperature would be 5 °C in winter and 4 °C in summer. Such shifts in temperature may have no pronounced direct effect on biological quality elements considering the large natural temperature fluctuation of the Baltic Sea basin. However, the increase in temperature significantly affects ice conditions reducing the ice extent by some 50% and therefore indirectly amplifying the effects of wind conditions. Furthermore, it is also expected that the mean daily wind speed over sea areas would increase up to 18% in winter. Finally, the average salinity of the Baltic Sea is projected to decrease by 25% of the recent level (BACC, 2008). Such shifts plausibly result in the doubling of phytoplankton biomass (Hense et al., 2013). Besides, water transparency is expected to be reduced as a function of water salinity (Stramska and Świrgoń, 2014). These stressors do not act in isolation but in combination their impacts on submerged aquatic vegetation may be greater than the sum of the single factor effects (Crain et al., 2008; Holmer et al., 2011). The modelling exercise used in this study incorporated all important environmental variables both at current and future climate levels. Hence our models suggest those stress-combinations and environmental conditions where impacts are synergistic and ecosystem degradation may occur.

2.3. Biotic and environmental data

2.3.1. Field sampling

The depth limit of submerged aquatic vegetation does not exceed 10 m in the Baltic Sea (Nielsen et al., 2002; Boström et al., 2003; Steinhardt and Selig, 2007) and therefore the sampling was carried out between seashore down to 10 m depth. Altogether, 6516 stations were sampled during the summers between 2005 and 2012 (Fig. 1). The dataset contains 1891 stations that include submerged aquatic vegetation. Using a remote underwater video device the cover patterns of submerged aquatic vegetation was estimated. The camera was set at an angle of 35° below horizontal to maximize the field of view and the range of the forward view was approximately 2 m in clear waters. The camera sled was towed from a 5-m-long boat 1 m above the sea floor at an average speed of 50 cm s^{-1}. Real-time video was captured with a digital video recorder. For each site a 50 m length transect was recorded. Depth and navigational data (from GPS) were recorded at 1-s intervals during camera deployments. In each transect the coverage of different sediment type (rock, boulders, pebbles, gravel, sand, silt) and submerged aquatic vegetation was estimated. Six different submerged plant species were investigated: *Myriophyllum spicatum* L., *Potamogeton perfoliatus* L., *Ruppia maritima* L., *Stuckenia pectinata* (L.) Börner, *Zannichellia palustris* L. and *Zostera marina* L. When it was difficult to identify submerged vegetation species in field, community samples were collected by diver for later taxonomic analysis.

2.3.2. Supporting environmental data

In the following paragraphs we describe environmental proxies that were used to link physical environment to the coverage of the submerged aquatic plants (for detailed modelling procedures see Section 2.4). The Baltic Sea lacks important biotic modifiers of seabed structure such as corals and oysters that are commonly present in true marine areas. Furthermore, the seabed sediment depends on the bedrock formations, glacial and post-glacial sediments, hydrodynamic conditions and seabed topographic features. The geographic information system (GIS) layer of the proportion of soft sediment was derived from a generalized additive model (GAM) where depth, wave exposure, seabed slope and large-scale geological seabed types (stored at the database of the Estonian Marine Institute) were used as predictive variables. The package mgcv (Wood, 2006) in statistical software R (RDC Team, 2013) was used to build the GAM. Data from nearly 10,000 benthos sampling points from the north-eastern Baltic Sea were used as input data for the proportion of soft sediment. Altogether 90% of the data were used as model training data and 10% for validating the model predictions using Pearson correlation (0.72 for the final model). After fitting the model, the GIS layers of predictive variables were used to produce the spatial prediction of the proportion of soft sediment at a resolution of 200 m (Herkül et al., 2013).

Based on bathymetry charts (available at the Estonian Marine Institute, University of Tartu) the inclination of coastal slopes was calculated at 50 m pixel resolutions using the Spatial Analyst tool of ArcInfo software (ESRI, 2011). High values of coastal slopes indicate the occurrence of topographic depressions or humps at the measured spatial scale. Low values refer to flat bottoms.

The values of water temperature, salinity and water velocity were obtained from the results of hydrodynamical model calculations from summers 2005–2012. The calculations were based on the COHERENS model which is a primitive equation ocean circulation model. It was formulated with spherical coordinates on a $1' \times 1'$ minute horizontal grid and 30 vertical sigma layers. The model was forced with hourly meteorological fields of 2 m air temperature, wind speed, wind stress vector, cloud cover and relative humidity. The meteorological fields were obtained from an operational atmospheric model. The model was validated against water level, temperature, salinity and water velocity measurements from the study area (Bendtsen et al., 2009).

Finnish Meteorological Institute provided ice cover over the study area for the investigated period. Ice cover was produced on daily basis at a nominal resolution of 500 m and was based on the most recent available ice chart and synthetic aperture radar (SAR) image. The ice regions in the ice charts were updated according to a SAR segmentation and new ice parameter values were assigned to each SAR segment based on the SAR backscattering and the ice range at that location.

As a proxy of eutrophication we used the MODIS satellite derived water transparency (K_d) and water chlorophyll a values. The frequency of satellite observations was generally weekly over the whole ice-free period, however, several observations were discarded due to cloudiness. The spatial resolution of satellite data was 1 km. False zeroes were removed from the data prior to the statistical analysis.

The ESRI Spatial Analyst tool was used to calculate the average of all abiotic and biotic variables (those obtained from field sampling as well as from modelling) for local i.e. sampling scale, 1 km and 10 km spatial scales. These values were used to link environmental and biotic patterns at larger spatial scales. The abiotic environmental variables with means, minima and maxima are presented in Table 1.

2.4. Modelling

2.4.1. Environmental niche analysis

All abiotic and biotic geo-referenced environmental data was used for environmental niche analysis. Niche breadth and

separation of habitat niche between submerged aquatic plant species were assessed using analysis of outlying mean index (OMI). OMI measures the distance between the mean habitat conditions used by the species (niche centre), and the mean habitat conditions of the sampling area (Dolédec et al., 2000). The higher the value of OMI index of a species, the higher its habitat specialization. OMI analysis is a multivariate coinertia analysis that unlike canonical correspondence analysis and redundancy analysis, can handle non-unimodal and non-linear species–environment relationships. Compared to the traditional multivariate methods, OMI gives a more even weight to all sampling units even if they exhibit low number of species or individuals. Thus, OMI captures more adequately the multivariate environmental space represented by sampling units (Dolédec et al., 2000). The package "ade4" (Dray and Dufour, 2007) was used for running OMI analysis in the statistical software R (RDC Team, 2013). The environmental niche space of submerged aquatic vegetation was visualized by drawing a convex hull over the points of OMI ordination where the species were present. When drawing the border of niche space, a total of 5% of the most distant observations of species occurrences were considered as outliers and excluded in the analysis.

2.4.2. Species distribution modelling

The contribution of different environmental variables on the coverages of submerged aquatic plant species was explored using the Boosted Regression Tree method (BRT) and the BRT models were also used to predict the species coverages for the whole study area given ambient and projected climate conditions. BRT models are capable of handling different types of predictor variables and their predictive performance is superior to most traditional modelling methods. The BRT method iteratively develops a large ensemble of small regression trees constructed from random subsets of the data. Each successive tree predicts the residuals from the previous tree to gradually boost the predictive performance of the overall model. Although BRT models are complex, they can be summarized in ways that give powerful ecological insight (Elith et al., 2008).

In the BRT models, all studied environmental variables were regressed to predict the coverage of submerged aquatic plant species. When fitting a BRT the learning rate and the tree complexity must be specified. The learning rate determines the contribution of each successive tree to the final model, as it proceeds through the iterations. The tree complexity fixes whether only main effects (tree complexity = 1) or interactions are also included (tree complexity >1). Ultimately, the learning rate and tree complexity combined determine the total number of trees in the final model. For each species, multiple models were run varying both the model learning rate (between 0.1 and 0.001) and the number of trees (between 1000 and 10,000). Then the optimum model was selected based on model performance. Typically, optimal learning rates, number of trees and interaction depth were 0.01, 2000 and 5, respectively. In order to avoid potential problems of overfitting, unimportant variables were dropped using a simplify tool. Such simplification is most useful for small data sets where redundant predictors may degrade performance by increasing variance. As a consequence, our final models did not include any autocorrelating variables. Model performance was evaluated using the cross validation statistics calculated during model fitting (Hastie et al., 2009). A random 20% of the data was assigned for testing model accuracy. The best models were then used for making the spatial prediction of the cover of submerged aquatic plant species in the Estonian coastal sea area. In order to model the cover of submerged aquatic vegetation in the predicted future climate we used the established relationships of today's plants to the environmental factors (and their interactions) in interpreting the influence of the future climate. Both present and future predictions were modelled over a 200 × 200 m grid covering water depths of 0–10 m. The BRT modelling was done in the statistical software R using the gbm package (RDC Team, 2013).

3. Results

Submerged aquatic vegetation was found at 1891 stations out of 6516. Other sites were devoid of vegetation or dominated by perennial or ephemeral algae. Altogether, six submerged aquatic plant species were observed with the number of records indicated in brackets: *M. spicatum* (437), *P. perfoliatus* (381), *R. maritima* (333), *S. pectinata* (1274), *Z. palustris* (433) and *Z. marina* (293). Both single species and mixed stands of submerged aquatic vegetation were observed.

The distributional range of the submerged plant species was similar and they inhabited practically the whole Estonian coastal range. In general the studied species were not found in the easternmost parts of the Gulf of Finland and *Z. marina* also tended to avoid the turbid and diluted Pärnu Bay area. Plants were recorded up to 8 km distance from the shore (Fig. 2). Higher order plants prevailed on soft and mixed substrates; *R. maritima* and *Z. palustris* were recorded also on rock crevices. No higher order plants were recorded deeper than 7 m and usually they were found at the depth range of 0.3 and 4.5 m. Similarly, the niche modelling indicated that there was a large overlap in niche space among all submerged plant species. Only *Z. marina* and *P. perfoliatus* inhabited somewhat opposing niche space. *P. perfoliatus* and *M. spicatum* had the narrowest niche space whereas *Z. palustris* had the broadest niche space (Fig. 3).

The BRT modelling described a significant proportion of variability in the cover of submerged aquatic vegetation and as expected the model performance varied among plant species. In general, the majority of the studied species are sensitive to changes in water temperature, current velocity and winter ice scour. Surprisingly, water salinity, turbidity and trophic state have a low impact on the biota. For the majority of submerged aquatic plant species, the distributional pattern is a function of a few environmental variables. Only *Z. palustris* and *R. maritima* are equally described by many environmental variables (Table 2).

Both local and seascape-scale environmental variability are important in the models of submerged aquatic plant species with local-scale variability, in general, exceeding that of 1 and 10 km scale variability. The contribution of 1 km scale variability is as important as local-scale variability in the models of *S. pectinata* and *Z. palustris* and that of 10 km scale in the model of *P. perfoliatus*, respectively (Table 3). In general there is no difference between the studied variables in how they contributed to the models along spatial scale. The only difference is due to their relative contribution.

When modelling species distribution under the projected influences of climate change, all of the studied submerged aquatic species seem to benefit from climate change with no indication of local extinction. Only the coverage of *Z. palustris* does not change in time (Figs. 4 and 5). Interestingly, this species has the lowest OMI index value i.e. broadest niche space.

All submerged plant species benefit from the warming climate. In general there is an abrupt increase in the vegetation cover over a certain threshold value and such a tipping point varied among species. Those species that have the highest temperature threshold value are mostly favoured by the future climate. If the temperature is too high, the coverage of *R. maritima* decreases again. *Z. palustris* have a narrow depth range whereas other species have either moderate to large depth range. Except for *S. pectinata* and *Z. marina*, all submerged plant species reduce their depth range under the

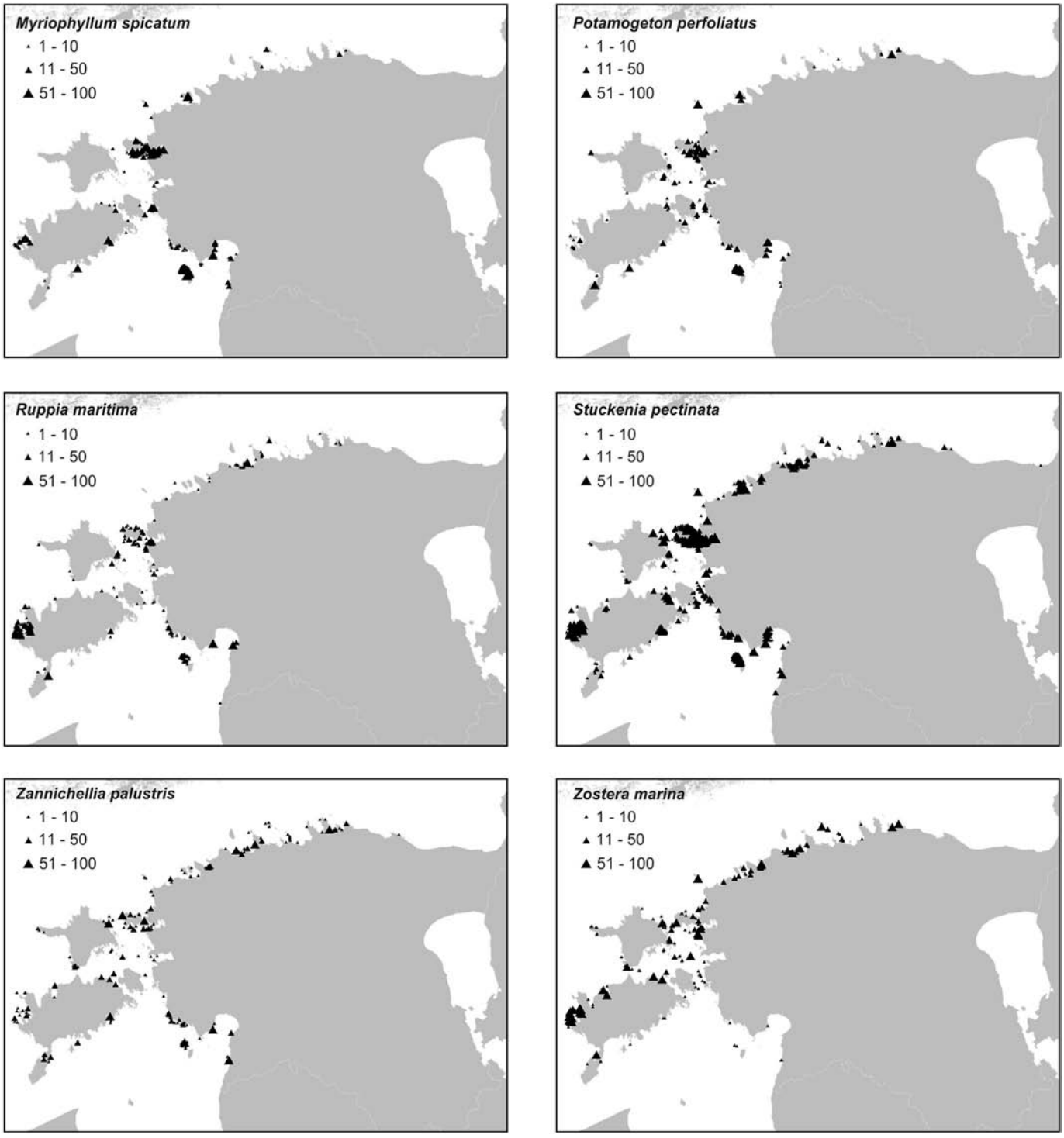

Fig. 2. The coverage of submerged aquatic plant species (%) in the study area.

projected influences of climate change. The majority of species are confined to areas where the wave-induced current velocity is the lowest. Only *M. spicatum* benefits from the elevated exposure to waves. *P. perfoliatus*, *M. spicatum* and *S. pectinata* reduce their cover and *Z. marina*, *R. maritima* and *Z. palustris* increase their cover under a reduced ice extent of the projected climate change (Fig. 6). To conclude, an overall increase in the cover of submerged aquatic vegetation under the projected influences of climate change is triggered both by a separate effect of seawater warming and an interactive effect of temperature and other environmental variables.

4. Discussion

Our study suggests that (1) local and seascape-scale environmental variability affect the cover patterns of submerged aquatic species with local variability exceeding seascape-scale variability, (2) physical disturbance such as seawater warming, elevated wave-

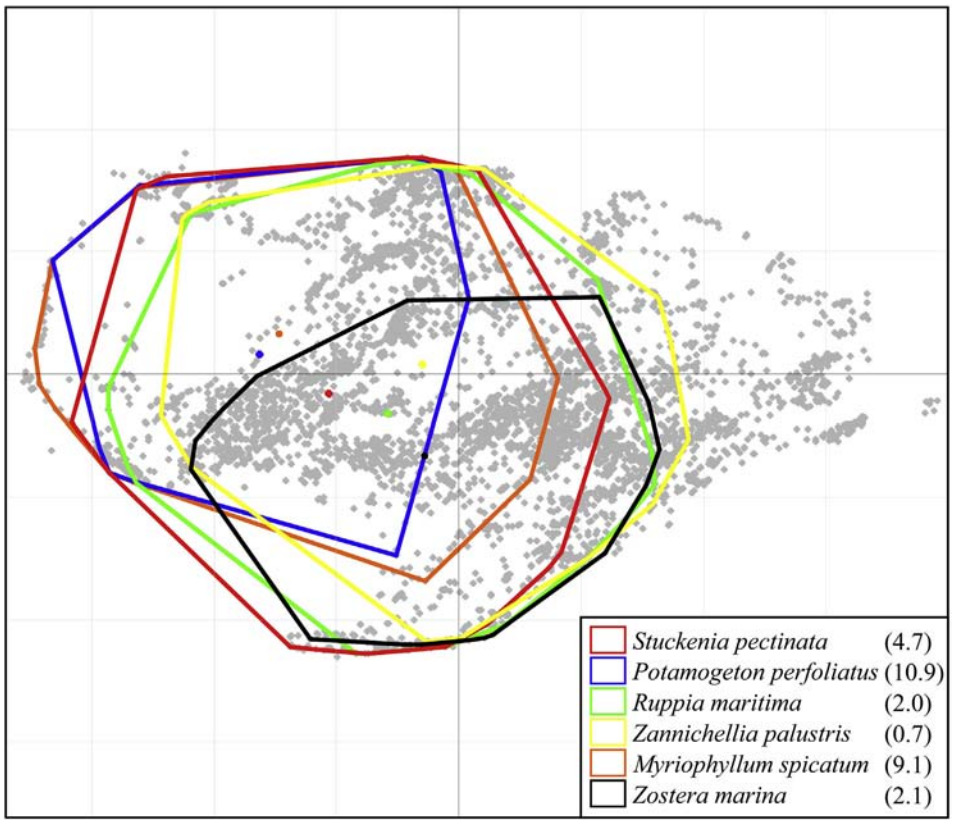

Fig. 3. Niche breadth analysis of the studied species. The borders of niche space and separation of habitat niche between the studied submerged aquatic species are shown by coloured lines. Coloured dots on the plot indicate the centres of niche space of the species. Grey dots represent sampling sites. The value of outlying mean index (OMI) is shown in brackets. OMI measures the distance between the mean habitat conditions used by species (niche centre), and the mean habitat conditions of the sampling area. The higher is the value of OMI index of a species, the higher is its habitat specialization. (For interpretation of the references to colour in this figure legend, the reader is referred to the web version of this article.)

induced current velocity and reduced ice scour override the effects of salinity reduction, elevated turbidity and pelagic production and (3) finally, practically all of the studied submerged aquatic species benefit from the projected influences of climate change with no indication of local extinction.

These findings suggest that there is no key spatial factor affecting the distributional patterns of submerged plant species and that in fact, the species distributional patterns seemingly having scale invariance in the Baltic Sea (in sensu Halley, 1996; Gisiger, 2001). This is not in accordance with earlier observations from various marine areas and for different organisms. Often the variation of physical characteristics at larger spatial scales (e.g. from hundreds of metres to hundreds of kilometres) has been seen to have a significant effect on species abundance (Turner et al., 1999; Witman et al., 2004), whereas small-scale environmental variability explained only a little of the variation in species abundance, especially when considered independently of large-scale variability (e.g. Zajac et al., 2003). More recently, however, it has been shown that the submerged plant species interacted with the environment across multiple spatial scales. In results similar to our study, the response to environmental forcing varied among different macrophyte species and many species showed constant variability through a wide range of spatial scales (Kendrick et al., 2008).

It is likely that high variability in submerged plant species at small scales is related to the mosaic of sediment and bottom topography at this scale in the study area (Kotta et al., 2008a; 2008b). Firstly, the availability of soft substrate is a pre-requisite for the establishment of the species. Secondly, sediment

Table 2
The percentage of variance explained by the BRT species models. Environmental variables are as follows: T – average water temperature, Vel – average current velocity, D – sampling depth, Ice – average ice cover over the study site, Slope – inclination of coastal slope, Chl – average chlorophyll a content in water, K_d – average water attenuation coefficient, Sed – percentage cover of soft sediment fractions, Sal – average water salinity. Total variance of the BRT models explained by the models is given in bold.

Species	T	Vel	D	Ice	Slope	Chl	K_d	Sed	Sal	Total
Myriophyllum spicatum	27	30	6	13	7	7	0	7	3	**0.81**
Potamogeton perfoliatus	40	28	5	8	6	6	2	4	1	**0.75**
Ruppia maritima	27	16	12	11	6	13	10	2	3	**0.50**
Stuckenia pectinata	22	30	12	4	8	9	5	5	5	**0.83**
Zannichellia palustris	20	18	17	18	10	0	17	0	0	**0.64**
Zostera marina	32	16	12	4	16	4	6	5	5	**0.61**
Average	**28**	**23**	**11**	**10**	**9**	**7**	**7**	**4**	**3**	**0.69**

Table 3
The percentage of explained variance by the BRT species models by different spatial scales.

Species	Local	1 km	10 km
Myriophyllum spicatum	42	35	23
Potamogeton perfoliatus	38	22	40
Ruppia maritima	53	22	25
Stuckenia pectinata	40	36	24
Zannichellia palustris	38	38	24
Zostera marina	45	26	29
Average	43	30	28

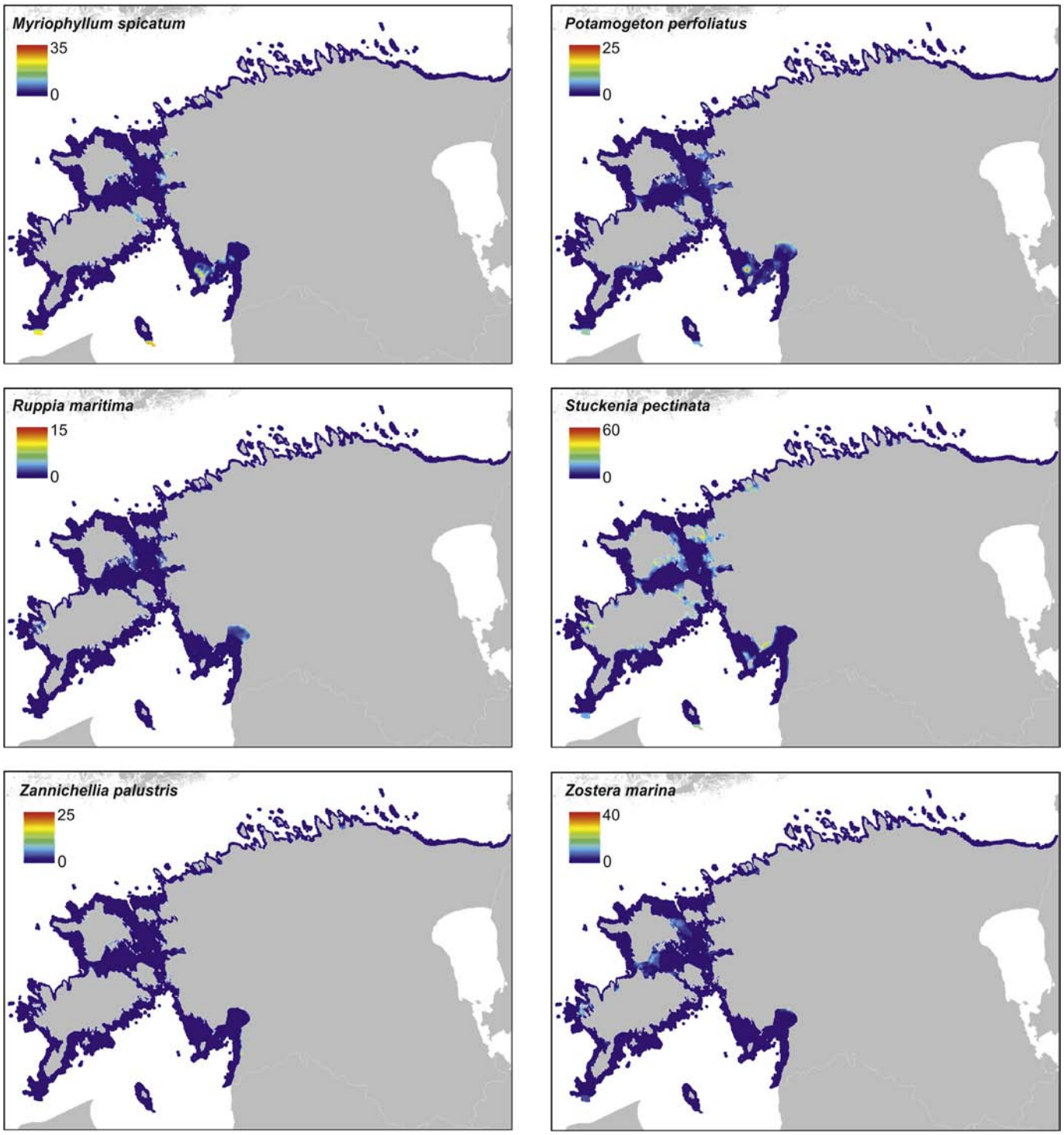

Fig. 4. Modelled distribution of the submerged aquatic plant species for current climate conditions. For modelling the Boosted Regression Tree technique (BRT) was used. Colour diagram shows the species cover in percentage. (For interpretation of the references to colour in this figure legend, the reader is referred to the web version of this article.)

modulates the flow above the seabed (e.g. Prasad et al., 2000; Håkanson and Eckhéll, 2005) and the intensity of flows is directly related to the cover pattern of the macrophytes (van Katwijk and Hermus, 2000; Madsen et al., 2001). In soft sediments, water flow also determines the light climate; i.e., large waves may cause considerable re-suspension of sediments and prolonged periods of poor light conditions (Madsen et al., 2001). Thirdly, small scale topographic heterogeneity may provide the species refuges against physical disturbances including ice scouring and mechanical stress due to waves (Kautsky, 1988; Heine, 1989). For some submerged aquatic species the contribution of seascape-scale variability was as important as local-scale variability. Those species were characterised by lower sensitivity to the variability in substrate characteristics compared to others. For example, *Z. palustris* inhabits different types of soft bottoms but also hard substrates i.e. rock crevices. In such habitats, this species

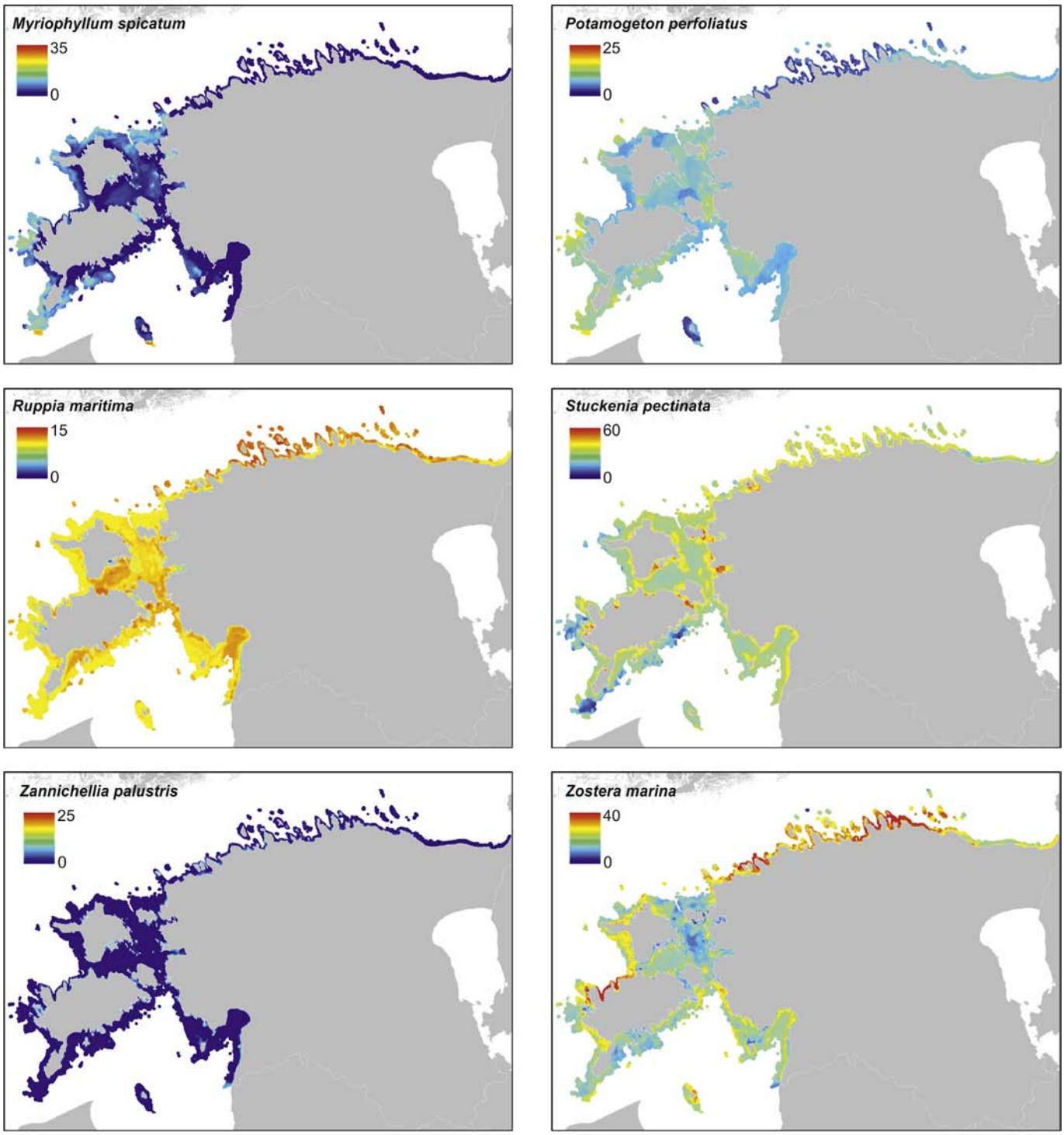

Fig. 5. Modelled distribution of the submerged aquatic plant species for projected future climate. The projected future scenario is described in the section "2.2. Predicted climate change." For modelling the Boosted Regression Tree technique (BRT) was used. Colour diagram shows the species cover in percentage. (For interpretation of the references to colour in this figure legend, the reader is referred to the web version of this article.)

can actually grow outside of its "normal" environment i.e. at exposed conditions and far away from the coast. High variability in macrophyte communities at seascape-scales is related to broad patterns of seawater warming, exposure to waves and winter ice scour and an interaction of all these variables defines the suitability of seascape for the growth of submerged aquatic vegetation (Kautsky and van der Maarel, 1990).

One of the fundamental challenges facing ecologists is to understand how natural systems will respond to environmental conditions that have no analogue at present or in the recent past (Harley et al., 2006). There is always a risk of non-linearities that are specific to climatic conditions we have not yet experienced. Although such source of error is acknowledged, the study area covered a large gradient of water temperature, salinity, wave

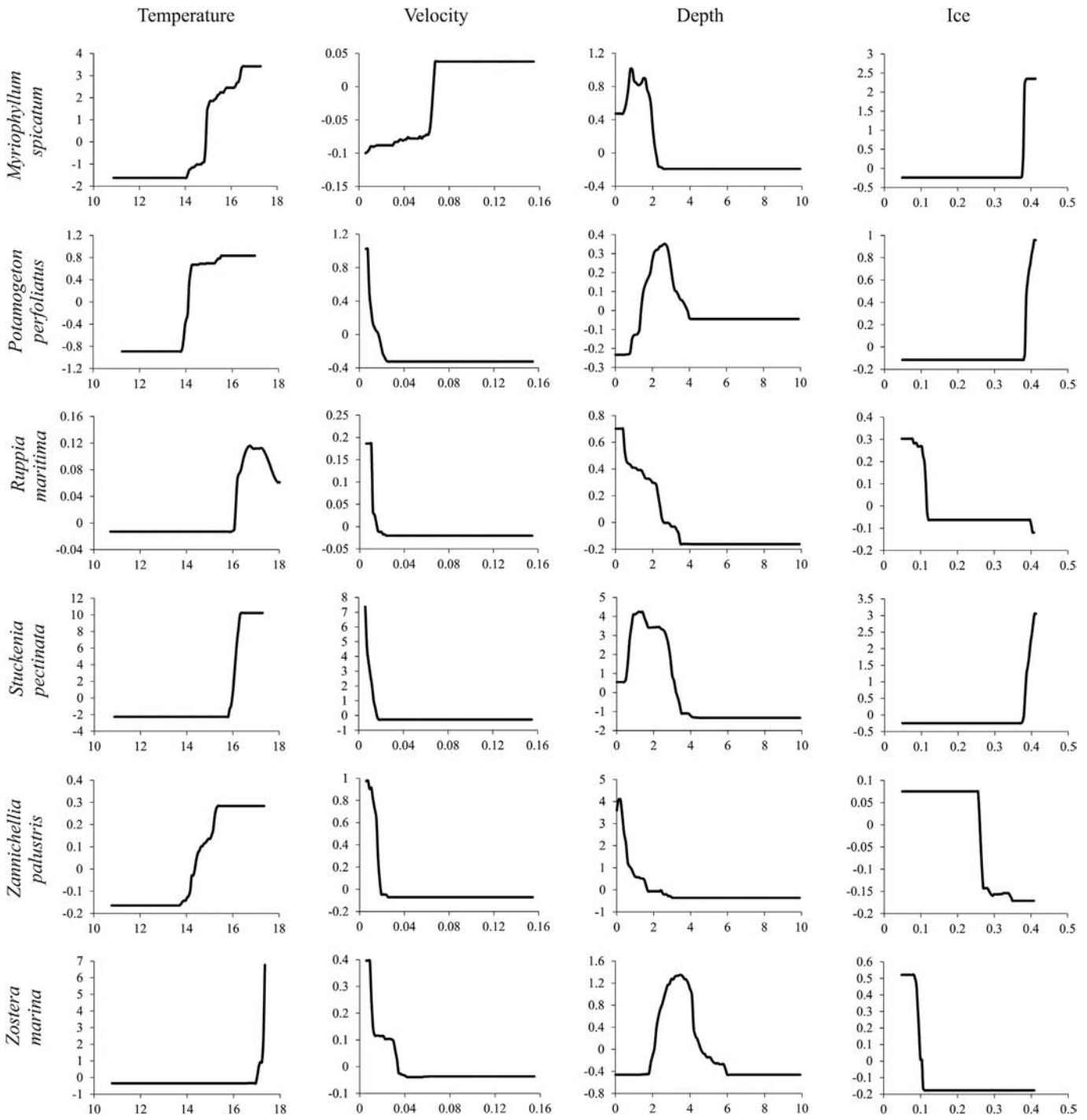

Fig. 6. "Partial dependence" plots of the Boosted Regression Tree technique modelling (BRT) showing the effect of environmental variables on the cover of submerged aquatic plant species whilst all other variables are held at their means.

exposure, etc. and the modelled ranges of environmental variability did not exceed those observed in the field.

The individualistic response of species to the environmental change was expected (e.g. Schiel, 2004; Bulleri et al., 2012) and this was confirmed by the BRT models (e.g. Fig. 6). The future climate would be also expected to be highly idiosyncratic and therefore shift in the patterns of submerged vegetation be species-specific. However, this was not the case as our future climate models showed a generic increase of the cover of submerged aquatic vegetation.

As expected, non-linearities between environment and biota result in situations where even gradual changes in future climate may provoke sudden and perhaps unpredictable biological responses as populations shift from one state to another. Moreover, the combined influence of several stressors might push population beyond a critical threshold that would not be reached via variation in any forcing variable operating in isolation (e.g. Hoffman et al., 2003).

This study shows that the species that has the broadest niche space is insensitive to the projected influences of climate change.

However, moderate to high selectivity to environmental conditions does not couple with the species sensitivity to climate change. It is expected that species with a broad environmental tolerance can cope with different stresses including those subjected by the future climate. The lack of differences in responses to the future climate among medium to highly selective species may be attributed to the species-specific reaction of environmental change (e.g. Schiel, 2004; Bulleri et al., 2012). Specifically, *S. pectinata* and *Z. marina* have the strongest responses to the projected influences of climate change. Both species have relatively broad depth range and this attribute may facilitate the species to persist under impoverished light conditions induced by the future climate. In fact, although the distribution maps of the submerged aquatic vegetation show that the majority of species benefit from the future climate, all species except for *S. pectinata* and *Z. marina* also retract from the deepest parts of their distributional range. Those species that can naturally inhabit broad depth ranges i.e. different light conditions, are insensitive to the impoverished light conditions and thereby are disproportionally favoured by a reduction of ice scour and an increment of temperature and nutrient availability as compared those species acclimated to the narrower ranges of light conditions and/or depth ranges. As an extreme, *Z. palustris* has a very narrow depth range inhabiting only at the shallowmost study areas. Concurrent with the declined transparency of the future climate, the species cannot possibly migrate into shallower areas and benefit from e.g. reduced ice disturbance and prolonged vegetative season.

This study suggests that elevated coverages of submerged vegetation associated to the future climate are largely triggered by elevated temperatures. A primary effect of increased global temperature on seagrasses but likely other submerged vegetation is related to the alteration of growth rates of the plants themselves (Short and Neckles, 1999). In general net photosynthesis of macrophytes increases with temperature up to an optimum value and then decreases dramatically. For seagrasses the rate of leaf respiration increases more rapidly with rising temperature than does that of photosynthesis, leading to both a steady decrease in the photosynthesis-to-respiration ratio with increasing temperature. A sharp decline of gross photosynthesis, however, is reached beyond 30 °C (Marsh et al., 1986). Obviously, the Baltic Sea is far too cold an environment characterised by a short vegetation season. Any elevated temperatures of the projected influences of climate change only prolong the vegetation season i.e. increase growth of the submerged aquatic vegetation and shoot to root ratio (Zimmerman et al., 1989) with no adverse effects on their carbon balances.

Water motion is known to affect the plant structure of submerged aquatic vegetation (Fonseca et al., 1983; Worcester, 1995) with elevating current velocity increasing leaf biomass, width, and canopy height (Fonseca and Kenworthy, 1987; Short, 1987). However, our study shows opposite results with only the cover of *M. spicatum* being facilitated by increased current velocities. This pattern may be due to specific light conditions in our study area. Specifically, clayey bottom deposits prevail in deeper parts of the study area and wind speeds higher than 5 m s^{-1} already result in considerable resuspension of these sediments and, thus, the reduction of water transparency in the coastal water. *M. spicatum*, however, can thrive in nutrient rich turbid habitats where other submerged aquatic plant species are missing due to poor light conditions (Menéndez and Comin, 1989; Eriksson et al., 2004; Gustafsson, 2013). In addition, *M. spicatum* is also very resistant to different mechanical disturbances e.g. a clipping experiment by Cohen et al. (1986) demonstrated that *M. spicatum* regenerated from below the damaged point, while other submerged plant species regenerated from the roots. Finally, *M. spicatum* can remain photosynthetically active through winter opposing to other submerged aquatic vegetation (Aiken and Walz, 1979). This wintertime growth allows the species to outcompete other submerged algal species especially in exposed areas where light conditions due to the lack of ice cover is relatively good all year round. On the other hand, there is also evidence that the resource allocation of some submerged plant species such as *S. pectinata* is strongly influenced by wave exposure. At sheltered areas more resources are allocated to vegetative shoots and rhizomes whereas at exposed sites more resources are allocated to reproduction (Kautsky, 1987).

Submerged aquatic vegetation is affected by changing salinity values by water and nutrient imbalance resulting from large difference in osmotic potentials between internal and external environments (Gorham et al., 1985). Salinity resistance is related to diverse physiological adaptations (Flowers et al., 1977; Greenway and Munns, 1980). Although seagrass photosynthesis is maintained at low salinities, a large reduction in productivity has been measured for various species at reduced salinities (Pinnerup, 1980; Kerr and Strother, 1985; Dawes et al., 1987). The submerged aquatic vegetation of fresh water origin are expected to increase their photosynthetic performance and hence their growth together with reduction in salinity (Riddin and Adams, 2010). Within a range of the projected influences of climate change, salinity seemed to have only a minor effect on the distributional patterns of submerged aquatic plant species. Plausibly, the submerged aquatic vegetation inhabiting the Baltic Sea range are adapted to a broad range of salinity variation and a 25% reduction of salinity values did not overweigh the gains resulted from elevated seawater temperature, prolonged vegetative season and reduced winter time ice scour. Other authors have also demonstrated a marginal role of salinity in the models of benthic vegetation compared to its potential role for species distributions in the brackish Baltic Sea (Rosqvist et al., 2010).

The models in this study demonstrate that different submerged aquatic species respond differently to changing winter ice cover. Winter ice scouring periodically destroys submerged aquatic vegetation. During harsh winters, prevailing fast growing species such as *M. spicatum*, *P. perfoliatus* and *S. pectinata* are favoured as those species can gain a large size and/or high biomass within a short vegetative season. Moreover, harsh winters seemingly bury the seeds of submerged vegetation deep in sediment and thereby dramatically reduces the species germination percentage, especially those of slow growing species (Xiao et al., 2010). The reduction of ice cover, in turn, favours slow growing species. The slow growing species are often the late successional species i.e. being once established they keep fast growing species away from the community.

The current study also suggests that those species that are weakly related to the multitude of environmental variables have a broad distributional range. For example, among the studied species *R. maritima* is the most widely distributed seagrass, occurring in tropical and temperate zones in a wide variety of habitats (Short et al., 2007). Weak responses of *R. maritima* to a range of environment variables may be related to the opportunistic character of the species. Specifically, it has been demonstrated that the response of submerged aquatic vegetation to the environmental perturbation is often a function of organism size (Kotta et al., 2013). For example, the large Mediterranean seagrass species *Posidonia oceanica* requires centuries for recolonization due to slow rhizome elongation rates and rare sexual reproduction (Duarte, 1995; Meehan and West, 2000). On the other hand, small, fast-growing seagrass species such as *R. maritima* recover within just one or a few years (Duarte, 1995). Moreover, submerged aquatic vegetation is known to modify their local abiotic environment by trapping and stabilizing suspended sediments and thereby improving water clarity and plant growth conditions (van

der Heide et al., 2011). This effect is expected to increase with the size of plants. Thus, the distribution of large submerged species is expected to be less coupled with their adjacent abiotic environment compared to their smaller counterparts and, their cover is therefore a function of a colonization history that spans decades to centuries (Kendrick et al., 2000).

The observed results are study area specific and possibly cannot be extrapolated to other seas. This is because different seas (e.g. Baltic Sea and the Atlantic coast) differ greatly with respect to salinity and wave exposure, and that the range of the studied environmental variables defines how those factors influence the distribution of a species. This is also because the habitat selection of seagrasses are known to vary among water bodies e.g. *Z. marina* having different habitat requirements in the Atlantic coasts and the Baltic Sea (Boström et al., 2003; Bekkby et al., 2008). The mechanisms behind the niche differentiation among brackish and marine seagrass populations stem from differences in both interspecific competition and genetic background. Although our study did not account for genetic adaptation, this likely does not affect our main conclusions. Specifically, many seagrass and other submerged plant populations are highly clonal, largely relying on asexual reproduction for population maintenance (Rasheed, 1999; Waycott et al., 2006). In the Baltic Sea submerged aquatic vegetation has very small genetic variability, often consisting of one or a few clones only (Reusch et al., 1999). Therefore, they are expected to be highly sensitive to extrinsic stressors and potentially have very low genetic adaptation potential (Lasker and Coffroth, 1999; Santamaría, 2002). Nevertheless, considering of a large variability in salinity, ice cover and eutrophication in the Baltic Sea range in last thousands of years these genotypes are characterised by wide reaction norms enabling the persistence of species under highly fluctuating environmental conditions. This is also supported by our study suggesting a strong resistance of vegetation to a dramatic change in the environment.

Besides genetic variability, our study did not account for the elevated growth of ephemeral epiphytic macroalgae stimulated by increased temperature under the projected climate change scenario (Lotze et al., 1999; Taylor et al., 2001). Nevertheless, the Baltic Sea is one of the most eutrophicated water basins in the world and the blooms of filamentous algae and the formation of the drifting macroalgal mats have not shown to have a dramatic consequence on the submerged aquatic vegetation including seagrasses (Lauringson and Kotta, 2006; Lyons et al., in press). However, such blooms likely reduce light availability and consequently lead to a reduced depth penetration and abundance of submerged vegetation (Duarte, 1991). The consequences of such interspecific interaction are expected to be much weaker compared to the facilitative effects of seawater warming. The most dramatic macroalgal blooms are developing during the summer months. Since then, however, the submerged aquatic vegetation has gained their maximum size and the algal blooms just reduce the photosynthetic performance of the host plant.

5. Conclusions

Our study did not confirm the hypothesis that large scale abiotic processes define broad patterns of distribution and are the most significant factors in community variability. Instead, small and large-scale environmental variability both interactively contribute to the variability in the cover of submerged aquatic vegetation. Physical disturbance such as seawater warming, elevated wave-induced current velocity and reduced ice scour override the effects of salinity reduction, elevated turbidity and pelagic production.

All predictions of future climate are far from certain and opposite changes in the abiotic environment might also occur under other climate change scenarios. Nevertheless, our modelling study showed that the submerged aquatic vegetation is very resilient to a broad range of environmental perturbation and biomass gains are expected when seawater temperature increases (e.g. Asaeda et al., 2001). This is mainly because vegetation develops faster in spring and has a longer growing season under the projected climate change scenario.

Although it is impossible to halt global warming within the coming years, a modelling of the cover of submerged aquatic species under the future climate is essential in order to help managers to establish marine protected areas that can resist the projected influences of climate change and thereby minimizing the risk of population collapses.

Acknowledgements

The authors acknowledge Dr. Kristjan Herkül for providing technical support at various stages of this study. Funding for this research was provided by Institutional research funding grant IUT02-20 of the Estonian Research Council. The project has received funding from BONUS project BIO-C3, the joint Baltic Sea research and development programme (Art 185), funded jointly from the European Union's Seventh Programme for research, technological development and demonstration and from the Estonian Research Council. The study has been also supported by the projects "The status of marine biodiversity and its potential futures in the Estonian coastal sea" grant no 3.2.0801.11-0029 and "Estkliima" grant no 3.2.0802.11-0043 of Environmental protection and technology program of European Regional Fund.

References

Aiken, S.G., Walz, K.F., 1979. Turions of *Myriophyllum exalbescens*. Aquat. Bot. 6, 357–363.
Appelgren, K., Mattila, J., 2005. Variation in vegetation communities in shallow bays of the northern Baltic Sea. Aquat. Bot. 83, 1–13.
Asaeda, T., Trung, V.K., Manatunge, J., Bon, T.V., 2001. Modelling macrophytes-nutrient-phytoplankton interactions in shallow eutrophic lakes and the evaluation of environmental impacts. Ecol. Eng. 16, 341–357.
BACC, 2008. Assessment of Climate Change for the Baltic Sea Basin. In: Regional Climate Studies, vol. 22. Springer, 474 pp.
Bekkby, T., Rinde, E., Erikstad, L., Bakkestuen, V., Longva, O., Christensen, O., Isaeus, M., Isachsen, P.E., 2008. Spatial probability modeling of eelgrass *Zostera marina* L. distribution on the west coast of Norway. ICES J. Mar. Sci. 65, 1093–1101.
Bendtsen, J., Gustafsson, K.E., Söderkvist, J., Hansen, J.L.S., 2009. Ventilation of bottom water in the North Sea–Baltic Sea transition zone. J. Mar. Syst. 75, 138–149.
Boström, C., Baden, S.P., Krause-Jensen, D., 2003. The seagrasses of Scandinavia and the Baltic Sea. In: Green, P., Short, F.T. (Eds.), The World Atlas of Seagrasses. University of California Press, Berkeley, USA, pp. 27–37.
Bulleri, F., Benedetti-Cecchi, L., Cusson, M., Maggi, E., Arenas, F., Aspden, R., Bertocci, I., Crowe, T.P., Davoult, D., Eriksson, B.K., Fraschetti, S., Golléty, C., Griffin, J.N., Jenkins, S.R., Kotta, J., Kraufvelin, P., Molis, M., Sousa Pinto, I., Terlizzi, A., Valdivia, N., Paterson, D.M., 2012. Temporal stability of European rocky shore assemblages: variation across a latitudinal gradient and the role of habitat-formers. Oikos 121, 1801–1809.
Burkholder, J.M., Tomasko, D.A., Touchette, B.W., 2007. Seagrasses and eutrophication. J. Exp. Mar. Biol. Ecol. 350, 46–72.
Byrne, M., Przeslawski, R., 2013. Multistressor impacts of warming and acidification of the ocean on marine invertebrates' life histories. Integr. Comp. Biol. 53, 582–596.
Chambers, P.A., Prepas, E.E., Hamilton, H.R., Bothwell, M.L., 1991. Current velocity and its effect on aquatic macrophytes in flowing waters. Ecol. Appl. 1, 249–257.
Cohen, Y., Moen, R., Schecterly, M., 1986. Interspecific interactions between *Potamogeton pectinatus* and *Myriophyllum exalbescens* in the face of grazing in a simulated ecosystem. In: Freshwater Wetlands and Wildlife: Perspectives on Natural, Managed and Degraded Ecosystems. Ninth Symposium, 24–27 March 1986. University of Georgia, Savanah River Ecological Laboratory 169.
Costanza, R., d'Arge, R., Groots, R., Farber, S., Grasso, M., Hannon, B., Limburg, K., Naeem, R.V., Paruelo, J., Raskin, R.G., Sutton, P., van den Belt, M., 1997. The value of the worlds ecosystem services and natural capital. Nature 387, 253–260.
Crain, C.M., Kroeker, K., Halpern, B.S., 2008. Interactive and cumulative effects of multiple human stressors in marine systems. Ecol. Lett. 11, 1304–1315.

Dawes, C., Chan, M., Chinn, R., Koch, E.W., Lazar, A., Tomasko, D., 1987. Proximate composition, photosynthetic and respiratory responses of the seagrass *Halophila engelmanni* from Florida. Aquat. Bot. 27, 195–201.
De Boer, W.F., 2007. Seagrass-sediment interactions, positive feedbacks and critical thresholds for occurrence: a review. Hydrobiologia 591, 5–24.
Dolédec, S., Chessel, D., Gimaret-Carpentier, C., 2000. Niche separation in community analysis: a new method. Ecology 81, 2914–2927.
Dray, S., Dufour, A.B., 2007. The ade4 package: implementing the duality diagram for ecologists. J. Stat. Softw. 22, 1–20.
Duarte, C.M., 1991. Seagrass depth limits. Aquat. Bot. 40, 363–377.
Duarte, C.M., 1995. Submerged aquatic vegetation in relation to different nutrient regimes. Ophelia 41, 87–112.
Duarte, C.M., 2002. The future of seagrass meadows. Environ. Conserv. 29, 192–206.
Elith, J., Leathwick, J.R., Hastie, T., 2008. A working guide to boosted regression trees. J. Anim. Ecol. 77, 802–813.
Eriksson, B.K., Sandström, A., Isæus, M., Schreiber, H., Karås, P., 2004. Effects of boating activities on aquatic vegetation in the Stockholm archipelago, Baltic Sea. Estuar. Coast. Shelf Sci. 61, 339–349.
ESRI, 2011. ArcGIS Desktop: Release 10. Environmental Systems Research Institute, Redlands, CA.
Flowers, T.J., Troke, P.F., Yeo, A.R., 1977. The mechanism of salt tolerance in halophytes. Annu. Rev. Plant Physiol. 28, 89–121.
Fonseca, M.S., Bell, S.S., 1998. Influence of physical setting on seagrass landscapes near Beaufort, North Carolina. Mar. Ecol. Prog. Ser. 171, 109–121.
Fonseca, M.S., Kenworthy, W.J., 1987. Effects of current on photosynthesis and distribution of seagrass. Aquat. Bot. 27, 59–78.
Fonseca, M.S., Kenworthy, W.J., Whitfield, P.E., 2000. Temporal dynamics of seagrass landscapes: a preliminary comparison of chronic and extreme disturbance events. In: Pergent, G., Pergent-Martini, C., Buia, M.C., Gambi, M.C. (Eds.), Proceedings of the Fourth International Seagrass Biology Workshop. September 25–October 2, 2000, Corsica, France. Biologia Marina Mediterranea, Instituto di Zoologia, Genova, Italy, pp. 373–376.
Fonseca, M.S., Zieman, J.C., Thayer, G.W., Fisher, J.S., 1983. The role of current velocity in structuring eelgrass *Zostera marina* meadows. Estuar. Coast. Shelf Sci. 17, 367–380.
Gisiger, T., 2001. Scale invariance in biology: coincidence or footprint of a universal mechanism? Biol. Rev. 76, 161–209.
Glemarec, M., LeFaou, Y., Cuq, F., 1997. Long-term changes of seagrass beds in the Glenan Archipelago (South Brittany). Oceanol. Acta 20, 217–227.
Gorham, J., Wyn Jones, R.G., McDonnell, E., 1985. Some mechanisms of salt tolerance in crop plants. Plant Soil. 89, 15–40.
Greenway, H., Munns, R., 1980. Mechanisms of salt tolerance in nonhalophytes. Annu. Rev. Plant Physiol. 31, 149–190.
Gustafsson, C., 2013. Biodiversity and Ecosystem Functioning in Angiosperm Communities in the Baltic Sea (PhD thesis). Åbo Akademi University, Department of Biosciences, Environmental and Marine Biology, Åbo, Finland, 59 pp.
Håkanson, L., Eckhéll, J., 2005. Suspended particulate matter (SPM) in the Baltic Sea – new empirical data and models. Ecol. Model. 189, 130–150.
Halley, J.M., 1996. Ecology, evolution and 1/f-noise. Trends Ecol. Evol. 11, 33–37.
Hällfors, G., Niemi, Å., Ackefors, H., Lassig, J., Leppäkoski, E., 1981. Biological oceanography (chapter 5). In: Voipio, A. (Ed.), The Baltic Sea, Elsevier Oceanography Series, vol. 30, pp. 219–274. Amsterdam, The Netherlands.
Harley, C.D.G., Hughes, A.R., Hultgren, K.M., Miner, B.G., Sorte, C.J., Thornber, C.S., Rodriguez, L.F., Tomanek, L., Williams, S.L., 2006. The impacts of climate change in coastal marine systems. Ecol. Lett. 9, 228–241.
Hastie, T., Tibshirani, R., Friedman, J.H., 2009. The Elements of Statistical Learning: Data Mining, Inference, and Prediction. Springer-Verlag, New York, 744 pp.
Hawkins, S.J., Firth, L.B., McHugh, M., Poloczanska, E.S., Herbert, R.J.H., Burrows, M.T., Kendall, M.A., Moore, P.J., Thompson, R.C., Jenkins, S.R., Sims, D.W., Genner, M.J., Mieszkowska, N., 2013. Data rescue and re-use: recycling old information to address new policy concerns. Mar. Policy 42, 91–98.
Heine, J.N., 1989. Effects of ice scour on the structure of sublittoral marine algal assemblages of St. Lawrence and St. Matthew Islands, Alaska. Mar. Ecol. Prog. Ser. 52, 253–260.
Heino, J., Virkkala, R., Toivonen, H., 2009. Climate change and freshwater biodiversity: detected patterns, future trends and adaptations in northern regions. Biol. Rev. Camb. Philos. Soc. 84, 39–54.
Hemminga, M.A., Duarte, C.M., 2000. Seagrass Ecology. Cambridge University Press, Cambridge, UK; New York, NY, USA, 198.
Hense, I., Meier, H.E.M., Sonntag, S., 2013. Projected climate change impact on Baltic Sea cyanobacteria. Climate change impact on cyanobacteria. Clim. Change 119, 391–406.
Herkül, K., Kotta, J., Kutser, T., Vahtmäe, E., 2013. Relating remotely sensed optical variability to marine benthic biodiversity. PLoS One 8 (2), e55624.
Hoffman, J.R., Hansen, L.J., Klinger, T., 2003. Interactions between UV radiation and temperature limit inferences from single-factor experiments. J. Phycol. 39, 268–272.
Holmer, M., Wirachwong, P., Thomsen, M.S., 2011. Negative effects of stress-resistant drift algae and high temperature on a small ephemeral seagrass species. Mar. Biol. 158, 297–309.
International Panel on Climate Change (IPCC), 2013. Climate Change 2013: the Physical Science Basis. Cambridge University Press, Cambridge, UK.
Kautsky, H., van der Maarel, E., 1990. Multivariate approaches to the variation in phytobenthic communities and environmental vectors in the Baltic Sea. Mar. Ecol. Prog. Ser. 60, 169–184.
Kautsky, L., 1988. Life strategies of aquatic soft bottom macrophytes. Oikos 53, 126–135.
Kendrick, G.A., Hegge, B.J., Wyllie, A., Davidson, A., Lord, D.A., 2000. Changes in seagrass cover on Success and Parmelia Banks, Western Australia between 1965 and 1995. Estuar. Coast. Shelf Sci. 50, 341–353.
Kendrick, G.A., Holmes, K.W., van Niel, K.P., 2008. Multi-scale patterns of three seagrass species with different growth dynamics. Ecography 31, 191–200.
Kerr, E.A., Strother, S., 1985. Effects of irradiance, temperature and salinity on photosynthesis of *Zostera muelleri*. Aquat. Bot. 23, 177–183.
Koch, M., Bowes, G., Ross, C., Zhang, X.-H., 2013. Climate change and ocean acidification effects on seagrasses and marine macroalgae. Glob. Change Biol. 19, 103–132.
Kotta, J., Jaanus, A., Kotta, I., 2008a. Haapsalu and Matsalu Bays. In: Schiewer, U. (Ed.), Ecology of Baltic Coastal Waters, Ecological Studies, vol. 197. Springer, pp. 245–258.
Kotta, J., Kutser, T., Teeveer, K., Vahtmäe, E., Pärnoja, M., 2013. Predicting species cover of marine macrophyte and invertebrate species combining hyperspectral remote sensing, machine learning and regression techniques. PLoS One 8 (6), e63946.
Kotta, J., Lauringson, V., Martin, G., Simm, M., Kotta, I., Herkül, K., Ojaveer, H., 2008b. Gulf of Riga and Pärnu Bay. In: Schiewer, U. (Ed.), Ecology of Baltic Coastal Waters, Ecological Studies, vol. 97. Springer, pp. 217–243.
Krause-Jensen, D., Pedersen, M.F., Jensen, C., 2003. Regulation of eelgrass (*Zostera marina*) cover along depth gradients in Danish coastal waters. Estuaries 26, 866–877.
Krause-Jensen, D., Sagert, S., Schubert, H., Boström, C., 2008. Empirical relationships linking distribution and abundance of marine vegetation to eutrophication. Ecol. Indic. 8, 515–529.
Larkum, A.W.D., Orth, R.J., Duarte, C.M., 2006. Seagrasses: Biology, Ecology, and Conservation. Springer.
Lasker, H.R., Coffroth, M.A., 1999. Responses of clonal reef taxa to environmental change. Am. Zool. 39, 92–103.
Lauringson, V., Kotta, J., 2006. Influence of the thin drift algal mats on the distribution of macrozoobenthos in Kõiguste Bay, NE Baltic Sea. Hydrobiologia 554, 97–105.
Lotze, H.K., Schramm, W., Schories, D., Worm, B., 1999. Control of macroalgal blooms at early developmental stages: *Pilayella littoralis* versus *Enteromorpha* spp. Oecologia 119, 46–54.
Lyons, D.A., Arvanitidis, C., Blight, A.J., Chatzinikolaou, E., Guy-Haim, T., Kotta, J., Orav-Kotta, H., Queirós, A.M., Rilov, G., Somerfield, P.J., Crowe, T.P., 2014. Effects of macroalgal blooms on marine biodiversity and ecosystem functioning: a global meta-analysis. Glob. Change Biol. in press.
Madsen, J.D., Chambers, P.A., James, W.F., Koch, E.W., Westlake, D.F., 2001. The interaction between water movement, sediment dynamics and submersed macrophytes. Hydrobiologia 444, 71–84.
Marsh Jr., J.A., Dennison, W.C., Alberte, R.S., 1986. Effects of temperature on photosynthesis and respiration in eelgrass (*Zostera marina* L.). J. Exp. Mar. Biol. Ecol. 101, 257–267.
Meehan, A.J., West, R.J., 2000. Recovery times for a damaged *Posidonia australis* bed in South Eastern Australia. Aquat. Bot. 67, 161–167.
Menéndez, M., Comin, F.A., 1989. Seasonal patterns of biomass variation of *Ruppia cirrhosa* (Petagna) Grande and *Potamogelon pectinatus* L. in a coastal lagoon. Sci. Mar. 53, 633–638.
Müller, R., Laepple, T., Bartsch, I., Wiencke, C., 2009. Impact of oceanic warming on the distribution of seaweeds in polar and cold-temperate waters. Bot. Mar. 52, 617–638.
Nielsen, S.L., Sand-Jensen, K., Borum, J., Geertz-Hansen, O., 2002. Depth colonization of eelgrass (*Zostera marina*) and macroalgae as determined by water transparency in Danish coastal waters. Estuaries 25, 1025–1032.
Orth, R.J., 1977. Effect of nutrient enrichment on growth of the seagrass *Zostera marina* in the Chesapeake Bay, Virginia, USA. Mar. Biol. 44, 187–194.
Orth, R., Carruthers, T.J.B., Dennison, W.C., Duarte, C.M., Fourqurean, J.W., Heck, J.K.L., Hughes, A.R., Kendrick, G., Kenworthy, W.J., Olyarnik, S., Short, F.T., Waycott, M., Williams, S.L., 2006. A global crisis for seagrass ecosystems. BioScience 56, 987–996.
Peralta, G., Perez-Llorens, J.L., Hernandez, I., Vergara, J.J., 2002. Effects of light availability on growth, architecture and nutrient content of the seagrass *Zostera noltii* Hornem. J. Exp. Mar. Biol. Ecol. 269, 9–26.
Pinnerup, S.P., 1980. Leaf production of Zostera marina L. at different salinities. Ophelia 1, 219–224.
Prasad, S.N., Pal, D., Römkens, M.J.M., 2000. Wave formation on a shallow layer of flowing grains. J. Fluid Mech. 413, 89–110.
Rasheed, A.M., 1999. Recovery of experimentally created gaps within a tropical *Zostera capricorni* (Aschers.) seagrass meadow, Queensland, Australia. J. Exp. Mar. Biol. Ecol. 235, 183–200.
RDC Team, 2013. R: a Language and Environment for Statistical Computing. R Foundation for Statistical Computing, Vienna, Austria. Available. http://www.R-project.org/ (accessed 20.07.13.).
Reusch, T.B.H., Boström, C., Stam, W.T., Olsen, J.L., 1999. An ancient eelgrass clone in the Baltic Sea. Mar. Ecol. Prog. Ser. 183, 301–304.
Reusch, T.B.H., Ehlers, A., Hämmerli, A., Worm, B., 2005. Ecosystem recovery after climatic extremes enhanced by genotypic diversity. Proc. Natl. Acad. Sci. U. S. A. 102, 2826–2831.
Reynaud, S., Leclercq, N., Romaine-Lioud, S., Ferrier-Pagès, C., Jaubert, J., Gattuso, J.-P., 2003. Interacting effects of CO_2 partial pressure and temperature on

photosynthesis and calcification in a scleractinian coral. Glob. Change Biol. 9, 1660–1668.
Riddin, T., Adams, J.B., 2010. The effect of a storm surge event on the macrophytes of a temporarily open/closed estuary, South Africa. Estuar. Coast. Shelf Sci. 89, 119–123.
Robertson, A.I., Mann, K.H., 1984. Disturbance of ice and life-history adaptations of the seagrass *Zostera marina*. Mar. Biol. 80, 131–141.
Rosqvist, K., Mattila, J., Sandstrom, A., Snickars, M., Westerbom, M., 2010. Regime shifts in vegetation composition of Baltic Sea coastal lagoons. Aquat. Bot. 93, 39–46.
Santamaría, L., 2002. Why are most aquatic plants widely distributed? Dispersal, clonal growth and small-scale heterogeneity in a stressful environment. Acta Oecol. 23, 137–154.
Schanz, A., Asmus, H., 2003. Impact of hydrodynamics on development and morphology of intertidal seagrasses in the Wadden Sea. Mar. Ecol. Prog. Ser. 261, 123–134.
Schiel, D.R., 2004. The structure and replenishment of rocky shore intertidal communities and biogeographic comparisons. J. Exp. Mar. Biol. Ecol. 300, 309–342.
Schneider, F.I., Mann, K.H., 1991. Rapid recovery of fauna following simulated ice rafting in a Nova Scotian seagrass bed. Mar. Ecol. Prog. Ser. 78, 57–70.
Short, F.T., 1987. Effects of sediment nutrients on seagrasses: literature review and mesocosm experiment. Aquat. Bot. 27, 41–57.
Short, F., Carruthers, T., Dennison, W., Waycott, M., 2007. Global seagrass distribution and diversity: a bioregional model. J. Exp. Mar. Biol. Ecol. 350, 3–20.
Short, F.T., Neckles, A.H., 1999. The effects of global climate change on seagrasses. Aquat. Bot. 63, 169–196.
Short, F.T., Polidoro, B., Livingstone, S.R., Carpenter, K.E., Bandeira, S., Bujang, J.S., Calumpong, H.P., Carruthers, T.J.B., Coles, R.G., Dennison, W.C., Erftemeijer, P.L.A., Fortes, M.D., Freemen, A.S., Jagtap, T.G., Kamal, A.H.M., Kendrick, G.A., Kenworthy, W.J., Nafie, Y.A.L., Nasution, I.M., Orth, R.J., Prathep, A., Sanciangco, J.C., van Tussenbroek, B., Vegara, S.G., Waycott, M., Zieman, J.C., 2011. Extinction risk assessment of the world's seagrass species. Biol. Conserv. 144, 1961–1971.
Snoeijs, P., 1999. Marine and brackish waters. In: Snoeijs, P., Diekmann, M. (Eds.), Swedish Plant Geography, Acta Phytogeographica Suecica 84. Opulus Press, Uppsala, pp. 187–212.
Steele, J.H., Henderson, E.W., 1994. Coupling between physical and biological scales. Philos. Trans. R. Soc. Lond. B 343, 5–9.
Steinhardt, T., Selig, U., 2007. Spatial distribution patterns and relationship between recent vegetation and diaspore bank of a brackish coastal lagoon on the southern Baltic Sea. Estuar. Coast. Shelf Sci. 74, 205–214.
Stevenson, J.C., 1988. Comparative ecology of submersed grass beds in freshwater, estuarine, and marine environments. Limnol. Oceanogr. 33, 867–893.
Stramska, M., Świrgoń, M., 2014. Influence of atmospheric forcing and freshwater discharge on interannual variability of the vertical diffuse attenuation coefficient at 490 nm in the Baltic Sea. Rem. Sens. Environ. 140, 155–164.
Taylor, R., Fletcher, R.L., Raven, J.A., 2001. Preliminary studies on the growth of selected 'Green Tide' algae in Laboratory Culture: effects of irradiance, temperature, salinity and nutrients on growth rate. Bot. Mar. 44, 327–336.
Touchette, B.W., 2007. Seagrass-salinity interactions: physiological mechanisms used by submersed marine angiosperms for a life at sea. J. Exp. Mar. Biol. Ecol. 350, 194–215.
Turner, S.J., Hewitt, J.E., Wilkinson, M.R., Morrisey, D.J., Thrush, S.F., Cummings, V.J., Funnell, G., 1999. Seagrass patches and landscapes: the influence of wind-wave dynamics and hierarchical arrangements of spatial structure on macrofaunal seagrass communities. Estuaries 22, 1016–1032.
van den Berg, M., Coops, H., Simons, J., de Keizer, A., 1998. Competition between *Chara aspera* and *Potamogeton pectinatus* as a function of temperature and light. Aquat. Bot. 60, 241–250.
van der Heide, T., van Nes, E.H., van Katwijk, M.M., Olff, H., Smolders, A.J.P., 2011. Positive feedbacks in seagrass ecosystems – evidence from large-scale empirical data. PLoS One 6, e16504.
van Katwijk, M.M., Hermus, D.C.R., 2000. Effects of water dynamics on *Zostera marina*: transplantation experiments in the intertidal Dutch Wadden Sea. Mar. Ecol. Prog. Ser. 208, 107–118.
Viaroli, P., Bartoli, M., Fumagalli, I., Giordani, G., 1997. Relationship between benthic fluxes and macrophyte cover in a shallow brackish lagoon. Water Air Soil Pollut. 99, 533–540.
Waycott, M., Duarte, C.M., Carruthers, T.J.B., Orth, R.J., Dennison, W.C., Olyarnik, S., Calladine, A., Fourqurean, J.W., Heck, J.K.L., Hughes, A.R., Kendrick, G.A., Kenworthy, W.J., Short, F.T., Williams, S.L., 2009. Accelerating loss of seagrasses across the globe threatens coastal ecosystems. Proc. Natl. Acad. Sci. U. S. A. 106, 12377–12381.
Waycott, M., Procaccini, G., Les, D.H., Reusch, T.B.H., 2006. Seagrass evolution, ecology, and conservation: a genetic perspective. In: Larkum, A.W.D., Orth, R.J., Duarte, C. (Eds.), Seagrasses: Biology, Ecology, and Conservation. Springer, The Netherlands, pp. 25–50.
Witman, J.D., Etter, R.J., Smith, F., 2004. The relationship between regional and local species diversity in marine benthic communities: a global perspective. Proc. Natl. Acad. Sci. U. S. A. 101, 15664–15669.
Wood, S.N., 2006. Generalized Additive Models: an Introduction with R. Chapman and Hall/CRC.
Worcester, S.E., 1995. Effects of eelgrass beds on advection and turbulent mixing in low current and low shoot density environments. Mar. Ecol. Prog. Ser. 126, 223–232.
Wortmann, J., Hearne, J.W., Adams, J.B., 1997. A mathematical model of an estuarine seagrass. Ecol. Model. 98, 137–149.
Xiao, C., Wang, X., Xia, J., Liu, G., 2010. The effect of temperature, water level and burial depth on seed germination of *Myriophyllum spicatum* and *Potamogeton malaianus*. Aquat. Bot. 92, 28–32.
Zajac, R.N., Lewis, R.S., Poppe, L.J., Twichell, D.C., Vozarik, J., DiGiacomo-Cohen, M.L., 2003. Responses of infaunal populations to benthoscape structure and the potential importance of transition zones. Limnol. Oceanogr. 48, 829–842.
Zimmerman, R.C., Smith, R.D., Alberte, R.S., 1989. Thermal acclimation and whole-plant carbon balance in *Zostera marina* L. (eelgrass). J. Exp. Mar. Biol. Ecol. 130, 93–109.

Mapping benthic biodiversity using georeferenced environmental data 1 **and predictive modeling**

Anneliis Peterson* and Kristjan Herkül

Embargoed until publication, for information please contact Anneliis Peterson, email: anneliis.peterson@ut.ee

frontiers in Marine Science

ORIGINAL RESEARCH
published: 08 February 2017
doi: 10.3389/fmars.2017.00027

Influence of Natural Oxygenation of Baltic Proper Deep Water on Benthic Recycling and Removal of Phosphorus, Nitrogen, Silicon and Carbon

Per O. J. Hall[1], Elin Almroth Rosell[2], Stefano Bonaglia[3†], Andrew W. Dale[4], Astrid Hylén[1], Mikhail Kononets[1], Madeleine Nilsson[1], Stefan Sommer[4], Sebastiaan van de Velde[5] and Lena Viktorsson[2]*

[1] Department of Marine Sciences, University of Gothenburg, Gothenburg, Sweden, [2] Swedish Meteorological and Hydrological Institute, Oceanographic Research, Västra Frölunda, Sweden, [3] Department of Geology, Lund University, Lund, Sweden, [4] GEOMAR Helmholtz-Zentrum für Ozeanforschung Kiel, Kiel, Germany, [5] Department of Analytical, Environmental and Geo-Chemistry, Vrije Universiteit Brussel, Brussels, Belgium

OPEN ACCESS

Edited by:
Osvaldo Ulloa, University of Concepción, Chile

Reviewed by:
Jake Bailey, University of Minnesota, USA
William Berelson, University of Southern California, USA

***Correspondence:**
Per O. J. Hall
per.hall@marine.gu.se

†Present Address:
Stefano Bonaglia, Department of Ecology, Environment and Plant Sciences, Stockholm University, Stockholm, Sweden

Specialty section:
This article was submitted to Marine Biogeochemistry, a section of the journal Frontiers in Marine Science

Received: *31 October 2016*
Accepted: *24 January 2017*
Published: *08 February 2017*

Citation:
Hall POJ, Almroth Rosell E, Bonaglia S, Dale AW, Hylén A, Kononets M, Nilsson M, Sommer S, van de Velde S and Viktorsson L (2017) Influence of Natural Oxygenation of Baltic Proper Deep Water on Benthic Recycling and Removal of Phosphorus, Nitrogen, Silicon and Carbon. Front. Mar. Sci. 4:27. doi: 10.3389/fmars.2017.00027

At the end of 2014, a Major Baltic Inflow (MBI) brought oxygenated, salty water into the Baltic proper and reached the long-term anoxic Eastern Gotland Basin (EGB) by March 2015. In July 2015, we measured benthic fluxes of phosphorus (P), nitrogen (N) and silicon (Si) nutrients and dissolved inorganic carbon (DIC) *in situ* using an autonomous benthic lander at deep sites (170–210 m) in the EGB, where the bottom water oxygen concentration was 30–45 μM. The same *in situ* methodology was used to measure benthic fluxes at the same sites in 2008–2010, but then under anoxic conditions. The high efflux of phosphate under anoxic conditions became lower upon oxygenation, and turned into an influx in about 50% of the flux measurements. The C:P and N:P ratios of the benthic solute flux changed from clearly below the Redfield ratio (on average about 70 and 3–4, respectively) under anoxia to approaching or being well above the Redfield ratio upon oxygenation. These observations demonstrate retention of P in newly oxygenated sediments. We found no significant effect of oxygenation on the benthic ammonium, silicate and DIC flux. We also measured benthic denitrification, anammox, and dissimilatory nitrate reduction to ammonium (DNRA) rates at the same sites using isotope-pairing techniques. The bottom water of the long-term anoxic EGB contained less than 0.5 μM nitrate in 2008–2010, but the oxygenation event created bottom water nitrate concentrations of about 10 μM in July 2015 and the benthic flux of nitrate was consistently directed into the sediment. Nitrate reduction to both dinitrogen gas (denitrification) and ammonium (DNRA) was initiated in the newly oxygenated sediments, while anammox activity was negligible. We estimated the influence of this oxygenation event on the magnitudes of the integrated benthic P flux (the internal P load) and the fixed N removal through benthic and pelagic denitrification by comparing with a hypothetical

scenario without the MBI. Our calculations suggest that the oxygenation triggered by the MBI in July 2015, extrapolated to the basin-wide scale of the Baltic proper, decreased the internal P load by 23% and increased the total (benthic plus pelagic) denitrification by 18%.

Keywords: major baltic inflow, benthic nutrient and DIC fluxes, internal P load, denitrification, DNRA

INTRODUCTION

Biogeochemical and early diagenetic processes (recently reviewed by Aller, 2014) make sediments act as both sources and sinks for N, P, Si, and C. Sediments supply dissolved inorganic N (DIN; in the form of ammonium and often nitrate), P (phosphate), Si (silicate), and C (DIC) to overlying waters, and act in this way as a source to the water column of these dissolved inorganic forms of the elements. Mineralization of organic matter containing N, P, and C, and dissolution of biogenic Si, in sediment produces nutrients and DIC, which are dissolved in the sediment pore water and then released to the water column as a benthic flux. Degradation of organic matter in sediments also produces dissolved organic N (DON), P (DOP), and C (DOC), which may be released to the water column and contribute to the benthic flux (Ståhl et al., 2004; Ekeroth et al., 2012, 2016a,b). A fraction (in some sediments significant) of the particulate organic matter containing N, P, and C, and of biogenic Si, which is deposited from overlying waters on the sea-floor, is not mineralized and recycled, but will undergo burial in the sediment (reviewed by Burdige, 2007). The elements are hereby removed from the oceanic-atmospheric biogeochemical cycles for very long time-scales. The sediment in this way acts as a sink for the elements. Another sink for fixed N in sediments is the transformation of bioavailable dissolved inorganic N to dinitrogen gas, N_2, via denitrification and anammox (e.g., Thamdrup and Dalsgaard, 2002; Dalsgaard et al., 2005).

The Baltic Sea is the second largest brackish water basin in the world after the Black Sea. There is a strong stratification of the water column with a permanent halocline at around 60–80 m depth. Since the residence time of the water in the Baltic is as long as 25–35 years, and the average depth is not more than about 60 m, sediments here play an essential role in the biogeochemical cycles of nutrient elements and carbon. The semi-permanent anoxic conditions in the Baltic are due to the limited water exchange with the Kattegat and the strong vertical stratification (e.g., Kullenberg and Jacobsen, 1981; Stigebrandt, 2001). These physical characteristics in combination with an increased nutrient supply have led to an increased frequency of cyanobacteria blooms in the Baltic proper since the 1960s (e.g. Finni et al., 2001; Wasmund et al., 2001). The frequent, sometimes toxic, cyanobacteria blooms and high P concentrations in the basin water have been explained by a positive feedback between increased bottom hypoxia and release of P from iron oxyhydroxides (e.g., Conley et al., 2002; Gustafsson and Stigebrandt, 2007; Vahtera et al., 2007). Roughly 0.5 million tons N is imported to the Baltic Sea annually through N_2 fixation by pelagic cyanobacteria (Vahtera et al., 2007; Nausch et al., 2012, and references therein). Nitrogen-fixing cyanobacteria are limited by P, and the blooms are triggered by low N:P ratios in the nutrient pool (e.g., Nausch et al., 2012). The low N:P ratios are caused by removal of fixed nitrogen (denitrification and anammox) at both the oxycline/nitracline in water column (Dalsgaard et al., 2013) and in sediments underlying oxygenated or at least nitrate containing bottom water (Tuominen et al., 1998; Deutsch et al., 2010) together with enhanced benthic P regeneration due to oxygen depletion in deep waters (Jilbert et al., 2011; Viktorsson et al., 2013a). The change in the bottom area covered by hypoxic water in the Baltic Sea, but not the external P load, has been found to correlate well with variations in the dissolved water column P pool size (Conley et al., 2002; Stigebrandt et al., 2014). This correlation indirectly indicates the importance of oxygen in regulating the capacity of sediments to release/retain P in the Baltic Sea. In addition, it was recently shown that the rate of sedimentary deposition and degradation of organic matter controls the benthic P flux under long term anoxic conditions in Baltic Sea basins and in west-Swedish fjords (Viktorsson et al., 2012, 2013a,b). Furthermore, the benthic solute flux under anoxic conditions in these basins was found to be very P rich in relation to both C and N. Hence, oxygen does not only control the magnitude of the dissolved bioavailable N, P (e.g., Bonaglia et al., 2013) and sometimes even Si flux (Ekeroth et al., 2016a), but may also have a strong influence on the N:P, C:P, and Si:P ratios in benthic fluxes, and thus indirectly on abundance and composition of phytoplankton and cyanobacteria communities in surface waters.

An intrusion of oxygenated salty water into the Baltic proper started at the end of 2014. This is the largest Major Baltic Inflow (MBI) since 1951, and the third largest since oceanographic measurements in the Baltic Sea began in 1880 (Mohrholz et al., 2015). MBIs are episodic and unpredictable, and on short time-scales the most effective way to ventilate and oxygenate the deep water of the Baltic proper. A majority of these inflows can be explained from variations in the atmospheric sea-level pressure fields, and the stagnation periods in the deep water are caused by the lack of atmospheric forcing (Schimanke et al., 2012). Causes and effects of MBIs were reviewed by Matthäus et al. (2008) and Reissmann et al. (2009) reviewed the physical dynamics and mixing processes of the inflowing waters.

We made repeated *in situ* measurements of benthic nutrient and DIC fluxes in the EGB during 2008–2010. In this time period the water column below about 100 m depth was anoxic, and these measurements comprised stations with fully anoxic bottom water conditions. The MBI of oxygenated salty water, which started at the end of 2014, reached the EGB in March 2015 (IOW Baltic Sea Research Institute Warnemünde, 2015). Nature thus gave us a unique opportunity to repeat the same type of measurements we previously did at fully anoxic stations,

but under oxygenated conditions generated by the recent MBI. This paper presents novel results on the effect of this natural oxygenation of previously long-term anoxic Baltic bottoms on rates and extent of recycling and removal of nutrient elements and carbon in sediments including denitrification, anammox and DNRA.

MATERIALS AND METHODS

Study Area

The Eastern Gotland Basin (EGB) is among the most well studied basins of the Baltic proper. The EGB comprises the water body between the island of Gotland (Sweden) and Latvia. The maximum depth is about 250 m.

We visited two stations in the EGB during an expedition with R/V "Skagerak" in early July 2015; station E and F at depths of about 170 and 210 m, respectively. We made two autonomous benthic lander (see below) deployments and collected sediment with a box-corer at each station. The study area and locations of the stations are shown in **Figure 1**, and exact dates of visits, coordinates and bottom water characteristics for the two lander deployments at each station are given in **Table 1**.

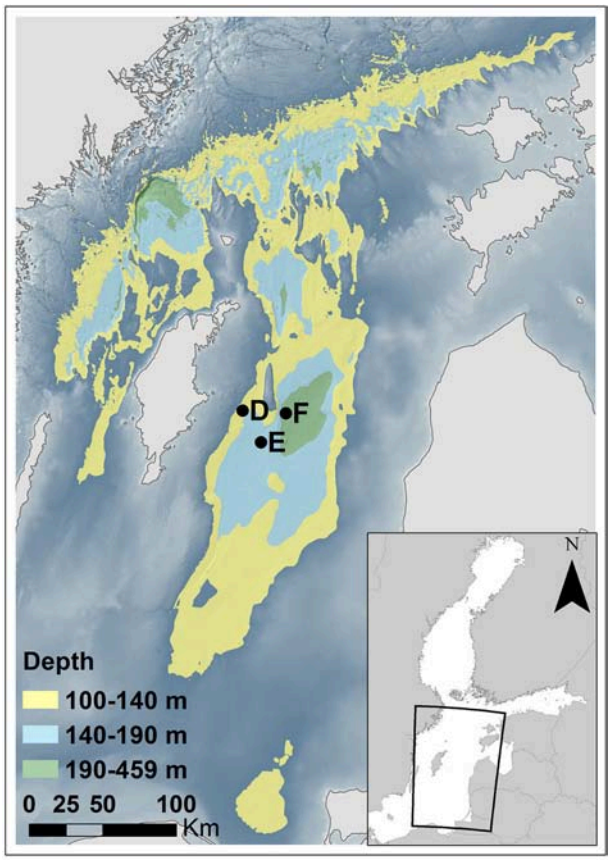

FIGURE 1 | Map of the northern and central Baltic proper. Stations E and F were visited in July 2015 (this study); at this time the water at these sites was oxygenated below 140 m depth due to the MBI. The coordinates and water depths of these stations are presented in **Table 1**. Stations D, E, and F were visited by Viktorsson et al. (2013a) in 2008 and 2010 under anoxic bottom water conditions. Bottom areas at water depths of 100–140, 140–190, and 190–459 m are indicated in yellow, light blue, and green color, respectively. The background color indicates bottom areas at water depths shallower than 100 m. Depth data from the Baltic Sea Hydrographic Commission (2013), Baltic Sea Bathymetry Database verstion 0.9.3, downloaded from http://data.bshc.pro/ on 2016-09-22. The figure was created using the software ArcGIS 10.3.1 for Desktop [Environmental Systems Research Institute (ESRI, 2015), Redlands, CA].

Benthic *In Situ* Flux Measurements

Benthic fluxes of nutrients, DIC and oxygen were measured *in situ* using chambers of the autonomous big Gothenburg benthic lander (e.g., Brunnegård et al., 2004; Almroth et al., 2009; Viktorsson et al., 2013a). This lander carries four square (20 × 20 cm) benthic chambers with rounded corners. Prior to the chamber incubations, and just after the lander had reached the seafloor, the chambers were ventilated in the bottom water just above seafloor for about 2 h with stirring on, and for 2–4 additional hours inserted into sediment with lid open and stirring on. This procedure was undertaken to allow oxygen dissolved in the material of the chamber (polycarbonate) to diffuse out into the low oxygen bottom water, and to ascertain that the chambers were completely filled with ambient bottom water. Sediment and overlying water were then incubated in the four chambers (with lids closed) for about 20 h during which nine samples were taken autonomously with syringes from each chamber. The lander was then recovered and water samples were collected from the syringes. Nutrient and DIC samples were filtered through pre-cleaned 0.45 μm pore size cellulose acetate filters on-board immediately after sampling. The nutrient samples were then stored at 4 to 6°C until analysis on land immediately after the expedition. Nutrients were determined with a standard colorimetric method (modified after Koroleff, 1983) applied in segmented-flow analysis (SFA). The measurement uncertainty was 0.5 μg L^{-1} for ammonium, 0.3 μg L^{-1} for nitrate + nitrite, 0.2 μg L^{-1} for nitrite, 0.5 μg L^{-1} for phosphate and 2.5% for silicate for the actual concentration ranges obtained.

Determination of DIC in chamber samples was performed on-board ship immediately after lander recovery using an automated system based on non-dispersive infrared detection of CO_2 (Goyet and Snover, 1993; O'Sullivan and Millero, 1998). Prior to detection, all of the dissolved carbonate species in the samples were driven to CO_2 gas by acidification with phosphoric acid followed by nitrogen gas stripping. Running replicate measurements ($n = 10$) of certified reference material (CRM, Dickson Laboratories, Scripps Inst. of Oceanography, California), using a sample loop of 4 ml, an analytical precision of 0.2% RSD (SD × 100/mean) was obtained. The instrument was furthermore calibrated and corrected for drift with this CRM.

Salinity, temperature, and oxygen sensors that continuously measured ambient conditions in the bottom water during the deployments were mounted on the lander. Each chamber was also equipped with oxygen (optodes), salinity and temperature sensors for calculation of chamber volume (salinity), detection of possible leakage (salinity and oxygen) and measurement of total

TABLE 1 | Dates, coordinates, water depths and bottom water (BW) characteristics (average and STD for temperature, salinity and oxygen concentration measured 0.5 m above the seafloor *in situ* by sensors on the benthic lander) for the two lander deployments (I and II) at each of stations E and F.

Station	Date 2015	Lat	Long	Depth (m)	BW Temp (°C)	BW Sal	BW O_2 (μM)
E I	July 2–3	57° 07.476′	19° 30.467'	171	6.74 ± 0.05	12.9 ± 0.1	30 ± 10
E II	July 5–6	57° 07.491′	19° 30.479'	171	6.74 ± 0.05	12.9 ± 0.1	30 ± 10
F I	July 1–2	57° 17.230′	19° 48.020'	210	6.80 ± 0.05	13.4 ± 0.1	45 ± 5
F II	July 3–4	57° 17.256′	19° 48.058'	210	6.80 ± 0.05	13.4 ± 0.1	45 ± 5

oxygen uptake rates. Chamber volume, a necessary parameter when calculating the benthic flux, was calculated by injection of a known volume of MQ water (around 56 to 59 mL, which normally is 0.5 to 1% of the chamber volume), and the chamber volume was then calculated from the measured salinity decrease and the MQ volume injected. Using data from sensors inside and outside chambers, occasional leakage of chambers could easily be detected. Flux data from leaking chambers were discarded. A more detailed description of the landers is given in e.g., Ståhl et al. (2004), and of the chambers and their hydrodynamics in e.g., Tengberg et al. (2004).

Benthic fluxes for each solute were calculated from the concentration change per unit of area and time in every chamber. First, the measured concentrations were corrected for the small dilution that occurred every time ambient bottom water, through a metal loop, entered the chamber when a sample was taken. A linear least squares regression (LLSR) was subsequently used to find the slope of the concentrations in the syringe samples vs. time. The model was applied using the function "lm" (CRAN:stats) in the open-source software R (https://www.r-project.org/), which implements the equations from Chambers (1992) and Wilkinson and Rogers (1973). Benthic fluxes were ultimately calculated by multiplying the slope value of the regression with the chamber height, which was obtained from chamber volume (see above) and the known sediment surface area incubated by the chambers (400 cm^2).

Prior to the LLSR, two different types of outliers were identified. The first type is based on the studentized deleted residual index (SDRI), which indicates if a data point is unusual for the fitted model. Since the increase or decrease of nutrient and DIC concentration over time in a benthic chamber is expected to be linear, observations with SDRIs higher than 2 were assumed to be outliers. The second type is called a leverage point and is based on the Cook's distance, which is a statistical value that indicates whether one observation strongly influences the estimated model parameters (i.e., slope and intercept). A Cook's distance value higher than 1 was assumed to be a leverage point. Both these outliers were identified using the functions "rstudent" and "cooks.distance" (CRAN:stats) from Fox and Weisberg (2011), based on well accepted outlier diagnostics described by e.g., Belsley et al. (1980), Cook and Weisberg (1982), and Williams (1987). If a point was identified as an outlier by either method, it was excluded from the calculations. We identified, at each station, 0–2 outliers for each solute in each chamber, i.e., 7–9 data points were used to determine each flux of each solute.

Fluxes were considered to be significant when the *p*-value of the LLSR was lower than 0.05. When the concentration change in a chamber was small and the regression slope was close to zero, minor scatter around the slope line could cause the *p*-value to rise above 0.05. In these cases, two more conditions were used in order to avoid systematically discarding low fluxes, following Ekeroth et al. (2016b) with minor modifications. First, the regression slope was multiplied with the total incubation time to calculate the expected concentration change. If this expected change was smaller than the analytical uncertainty, it was assumed that the incubation time had been too short to produce a change that was large enough to capture analytically. The second condition was the goodness-of-fit. In order to select only the high quality fits, fluxes with an R^2 value smaller than 0.3 were discarded, while fluxes with a higher R^2 value were retained. Since the identified low fluxes were not statistically different from 0, they were retained in the data set as zero fluxes.

Benthic solute fluxes from the anoxic (2008 and 2010; Viktorsson et al., 2013a; Nilsson et al., in prep; Hall et al., unpublished results) and newly oxygenated (2015; this study) bottoms were compared using *t*-tests. This was followed by a *post-hoc* power analysis performed with the software G*Power 3.1 (Faul et al., 2007).

Sediment Core Incubations Using ^{15}N

In order to determine rates of denitrification and DNRA a set of sediment cores was incubated after addition of $^{15}NO_3^-$ to the overlying water (De Brabandere et al., 2015). Briefly, plastic liners ($n = 15$, 3.6 cm inner diameter, 25 cm length) were used to subsample a sediment box-core, and half sediment and half water were collected. The sediment cores were transferred into a 25 L incubation tank that had been filled with ambient bottom water, situated in a temperature-controlled room kept at bottom water temperature. The oxygen concentration in the tank was adjusted to the bottom water oxygen concentration by bubbling with the appropriate mixture of N_2 and air. Subsequently, 7 mL of a 200 mM $^{15}NO_3^-$ solution - prepared by dissolving $Na^{15}NO_3$ (99.4 atom%, Sigma-Aldrich) in distilled water—was added to the water tank in order to reach a $^{15}NO_3^-$ concentration of ∼70 μM. The incubation started after a lag time of ∼2 h, which was necessary to homogeneously mix the added nitrate with the endogenous nitrate and to establish a linear production of $^{15}N_2$ within the sediment. At the beginning of the incubation the cores were capped with rubber stoppers, and the water phase was stirred by externally driven magnetic bars. The O_2 concentration was constantly monitored in one of the cores to make sure it did

not decrease below 30–35% of the initial value. Triplicate cores were sampled directly after the addition of the $^{15}NO_3^-$ and at regular intervals (∼3 h) during the incubation, which lasted 12 h. The incubation was terminated by mixing the water phase with the sediment. Slurry samples ($^{15}N_2$ analysis) were collected in 12 mL Exetainers to which 200 μL of a 37% formaldehyde solution was added. An additional sample of the slurry ($^{15}NH_4^+$ analysis) was taken from each core, the pore water extracted with a Rhizon sampler (Rhizon SMS, Rhizosphere), transferred into a plastic vial and immediately frozen.

Anoxic Slurry Incubations Using ^{15}N

Anoxic slurry incubations amended with $^{15}NO_3^-$ and $^{15}NH_4^+$ were performed in order to estimate the anammox contribution to total N_2 production (Thamdrup and Dalsgaard, 2002; Risgaard-Petersen et al., 2003). Our experiments followed the procedure described in Bonaglia et al. (2014). Briefly, the top 2 cm of two sediment cores (9 cm inner diameter) were extruded, homogenized and 100 ml of this sediment was transferred to a glass bottle filled with 900 mL filtered and anoxic bottom water. All operations were carried out in a temperature-controlled room kept at bottom water temperature. The bottle with the sediment slurry was purged with N_2 for 10 min to remove any oxygen entering during previous operations, and it was dispensed through a Viton™ tubing into a series of 12 mL Exetainers, each containing a 4 mm glass bead. Vigorous shaking of the bottle while filling the Exetainers maintained the slurry homogenous throughout dispensation. The Exetainers ($n = 35$) were filled to the top and capped right after avoiding bubbles. The samples were pre-incubated for ∼10 h on a rotating stirrer to remove any residual oxygen and nitrate. After that 15 Exetainers received 150 μL of an anoxic 9 mM $^{15}NO_3^-$ solution (final $^{15}NO_3^-$ concentration 113 μM); 15 Exetainers received 150 μL of an anoxic 9 mM $^{15}NH_4^+ + {}^{14}NO_3^-$ solution (final $^{15}NH_4^+$ and $^{14}NO_3^-$ concentrations 113 μM); and 5 Exetainers were left unamended and served as control. Triplicate vials from each treatment plus one control ($n = 7$) were sampled right after the addition by injecting 200 μL of a 37% formaldehyde solution into the Exetainers. The rest of the Exetainers ($n = 28$) were incubated on the rotating stirrer for 8 h. Triplicate vials plus one control were sampled at regular intervals of ∼2 h.

An illustration of the various steps in the sediment core and anoxic slurry incubations using ^{15}N is given in **Figure 2**.

^{15}N Incubations: Laboratory Analysis and Calculations

The isotopic composition of the N_2 samples from the denitrification and anammox experiments were determined by headspace analysis using gas chromatography-isotope ratio mass spectrometry (GC-IRMS, DeltaV plus, Thermo). Slopes of the linear regression of $^{29}N_2$ and $^{30}N_2$ concentration against time were used to calculate production rates of labeled N_2 ($p^{29}N_2$ and $p^{30}N_2$, respectively). Rates of N_2 production (=denitrification) were calculated based on Nielsen (1992) canonical isotope pairing technique (IPT) as the contribution of anammox to the N_2 production was found to be negligible. Denitrification rate was split into: (1) denitrification fuelled by water column nitrate (D_w), and (2) denitrification coupled to nitrification (D_n), using the equations described in Nielsen (1992).

Concentrations of labeled ammonium ($^{15}NH_4^+$) were quantified after oxidation of NH_4^+ to N_2 with alkaline hypobromite (Warembourg, 1993). Samples were analyzed by headspace technique at the GC-IRMS as for labeled N_2 analysis as described above. Slopes of the linear regression of $^{15}NH_4^+$ concentration against time were used to calculate production rates of labeled ammonium ($p^{15}NH_4^+$). DNRA rates were calculated according to Christensen et al. (2000). Since part of the $^{15}NH_4^+$ produced during incubation is adsorbed by sediment particles (Laima, 1994), the measured DNRA rate was further multiplied by a factor two (De Brabandere et al., 2015).

RESULTS

Water Column Oxygen Conditions

Several casts with a CTD, on which a Seabird 43 oxygen sensor was mounted, were made at each station. The obtained vertical profiles of oxygen distributions in the water column are displayed in **Figure 3**. It is obvious from these profiles that the water column below a depth of about 140 m was oxygenated in early July 2015. In 2008 and 2010, the water column was anoxic below about 100 m depth (Viktorsson et al., 2013a). The bottom water oxygen concentration, measured *in situ* with O_2 optodes mounted on the benthic lander in 2015, was 30 ± 10 μM at station E and 45 ± 5 μM at station F. Since the lander mounted sensors measured oxygen in the bottom water closer to the seafloor than the sensors on the CTD, the former recorded somewhat lower concentrations than the latter (**Table 1**, **Figure 3**).

Benthic Fluxes in the Newly Oxygenated Deep EGB

Examples of the evolution of nutrient concentrations during the *in situ* chamber incubations are shown in **Figure 4**. The evolution of each solute concentration during all chamber incubations at both stations is displayed in Supplementary Material (SM). The benthic fluxes of nutrients, DIC and oxygen, measured *in situ* with the benthic lander in July 2015, are presented in **Table 2**. Ammonium fluxes were consistently directed out of the sediment, whereas nitrate fluxes consistently were directed into the sediment. The flux of DIN (the sum of ammonium, nitrite and nitrate) was dominated by ammonium, whereas nitrite made the smallest contribution to the DIN flux. The average flux of each inorganic N component was higher at the deeper station F than at station E. The average oxygen uptake and DIC flux showed the same pattern with higher fluxes at station F than at station E (**Table 2**). The bottom water oxygen concentration was also higher at station F than E as mentioned above. The average phosphate (or DIP) flux was similar at the two stations (0.11 and 0.12 mmol m^{-2} d^{-1} at station E and F, respectively). The average silicate efflux was 5.5 and 6.2 mmol m^{-2} d^{-1} at station E and F, respectively. The results from the *t*-test are shown in **Table 3**. Since the bottom water was anoxic in 2008 and 2010, oxygen uptake rates could only be measured in 2015. The only flux that showed a statistically significant ($p < 0.05$) difference was the DIP

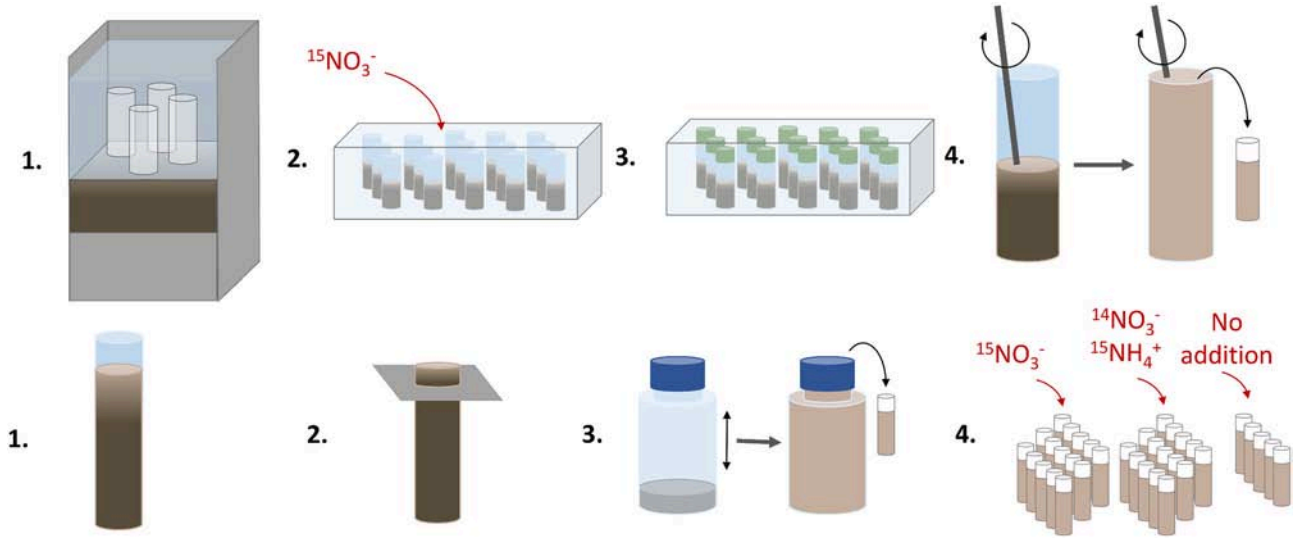

FIGURE 2 | An illustration of the various handling steps in the sediment core (upper panel) and anoxic slurry (lower panel) incubations using ^{15}N. The sediment core incubations were run to determine denitrification and DNRA rates, and the anoxic slurry incubations to estimate the anammox contribution to total N_2 production.

flux at station F, which was significantly lower in 2015 than in 2008–2010.

Denitrification and DNRA Rates in Newly Oxygenated EGB Sediments

Rates of nitrate reduction (= denitrification + DNRA since the contribution of anammox was found to be negligible) were detectable at both station E and F and were 0.32 mmol N m^{-2} d^{-1} and 0.58 mmol N m^{-2} d^{-1}, respectively (**Table 4**; **Figure 5**). The nitrate reduction rate, as well as the DNRA rate, was significantly higher at the deep station F than at the shallower station E (ANOVA, $p < 0.01$). On the other hand, denitrification rate was significantly higher at E than at F. DNRA rates were significantly higher than denitrification rates (ANOVA, $p < 0.001$) only at station F (**Figure 5**).

At the two investigated stations, significant differences (ANOVA, $p < 0.001$) in rates of coupled nitrification–denitrification (D_n) explained the conspicuous variation in total denitrification rates (**Table 4**). In other words, excluding the contribution of nitrification, rates of denitrification would be comparable at the two oxygenated sites. As a result of this, denitrification fuelled by nitrate diffusing from the overlying water (D_w) contributed very differently to total denitrification at the two stations (86% at F vs. 24% at E; **Table 4**).

DISCUSSION

Effect of Natural Oxygenation of Long-term Anoxic Baltic Bottoms on Benthic Solute Fluxes

The influence of oxygenation of long-term anoxic benthic systems on biogeochemical processes in sediments and solute exchange at the sediment-water interface is a function of duration of oxygenation and the actual bottom water oxygen concentration level (e.g., De Brabandere et al., 2015; Ekeroth et al., 2016a). The present study investigated the situation in the EGB in early July 2015, i.e., when the EGB had been oxygenated for 3–4 months by the 2014–2015 MBI. The observed bottom water oxygen concentration level (**Figure 3**, **Table 1**) is consistent with other observations in the EGB at about the same time (e.g., Sommer et al., 2017). Strong evidence of oxidized conditions in surficial sediments in the deep EGB in early July 2015 was obtained by sediment profile imagery (SPI) and reported by Rosenberg et al. (2016). These authors found the sediment surface at water depths below 140 m close to stations E and F to be orange colored, and suggested that this was due to newly formed iron and manganese oxides.

The *post-hoc* power analysis showed that the statistical power of the *t*-tests was generally low, meaning that the risk of making a type II error and failing to detect an actual difference was relatively large. Most of the measured fluxes varied considerably on each station each year (**Figure 6**), suggesting spatial heterogeneity of the seafloor. One clear example of this is the DIP fluxes at station E in 2015, which at one lander deployment were directed out of the sediment in two of the chambers and into the sediment in the other two (**Figure 4**). A plausible explanation for this observation is that the oxygen containing bottom water had oxygenated the sediment to a different extent even on the local scale in July 2015, e.g., due to a heterogeneous distribution of reactive organic matter in the sediment. Given the relatively low number of flux measurements in combination with the high natural variability, it is unlikely that we would have been able to find actual differences in fluxes, as indicated by the low power. For the significant difference in the DIP flux at station F, power was high (>0.80; **Table 3**). The risk

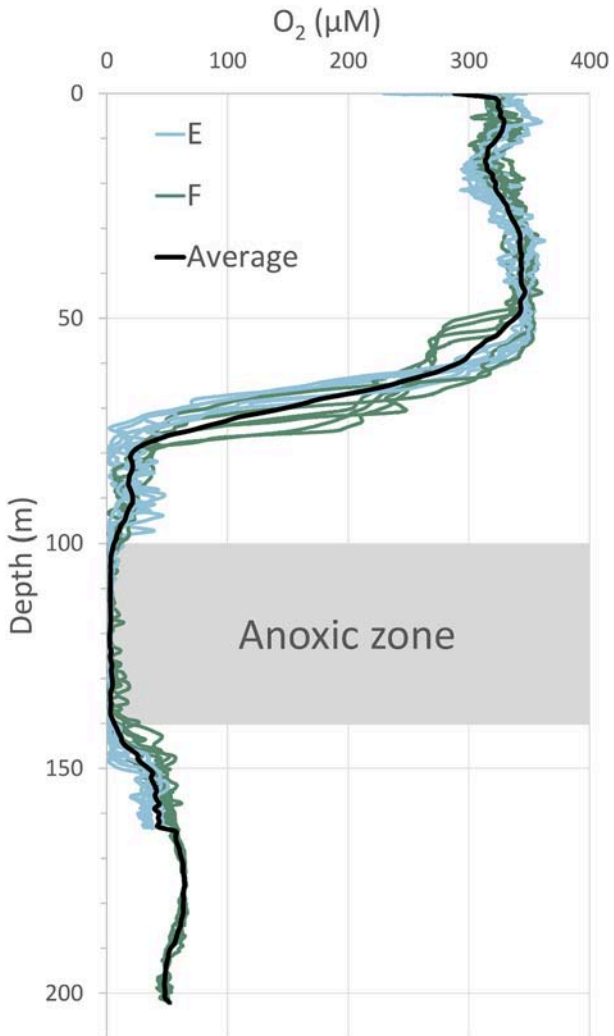

FIGURE 3 | Distribution of dissolved oxygen in the water column at stations E and F in July 2015. A Seabird 43 oxygen sensor, mounted on the CTD of the ship, was used for these measurements. The average of several profiles is indicated by the black line. Note the anoxic zone at 100–140 m depth and the oxygenated zone below; these zones were separated by a "second" oxycline at around 140 m depth.

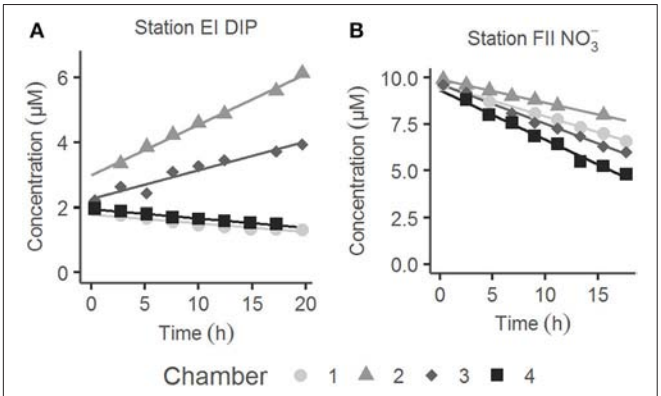

FIGURE 4 | Typical examples of the evolution of solute concentrations with time during benthic chamber incubations *in situ*. (A) Dissolved inorganic phosphorus (DIP) at station E during lander deployment I. **(B)** NO_3^- at station F during lander deployment II. The four chambers of each lander deployment are indicated in white and different tones of gray.

TABLE 2 | Average benthic fluxes with standard deviations at the two stations in July 2015.

	Station E Flux (mmol m^{-2} d^{-1})			Station F Flux (mmol m^{-2} d^{-1})		
	Average	**σ**	***n***	**Average**	**σ**	***n***
O_2	−7.31	3.66	8	−15.6	3.88	8
DIC	27.5	12.9	8	35.5	9.67	8
DIN	1.53	1.06	8	2.66	0.663	8
NH_4^+	1.98	1.20	8	3.37	0.702	8
NO_3^-	−0.477	0.293	8	−0.793	0.213	8
NO_2^-	0.0158	0.0300	6	0.0499	0.0295	7
DIP	0.107	0.316	8	0.120	0.192	5
Si	5.48	2.97	8	6.16	1.52	8

Two lander deployments were made at each station; the average was calculated from all approved fluxes (see Materials and Methods) of each solute measured during the two deployments. n is the number of individual chamber flux measurements. DIN (dissolved inorganic nitrogen) is the sum of ammonium, nitrite and nitrate. DIP is dissolved inorganic phosphorus.

that this difference was falsely found to be significant is therefore low.

Another clear effect of the oxygenation event in 2015 is that the DIP flux was directed into the sediment in about 50% of the flux measurements (**Figures 6**, **7**). An uptake of DIP by the sediment was never observed under anoxic conditions in 2008 and 2010 (Viktorsson et al., 2013a). The DIP uptake by EGB sediments in 2015 is consistent with the presence of iron and manganese oxides in these sediments as suggested by Rosenberg et al. (2016). Change of direction of the benthic DIP flux as a result of an altered oxygen regime has been observed previously in the Baltic Sea. An episodic oxygenation event of deep long-term anoxic accumulation bottoms in the western Gulf of Finland turned the high DIP efflux in 2003 into an influx in 2004. When the bottom water had returned to anoxia in 2005, the high DIP efflux was resumed (Viktorsson et al., 2012).

We suggest that the high spatial variability of the sediment caused the fluxes measured each year to be variable, and especially in 2015 when the oxygenated bottom water likely increased sediment heterogeneity as discussed above. Because of this, the statistical power to detect an actual difference between the anoxic years and 2015 became low. The risk of failing to detect an actual difference was therefore relatively large as mentioned above. Hence, we used the average DIP fluxes from stations E and F in 2015 to estimate the decrease of the internal DIP load due to the oxygenation event caused by the 2014–2015 MBI (see below; **Table 5**).

Yet another clear effect of the MBI oxygenation event is that bottom water nitrate concentrations of about 10 μM were observed in July 2015, and the flux of nitrate was consistently

directed into the sediment (**Figure 4**, **Table 2**). In 2008 and 2010, the bottom water contained no or very little nitrate, and the nitrate flux was not measurable or zero (**Figure 6**). The average nitrate flux in 2015 (**Table 2**) was on each station not significantly different (ANOVA, $p = 0.254$ for station E and $p = 0.365$ for station F) from the sum of the average denitrification and DNRA rates (**Table 4**). Since anammox rates were insignificant, this finding indicates that other nitrate removal processes, such as bacterial intracellular storage, did not play a major role in newly oxygenated Baltic proper sediments in July 2015.

Effect of Oxygenation on Composition of the Benthic Solute Flux

Oxygenation of surficial sediments effects transformation, retention and removal of various elements differently (e.g., Sundby et al., 1986; Ekeroth et al., 2016a). The composition and elemental ratios of benthic solute fluxes under anoxic conditions thus change upon oxygenation as suggested by several studies. Ekeroth et al. (2016a) found a very low DIN:DIP molar ratio (2.8) of the benthic flux measured under anoxia, but when these reduced Baltic proper sediments were experimentally oxygenated, the DIN:DIP ratio of the flux increased to about 12, which was due to a retention of DIP in the oxygenated azoic sediment rather than to a stimulation of the DIN flux. Viktorsson et al. (2012, 2013a,b) reported average DIC:DIP molar ratios of anoxic benthic fluxes of about 30 in the Gulf of Finland, and about 70 in the EGB and in west-Swedish fjords. The DIC:DIP molar ratio of fluxes measured in permanently oxygenated areas of the same basins was several fold higher and approached often a value of about 1000. N:P and C:P ratios of benthic solute fluxes in anoxic settings are thus well below the Redfield ratios of 16:1 and 106:1, respectively, due to preferential regeneration of P under anoxic conditions (e.g., Viktorsson et al., 2013b; Ekeroth et al., 2016a, and references therein).

We compared the composition of the benthic nutrient and DIC fluxes at stations E and F in the EGB under anoxic conditions in 2008 and 2010 (Viktorsson et al., 2013a; Nilsson et al., in prep; Hall et al., unpublished results) with those under newly oxygenated conditions in 2015 (this study; **Figure 7**). The DIC and DIN flux, as well as the DIC and Si flux, showed positive correlations both under anoxic and oxygenated conditions, and both the C:N and the C:Si molar ratios of fluxes were unaffected by the oxygenation event. The C:N molar ratio of fluxes was above the Redfield ratio all years (**Figure 7**). It was previously suggested that the benthic Si flux from reduced Baltic sediments slows down upon oxygenation (Ekeroth et al., 2016a; Tallberg et al., in press). We did not observe any such effect in the EGB (see above; **Figure 6**), and that would likely have made the C:Si ratio of the flux higher—contrary to our findings.

However, the oxygenation triggered by the MBI drastically changed the C:P and the N:P composition of the flux. While both the C:P (on average about 70) and the N:P (on average 3–4) molar ratio of the flux was much below the Redfield ratio under anoxia in 2008 and 2010 (Viktorsson et al., 2013a), these ratios became much higher and in most cases well above Redfield as a result of oxygenation in 2015 (**Figure 7**). The very P rich (in relation to both C and N) benthic flux under anoxia thus turned into a P poor flux under oxygenated conditions due to sedimentary P retention. A natural bottom water oxygenation event may thus increase the DIN:DIP ratio of the water column nutrient pool, and thus indirectly influence eutrophication status, and the abundance and composition of phytoplankton and cyanobacteria communities in surface waters.

Our aim with this study was not to explore the detailed mechanisms of P retention in the sediment upon oxygenation, but rather to show the existence and determine the magnitude of P retention. However, it is very likely that phosphate adsorption to metal (Fe) oxyhydroxides was an important mechanism as indicated above. Also polyphosphate storage by bacteria (e.g., sulfur bacteria) is likely. Our inorganic P concentrations (data not shown) for the solid phase of the sediment indicate enrichment close to the sediment-water interface and thus P adsorption to metal oxyhydroxides. However, these data are not comprehensive enough to rule out other P retention mechanisms.

TABLE 3 | *P*-value and power of Students *t*-test performed for fluxes from anoxic (2008 + 2010) and oxygenated (2015) bottoms.

		DIC	DIN	NH_4^+	DIP	Si
Station E	*p*	0.062	0.52	0.093	0.21	0.36
	Power	0.48	0.085	0.34	0.37	0.14
Station F	*p*	0.43	0.45	0.11	0.0058*	0.25
	Power	0.12	0.11	0.34	0.89	0.20

**Statistically significant ($p < 0.05$) difference.*

TABLE 4 | Average rates of denitrification, DNRA, denitrification fueled by water column nitrate (D_W), denitrification coupled to nitrification (D_n), and average contribution of D_W to total denitrification (D_W %).

Station	Denitrification (mmol N m^{-2} d^{-1})		DNRA (mmol N m^{-2} d^{-1})		D_W (mmol N m^{-2} d^{-1})		D_n (mmol N m^{-2} d^{-1})		D_W (%)
	Average	±SE	Average	±SE	Average	±SE	Average	±SE	
E	0.16	0.02	0.16	0.06	0.038	0.004	0.122	0.014	24
F	0.05	0.02	0.53	0.15	0.040	0.010	0.006	0.002	86

All rates ($n = 15$) are reported with associated standard errors (SE). Rates were measured by means of sediment core incubations with addition of $^{15}NO_3^-$ to the water phase (see Materials and Methods).

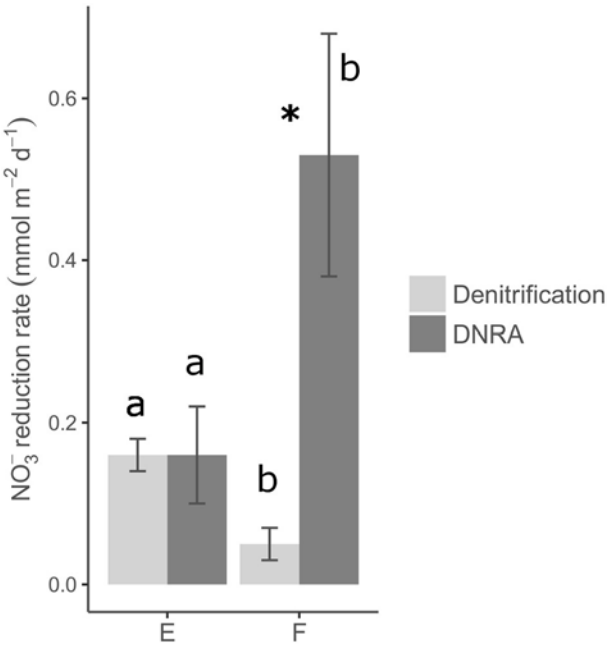

FIGURE 5 | Average rates of denitrification and DNRA and associated error bars (standard errors, $n = 15$). Rates were measured by means of sediment core incubations with addition of $^{15}NO_3^-$ to the water phase (see Materials and Methods). Different letters (i.e., a vs. b) represent statistically significant differences in denitrification rates and DNRA rates between the two stations (ANOVA, $p < 0.05$). Asterisk depicts statistically significant differences between denitrification and DNRA rates at station F (ANOVA, $p < 0.05$).

Change of the Internal P Load as a Result of Oxygenation: An Estimate on the Baltic Proper Scale

The statistical analysis showed that the benthic DIP flux was significantly lower in the oxygenated 2015 than in the anoxic 2008 and 2010 only at station F (**Table 3**). The statistical power of this significant difference was high (see above). However, the statistical power to detect an actual decrease of the DIP flux at station E between 2008–2010 and 2015 was low due to sediment heterogeneity. The risk of failing to detect an actual difference was therefore large as mentioned above. To this end, we used the average DIP fluxes from stations E and F in 2015 to estimate the decrease, up scaled to the Baltic proper basin, of the integrated benthic DIP flux (the internal DIP load) due to the oxygenation triggered by the 2014–2015 MBI.

To accomplish this we outlined two cases in July 2015: (a) The Baltic proper is anoxic below 100 m depth, and (b) the Baltic proper is anoxic in the depth interval 100–140 m and oxygenated below 140 m due to the MBI with a second oxycline in the water column at 140 m depth. Case (a) is hypothetical, and case (b) extrapolates the actual oxygenated situation in the EGB in July 2015 to the entire Baltic proper.

The bottom surface areas were calculated with the 'Surface Volume' tool in the software ArcGIS 10.3.1 (ESRI, 2015), using bathymetry data from the Baltic Sea Bathymetry Database (Baltic Sea Hydrographic Commission, 2013). Bottoms were divided into three groups: anoxic, type E and type F. Anoxic bottoms were situated at 100–140 m depth, where CTD measurements showed that the O_2 concentration was <5 μM, whereas bottoms below 140 m were oxygenated by the MBI in 2015. All bottoms below 100 m depth were anoxic in 2008 and 2010. Type E (140–190 m) and type F (190–459 m) bottoms were situated around the depths of station E (170 m) and F (210 m), respectively. Each bottom area was multiplied with the average DIP flux for that bottom type and time period. For the anoxic bottoms, the average flux from station D (at a depth of 130 m), E and F in 2008–2010 was used (Viktorsson et al., 2013a). It was assumed that the flux from the anoxic bottoms was the same in 2015 as in 2008 and 2010. Bottoms shallower than 100 m depth were assumed to give a negligible contribution to the internal DIP load (Viktorsson et al., 2013a).

The internal DIP load for the fully anoxic case a) was 144 ± 35.9 kton P yr^{-1} and for the MBI oxygenated case b) 111 ± 54.1 kton P yr^{-1} (**Table 5**). The internal DIP load had thus been lowered with 23% if the 2014–2015 MBI had oxygenated all of the Baltic proper below 140 m depth.

The reason the anoxic internal DIP load presented here is almost 10 kton yr^{-1} lower than that estimated by Viktorsson et al. (2013a) is that the latter study used an average DIP flux for the entire anoxic Baltic proper area, whereas we specified the anoxic flux for the different anoxic depth intervals (**Table 5**).

Sommer et al. (2017) reported a much lower influence of deep-water renewal, such as the MBI, on the Baltic proper internal DIP load. They reported a reduction of the DIP load with only 5%, which is much less the 23% we report. This discrepancy is most likely due to the presence of massive benthic microbial mats in the hypoxic transition zone at 80–120 m depth in the eastern part of the EGB (Noffke et al., 2016). These microbial mats were found to be very active in releasing DIP, but they exist at water depths above the influence of the MBI, and were thus not influenced by it. However, benthic microbial mats have not been found in the western part of the EGB despite attempts to find them (U. Marzocchi, pers. comm.). It thus appears that there are regional differences within the EGB indicating that extrapolations from stations in the eastern part of the basin may differ from those made from stations in the western and central parts of the basin.

Benthic DNRA Rates and Ammonium Effluxes

The DNRA rate was significantly higher at the deep station F than at the shallower station E (ANOVA, $p < 0.01$) as mentioned above. It is plausible that the H_2S pool in the sediment was higher at station F than at station E, since it is likely that sulfate reduction rates were higher at station F than at station E because of higher salinity (i.e., higher sulfate concentration) and plausibly higher content of labile sedimentary organic matter at the deeper station F (210 m) than at station E (170 m). Highly sulfidic conditions favor chemolithoautotrophic DNRA over heterotrophic denitrification and DNRA; Beggiatoa and

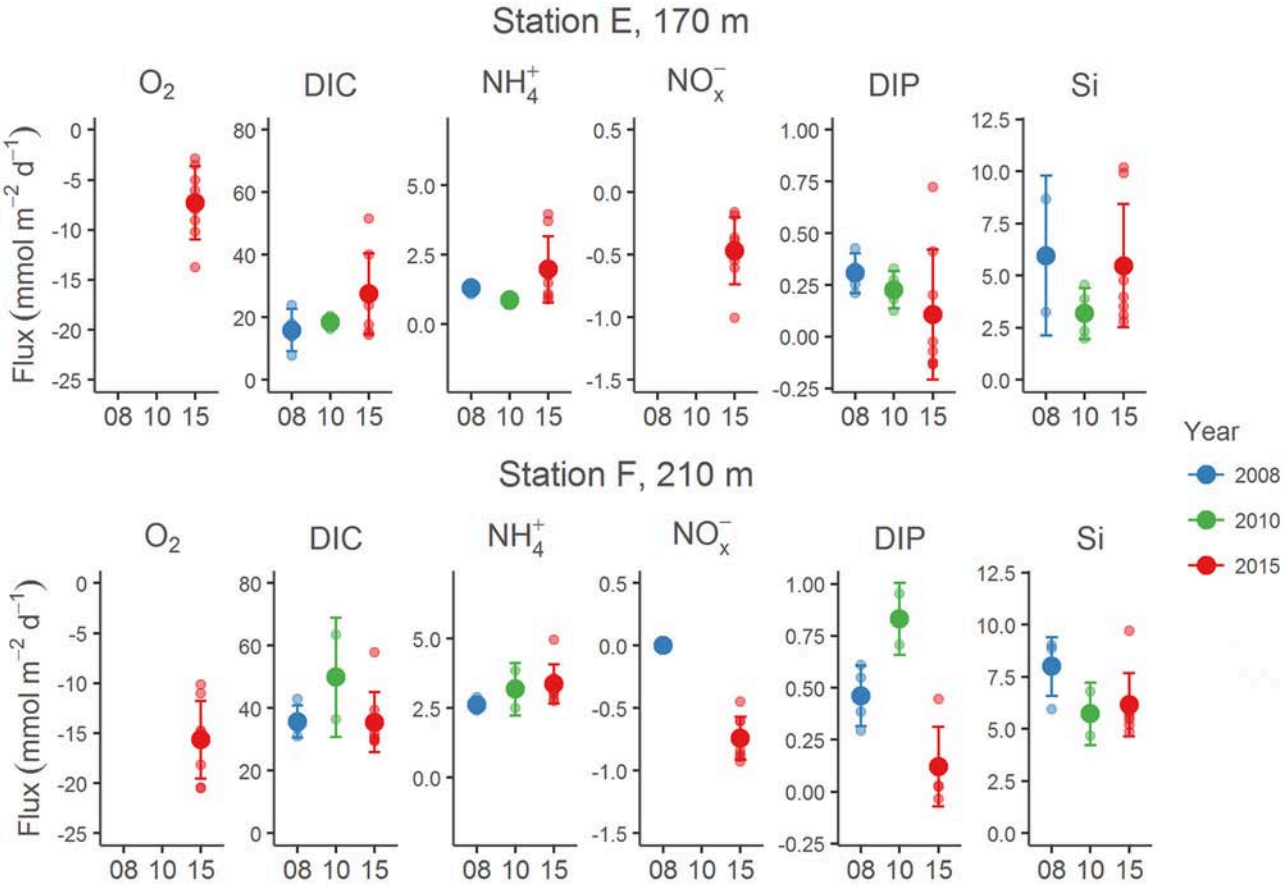

FIGURE 6 | Benthic fluxes of O_2, DIC, NH_4^+, NO_x (NO_2^- + NO_3^-), DIP and Si at stations E and F in 2008 (blue), 2010 (green), and 2015 (red). The years are given on the x-axis. The bottom water at these stations was anoxic in 2008 and 2010 (with essentially no NO_3^- present), but oxygenated in 2015 (this study). The fluxes from 2008 and 2010 are from Viktorsson et al. (2013a), Nilsson et al. (in prep.) and Hall et al. (unpublished results). Each individual chamber flux is indicated with a small circle, the average flux with a big circle, and the standard deviation with a bar.

other sulfide oxidizers can couple the reduction of NO_3^- to NH_4^+ with sulfide oxidation (Brunet and Garcia-Gil, 1996; Jørgensen and Nelson, 2004), whereas sulfide can inhibit denitrification (Sørensen et al., 1980). We thus speculate that the higher DNRA rates at station F than at E are linked to higher pore water sulfide concentration at station F than at E.

The ammonium effluxes measured *in situ* in the chambers were statistically significantly higher than the DNRA rates at both stations, and DNRA supported only 16 and 8% of the ammonium efflux at stations F and E, respectively. It is clear that the rate of ammonium regeneration via ammonification of organic matter and subsequent efflux from the sediment was much higher than the rate of ammonium regeneration via DNRA.

Influence of Bottom Water Oxygenation on Benthic and Pelagic Fixed N Removal through Denitrification: An Estimate on the Baltic Proper Scale

Our results clearly show that the natural major oxygenation event initiated benthic nitrogen removal (through denitrification) and recycling (through DNRA) in the formerly anoxic sediments. These two microbial processes were initially driven by the appearance of nitrate in the bottom water (De Brabandere et al., 2015). With time, a vast portion of these newly oxygenated sediments switched the nitrate source from the overlying water to benthic nitrification, as suggested by the significant discrepancy in D_n rates between station E and F.

Here we propose an integrated denitrification budget by up scaling the rates to the oxygenated, nitrate-containing areas of the Baltic proper, which are to be considered as new active sites of N loss. We estimated the annual sedimentary N loss from these newly oxygenated sites to be 10.3 kton N yr^{-1} (**Table 5**). Recently, Deutsch et al. (2010) estimated the integrated benthic denitrification in permanently oxygenated bottoms of the Baltic proper being 191 kton N yr^{-1}. This thus suggests that sedimentary N loss associated to the newly oxygenated sites is minimal compared to the total basin-wide benthic N loss.

However, recent up scaling of water column denitrification rates to the whole Baltic proper anoxic surface area indicated

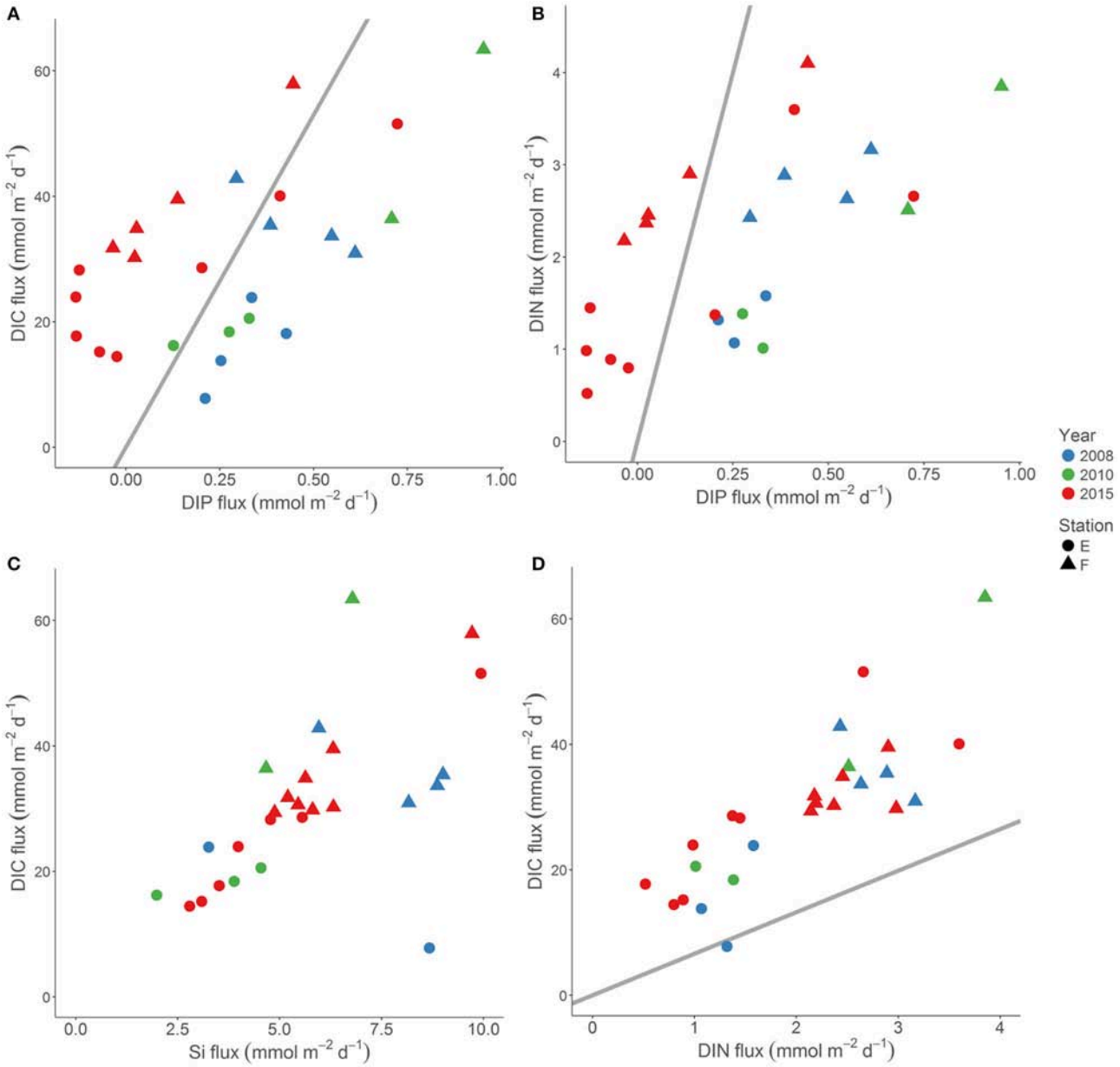

FIGURE 7 | The DIC flux vs. the DIP flux (A), the DIC flux vs. the DIN flux **(B)**, the DIC flux vs. the Si flux **(C)**, and the DIN flux vs. the DIP flux **(D)** at stations E (circles) and F (triangles) in 2008 (blue), 2010 (green), and 2015 (red). The bottom water was anoxic in 2008 and 2010, and oxygenated in 2015. The Redfield elemental ratio is indicated with a straight line.

that water column N loss exceeds sediment denitrification by up to a factor of three (Dalsgaard et al., 2013). It is important to note that the newly oxygenated sediments were lying underneath a double oxycline (cf **Figure 3**), as the MBI was constituted of dense water masses circulating on the bottom of the basins. Assuming that the upper and lower water column oxyclines would have the same denitrification rate (Dalsgaard et al., 2013), the estimated annual N loss associated to the second newly-established oxycline is 84.4 kton N yr^{-1} (**Table 5**), which is 44% of the total sedimentary Baltic proper N loss estimated by Deutsch et al. (2010). We suggest that, although the horizontal area of the second oxycline in the water column at 140 m depth and the bottom area below 140 m oxygenated by the MBI is limited (**Table 5**), the impact of these newly oxygenated areas on the total (pelagic plus benthic) N removal in the Baltic proper is remarkable (95 kton N yr^{-1} vs. 531 kton N yr^{-1}), where the total N removal rate (531 kton N yr^{-1}) is the average of the water column N removal range (132–547 kton N yr^{-1}, Dalsgaard et al., 2013) added to the average sedimentary N removal (191 kton N yr^{-1}, Deutsch et al., 2010). The natural oxygenation event may

TABLE 5 | Internal loading of DIP (DIP load) and fixed N removal by pelagic and benthic denitrification (N loss) scaled up to the Baltic proper basin for two cases in July 2015.

		Area (km^2)	Flux case (a) ($mmol\ m^2\ d^{-1}$)		Total flux case (a) ($kton\ yr^{-1}$)		Flux case (b) ($mmol\ m^2\ d^{-1}$)		Total flux case (b) ($kton\ yr^{-1}$)	
			Average	σ	Average	σ	Average	σ	Average	σ
DIP load	Anoxic 100 to 140 m	24,670	0.336	0.118	93.7	33.0	0.336	0.118	93.7	33.0
	Station E 140 to 190 m	11,965	0.267	0.096	36.1	13.0	0.107	0.316	14.5	42.7
	Station F 190 to 459 m	2,160	0.583	0.235	14.2	5.74	0.120	0.192	2.93	4.69
	Sum				144	35.9			111	54.1
			Average	SE	Average	SE	Average	SE	Average	SE
N loss	Second oxycline 140 m	14,121	–	–	–	–	1.17	–	84.4	–
	Station E 140 to 190 m	11,965	0	0	0	0	0.16	0.02	9.8	1.3
	Station F 190 to 459 m	2,160	0	0	0	0	0.05	0.02	0.51	0.20
	Sum				0	0			94.7	–

*a) The Baltic proper is anoxic below 100 m depth, and b) the Baltic proper is anoxic in the depth interval 100–140 m and oxygenated below 140 m due to the MBI with a second oxycline in the water column at 140 m depth. Case a) is hypothetical, and case b) extrapolates the actual situation in the EGB in July 2015 to the entire Baltic proper. The N loss presented here is an estimate of the N loss created by the MBI, and is additional to the N loss occurring in the first (upper) oxycline and in permanently oxygenated bottoms. The anoxic DIP fluxes were measured at station D (130 m), E and F in 2008 and 2010, and were reported by Viktorsson et al. (2013a). The DIP fluxes and benthic denitrification rates under oxygenated conditions were measured at station E and F in July 2015 (this study). Fluxes and rates measured at stations D, E, and F were assumed to be valid for the depth intervals 100–140, 140–190, and 190–459 m, respectively. The second oxycline N loss was calculated by using the water column denitrification rate from Dalsgaard et al. (2013) and up scaling it to the second oxycline area at 140 m depth. The bottom areas corresponding to the different depth intervals are displayed in **Figure 1**. See text for further explanations.*

thus have increased the total Baltic proper fixed N removal by denitrification by 18%.

CONCLUDING REMARKS

In the scenario that the 2014–2015 MBI oxygenated all of the Baltic proper below 140 m depth, we estimated that this natural oxygenation event would decrease the internal DIP load with 23% and enhance total (pelagic plus benthic) denitrification by 18%. Although there are several uncertainties and assumptions associated with our estimates, they indicate that MBIs may have a considerable influence on the Baltic proper P and N budgets.

AUTHOR CONTRIBUTIONS

PH, EA, SB, AH, and MK designed the study, and coordinated the ship operation and sediment sampling. MK coordinated the lander deployments. AH ran incubations on-board. EA, SB, AH, MK, MN and LV processed samples. AH and Sv made statistical analyses. All authors contributed to the evaluation of data and to writing the manuscript.

FUNDING

This work was supported financially by the Swedish Research Council (VR), the BIO-C3 project funded jointly by BONUS (Art 185) and the Swedish Research Council for Environment, Agricultural Sciences and Spatial Planning (FORMAS), the Helmholtz Alliance "ROBEX-Robotic Exploration of Extreme Environments", the Sonderforschungsbereich 754 "Climate-Biogeochemistry Interactions in the Tropical Ocean" supported by the Deutsche Forschungsgemeinschaft, and the Research Foundation Flanders (Ph.D. fellowship to Sv).

ACKNOWLEDGMENTS

We thank Nils Ekeroth for assistance with statistical analyses, Bo Thamdrup for making analytical instrumentation available at Southern Denmark University, and the captain and crew on University of Gothenburg R/V "Skagerak" for support at sea.

SUPPLEMENTARY MATERIAL

The Supplementary Material for this article can be found online at: http://journal.frontiersin.org/article/10.3389/fmars.2017.00027/full#supplementary-material

REFERENCES

Aller, R. C. (2014). "Sedimentary diagenesis, depositional environments, and benthic fluxes," in *Treatise on Geochemistry (2nd Edn)*, eds H. D. Holland and K. K. Turekian (Oxford: Elsevier), 293–334.

Almroth, E., Tengberg, A., Andersson, J. H., Pakhomova, S. V., and Hall, P. O. J. (2009). Effects of resuspension on benthic fluxes of oxygen, nutrients, dissolved inorganic carbon, iron and manganese in the Gulf of Finland, Baltic Sea. *Cont. Shelf Res.* 29, 807–818. doi: 10.1016/j.csr.2008.12.011

Baltic Sea Hydrographic Commission (2013). *Baltic Sea Bathymetry Database version 0.9.3*. Available online at: http://data.bshc.pro/ 2015-09-22

Belsley, D. A., Kuh, E., and Welsch, R. E. (1980). *Regression Diagnostics: Identifying Influential Data and Sources of Collinearity*. New York, NY: Wiley.

Bonaglia, S., Bartoli, M., Gunnarsson, J. S., Rahm, L., Raymond, C., Svensson, O., et al. (2013). Effect of reoxygenation and Marenzelleria spp. bioturbation on Baltic Sea sediment metabolism. *Mar. Ecol. Prog. Ser.* 482, 43–55. doi: 10.3354/meps10232

Bonaglia, S., Nascimento, F. A., Bartoli, M., Klawonn, I., and Brüchert, V. (2014). Meiofauna increases bacterial denitrification in marine sediments. *Nat. Commun.* 5:5133. doi: 10.1038/ncomms6133

Brunet, R. C., and Garcia-Gil, L. J. (1996). Sulfide-induced dissimilatory nitrate reduction to ammonia in anaerobic freshwater sediments. *FEMS Microbiol. Ecol.* 21, 131–138.

Brunnegård, J., Grandel, S., Ståhl, H., Tengberg, A., and Hall, P. O. J. (2004). Nitrogen cycling in deep-sea sediments of the Porcupine Abyssal Plain, NE Atlantic. *Prog. Oceanogr.* 63, 159–181. doi: 10.1016/j.pocean.2004.09.004

Burdige, D. J. (2007). Preservation of organic matter in marine sediments: controls, mechanisms, and an imbalance in sediment organic carbon budgets? *Chem. Rev.* 107, 467–485. doi: 10.1021/cr050347q

Chambers, J. M. (1992). "Linear models" in *Statistical Models in S*, eds J. M. Chambers and T. J. Hastie (Pacific Grove, CL: Wadsworth & Brooks/Cole). 95–144.

Christensen, P. B., Rysgaard, S., Sloth, N. P., Dalsgaard, T., and Schwærter, S. (2000). Sediment mineralization, nutrient fluxes, denitrification and dissimilatory nitrate reduction to ammonium in an estuarine fjord with sea cage trout farms. *Aquat. Microb. Ecol.* 21, 73–84. doi: 10.3354/ame021073

Conley, D. J., Humborg, C., Rahm, L., Savchuk, O. P., and Wulff, F. (2002). Hypoxia in the Baltic Sea and basin-scale changes in phosphorus biogeochemistry. *Environ. Sci. Tech.* 36, 5315–5320. doi: 10.1021/es025763w

Cook, R. D., and Weisberg, S. (1982). *Residuals and Influence in Regression*. London: Chapman and Hall.

Dalsgaard, T., De Brabandere, L., and Hall, P. O. J. (2013). Denitrification in the water column of the central Baltic Sea. *Geochim. Cosmochim. Acta* 106, 247–260. doi: 10.1016/j.gca.2012.12.038

Dalsgaard, T., Thamdrup, B., and Canfield, D. E. (2005). Anaerobic ammonium oxidation (anammox) in the marine environment. *Res. Microbiol.* 156, 457–464. doi: 10.1016/j.resmic.2005.01.011

De Brabandere, L., Bonaglia, S., Kononets, M. Y., Viktorsson, L., Stigebrandt, A., Thamdrup, B., et al. (2015). Oxygenation of an anoxic fjord basin strongly stimulates benthic denitrification and DNRA. *Biogeochemistry* 126, 131–152. doi: 10.1007/s10533-015-0148-6

Deutsch, B., Forster, S., Wilhelm, M., Dippner, J., and Voss, M. (2010). Denitrification in sediments as a major nitrogen sink in the Baltic Sea: an extrapolation using sediment characteristics. *Biogeosciences* 7, 3259–3271. doi: 10.5194/bg-7-3259-2010

Ekeroth, N., Blomqvist, S., and Hall, P. O. J. (2016a). Nutrient fluxes from reduced Baltic Sea sediment: effects of oxygenation and macrobenthos. *Mar. Ecol. Prog. Ser.* 544, 77–92. doi: 10.3354/meps11592

Ekeroth, N., Kononets, M., Walve, J., Blomqvist, S., and Hall, P. O. J. (2016b). Effects of oxygen on recycling of biogenic elements from sediments of a stratified coastal Baltic Sea basin. *J. Mar. Syst.* 154, 206–219. doi: 10.1016/j.jmarsys.2015.10.005

Ekeroth, N., Lindström, M., Blomqvist, S., and Hall, P. O. J. (2012). Recolonisation by macrobenthos mobilises organic phosphorus from reoxidised Baltic Sea sediments. *Aquatic Geochemistry* 18, 499–513. doi: 10.1007/s10498-012-9172-5

ESRI (2015). *ArcGIS 10.3.1 for Desktop*. Redlands, CA: ESRI.

Faul, F., Erdfelder, E., Lang, A.-G., and Buchner, A. (2007). G* Power 3: a flexible statistical power analysis program for the social, behavioral, and biomedical sciences. *Behav. Res. Methods* 39, 175–191. doi: 10.3758/BF03193146

Finni, T., Kononen, K., Olsonen, R., and Wallström, K. (2001). The history of cyanobacterial blooms in the Baltic Sea. *Ambio* 30, 172–178. doi: 10.1579/0044-7447-30.4.172

Fox, J., and Weisberg, S. (2011). *An R Companion to Applied Regression*. Thousand Oaks, CA:SAGE Publications.

Goyet, C., and Snover, A. K. (1993). High-accuracy measurements of total dissolved inorganic carbon in the ocean - Comparison of alternate detection methods. *Mar. Chem.* 44, 235–242.

Gustafsson, B. G., and Stigebrandt, A. (2007). Dynamics of nutrients and oxygen/hydrogen sulfide in the Baltic Sea deep water. *J. Geophys. Res. Biogeosci.* 112. doi: 10.1029/2006JG000304

IOW Baltic Sea Research Institute Warnemünde (2015). *Oxygen Arrived at the Bottom of the Central Baltic Sea*. Available at: http://www.io-warnemuende.de/tl_files/news/presse/2015/20150304_presse_Salzwassereinbruch2_engl.pdf

Jilbert, T., Slomp, C., Gustafsson, B. G., and Boer, W. (2011). Beyond the Fe-P-redox connection: preferential regeneration of phosphorus from organic matter as a key control on Baltic Sea nutrient cycles. *Biogeosciences* 8, 1699–1720. doi: 10.5194/bg-8-1699-2011

Jørgensen, B. B., and Nelson, D. C. (2004). Sulfide oxidation in marine sediments: geochemistry meets microbiology. *Geol. Soc. Am. Special Papers* 379, 63–81. doi: 10.1130/0-8137-2379-5.63

Koroleff, F. (ed.). (1983). *Methods of Seawater Analysis,* 2nd Edn. Verlag Chemie.

Kullenberg, G., and Jacobsen, T. (1981). The Baltic Sea: an outline of its physical oceanography. *Mar. Pollut. Bull.* 12, 183–186.

Laima, M. (1994). Is KCl a reliable extractant of $^{15}NH_4^+$ added to coastal marine sediments? *Biogeochemistry* 27, 83–95.

Matthäus, W., Nehring, D., Feistel, R., Nausch, G., Mohrholz, V., and Lass, H.-U. (2008). "The inflow of highly saline water into the Baltic Sea," in *State and Evolution of the Baltic Sea, 1952–2005* (John Wiley & Sons, Inc.), 265–309. doi: 10.1002/9780470283134.ch10

Mohrholz, V., Naumann, M., Nausch, G., Krüger, S., and Gräwe, U. (2015). Fresh oxygen for the Baltic Sea—An exceptional saline inflow after a decade of stagnation. *J. Mar. Syst.* 148, 152–166. doi: 10.1016/j.jmarsys.2015.03.005

Nausch, M., Nausch, G., Mohrholz, V., Siegel, H., and Wasmund, N. (2012). Is growth of filamentous cyanobacteria supported by phosphate uptake below the thermocline? *Estuar. Coast. Shelf Sci.* 99, 50–60. doi: 10.1016/j.ecss.2011.12.011

Nielsen, L. P. (1992). Denitrification in sediment determined from nitrogen isotope pairing. *FEMS Microbiol. Lett.* 86, 357. doi: 10.1111/j.1574-6968.1992.tb04828.x

Noffke, A., Sommer, S., Dale, A. W., Hall, P. O. J., and Pfannkuche, O. (2016). Benthic nutrient fluxes in the Eastern Gotland Basin (Baltic Sea) with particular focus on microbial mat ecosystems. *J. Mar. Syst.* 158, 1–12. doi: 10.1016/j.jmarsys.2016.01.007

O'Sullivan, D. W., and Millero, F. J. (1998). Continual measurement of the total inorganic carbon in surface seawater. *Mar. Chem.* 60, 75–83.

Reissmann, J. H., Burchard, H., Feistel, R., Hagen, E., Lass, H. U., Mohrholz, V., et al. (2009). Vertical mixing in the Baltic Sea and consequences for eutrophication – A review. *Prog. Oceanogr.* 82, 47–80. doi: 10.1016/j.pocean.2007.10.004

Risgaard-Petersen, N., Nielsen, L. P., Rysgaard, S., Dalsgaard, T., and Meyer, R. L. (2003). Application of the isotope pairing technique in sediments where anammox and denitrification coexist. *Limnol. Oceanogr. Methods* 1, 63–73. doi: 10.4319/lom.2003.1.63

Rosenberg, R., Magnusson, M., and Stigebrandt, A. (2016). Rapid re-oxygenation of Baltic Sea sediments following a large inflow event. *Ambio* 45, 130–132. doi: 10.1007/s13280-015-0736-7

Schimanke, S., Meier, M., Kjellström, E., Strandberg, G., and Hordoir, R. (2012). The climate in the Baltic Sea region during the last millennium simulated with a regional climate model. *Clim. Past* 8, 1419–1433. doi: 10.5194/cp-8-1419-2012

Sommer, S., Clemens, D., Yücel, M., Pfannkuche, O., Hall, P. O. J., Almroth Rosell, E., et al. (2017). Major bottom water ventilation events do not significantly reduce basin-wide benthic N and P release in the Eastern Gotland Basin. *Front. Mar. Sci.* 4:18. doi: 10.3389/fmars.2017.00018

Sørensen, J., Tiedje, J. M., and Firestone, R. B. (1980). Inhibition by sulfide of nitric and nitrous oxide reduction by denitrifying Pseudomonas fluorescens. *Appl. Environ. Microbiol.* 39, 105–108.

Ståhl, H., Tengberg, A., Brunnegård, J., Bjørnbom, E., Forbes, T. L., Josefson, A. B., et al. (2004). Factors influencing organic carbon recycling and burial in Skagerrak sediments. *J. Mar. Res.* 62, 867–907. doi: 10.1357/0022240042880873

Stigebrandt, A. (2001). "Physical oceanography of the Baltic sea," in *A System Analysis of the Baltic Sea,* eds F. Wulff, L. Rahm and P. Larsson (Berlin-Heidelberg: Springer-Verlag), 19–74.

Stigebrandt, A., Rahm, L., Viktorsson, L., Ödalen, M., Hall, P. O. J., and Liljebladh, B. (2014). A new phosphorus paradigm for the Baltic proper. *Ambio* 43, 634–643. doi: 10.1007/s13280-013-0441-3

Sundby, B., Anderson, L., Hall, P. O. J., Iverfeldt, Å., Rutgers van der Loeff, M. M., and Westerlund, S. (1986). The effect of oxygen on release and uptake

of cobalt, manganese, iron and phosphate at the sediment-water interface. *Geochim. Cosmochim. Acta* 50, 1281–1288.

Tallberg, P., Heiskanen, A.-S., Niemistö, J., Hall, P. O. J., and Lehtoranta, J. (in press). Are benthic fluxes important for the availability of Si in the Gulf of Finland? *J. Mar. Syst.* doi: 10.1016/j.jmarsys.2017.01.010

Tengberg, A., Stahl, H., Gust, G., Muller, V., Arning, U., Andersson, H., et al. (2004). Intercalibration of benthic flux chambers I. Accuracy of flux measurements and influence of chamber hydrodynamics. *Prog. Oceanogr.* 60, 1–28. doi: 10.1016/j.pocean.2003.12.001

Thamdrup, B., and Dalsgaard, T. (2002). Production of N_2 through anaerobic ammonium oxidation coupled to nitrate reduction in marine sediments. *Appl. Environ. Microbiol.* 68, 1312–1318. doi: 10.1128/aem.68.3.1312-1318.2002

Tuominen, L., Heinänen, A., Kuparinen, J., and Nielsen, L. P. (1998). Spatial and temporal variability of denitrification in the sediments of the northern Baltic Proper. *Mar. Ecol. Prog. Ser.* 172, 13–24.

Vahtera, E., Conley, D. J., Gustafsson, B. G., Kuosa, H., Pitkänen, H., Savchuk, O. P., et al. (2007). Internal ecosystem feedbacks enhance nitrogen-fixing cyanobacteria blooms and complicate management in the Baltic Sea. *Ambio* 36, 186–194. doi: 10.1579/0044-7447(2007)36[186:IEFENC]2.0.CO;2

Viktorsson, L., Almroth-Rosell, E., Tengberg, A., Vankevich, R., Neelov, I., Isaev, A., et al. (2012). Benthic phosphorus dynamics in the Gulf of Finland, Baltic Sea. *Aquat. Geochem.* 18, 543–564. doi: 10.1007/s10498-011-9155-y

Viktorsson, L., Ekeroth, N., Nilsson, M., Kononets, M., and Hall, P. O. J. (2013a). Phosphorus recycling in sediments of the central Baltic Sea. *Biogeosciences* 10, 3901–3916. doi: 10.5194/bg-10-3901-2013

Viktorsson, L., Kononets, M., Roos, P., and Hall, P. O. J. (2013b). Recycling and burial of phosphorus in sediments of an anoxic fjord—the By Fjord, western Sweden. *J. Mar. Res.* 71, 351–374. doi: 10.1357/002224013810921636

Warembourg, F. R. (1993). "Nitrogen Fixation in Soil and Plant Systems," in *Nitrogen Isotope Techniques,* eds R. Knowles and T. H. Blackburn (San Diego, CA: Academic Press), 127–156.

Wasmund, N., Voss, M., and Lochte, K. (2001). Evidence of nitrogen fixation by non-heterocystous cyanobacteria in the Baltic Sea and re-calculation of a budget of nitrogen fixation. *Mar. Ecol. Prog. Ser.* 214, 1–14. doi: 10.3354/meps214001

Wilkinson, G. N., and Rogers, C. E. (1973). Symbolic description of factorial models for analysis of variance. *J. R. Stat. Soc. C* 22, 392–399. doi: 10.2307/2346786

Williams, D. A. (1987). Generalized linear model diagnostics using the deviance and single case deletions. *J. R. Stat. Soc. C* 36, 181–191. doi: 10.2307/2347550

Conflict of Interest Statement: The authors declare that the research was conducted in the absence of any commercial or financial relationships that could be construed as a potential conflict of interest.

Clim Dyn
DOI 10.1007/s00382-017-3695-9

Sensitivity of the overturning circulation of the Baltic Sea to climate change, a numerical experiment

Robinson Hordoir[1] · Anders Höglund[1] · Per Pemberton[1] · Semjon Schimanke[1]

Received: 29 August 2016 / Accepted: 20 April 2017

Abstract An ocean model covering the Baltic Sea area is forced by several climate scenarios for a period extending from 1961 to 2100. The Baltic Sea overturning circulation is then analyzed. The analysis shows that this circulation decreases between the end of the 20th century and the end of the 21st century, and that the decrease is amplified in the case of the strongest greenhouse gas emission scenarios, which corresponds with the highest warming cases. The reasons behind this decrease in overturning circulation are investigated. A strong increase of thermal stratification is noticed at the level of the Baltic Sea mixed layer. Based on buoyancy flux considerations, we demonstrate that the decrease in overturning circulation coincides with the increase of thermal stratification. Evidence shows that the underlying process is linked to a smaller erosion of the halocline due to a higher shielding, itself linked with a stronger and longer seasonal thermocline. This theory works if surface wind mixing is not taken into account directly in the computation of buoyancy fluxes.

Keywords Baltic Sea · Climate change · Overturning circulation · Thermal stratification

1 Introduction

The Baltic Sea is a marginal sea in Central/Northern Europe which presents an interesting mixture of different dynamics. The amount of river runoff delivered to the Baltic Sea, and its narrow connection to the North Sea through the Danish Straits give the Baltic Sea typical sill estuarine dynamics. Although many dynamical features of the Baltic Sea are geostrophic, due to its size, it is still an estuary. As for any estuarine structure, the amount of freshwater delivered to the estuary generates an overturning circulation in the same sense as that described by Garvine and Whitney (2006). This means that the delivery of freshwater can be considered as a delivery of vorticity or energy (Hordoir et al. 2008). For this reason, one can define an overturning circulation in the Baltic Sea (Döös et al. 2004), which is much larger than the amount of runoff delivered to the estuary or coastal area. Of course any estuarine or freshwater driven circulation is influenced by many parameters, the most important ones being wind forcing (Fong and Geyer 2002; Hordoir et al. 2006) and tidal currents (Hordoir et al. 2006). In the case of the Baltic Sea, tides are negligible but wind forcing does play an important role in its overturning circulation. Wind forcing over the Baltic and North Seas, and especially wind forcing variability, drive Baltic Sea salt inflows and so-called "Major Baltic Inflows" (MBI hereafter) (Matthäus 2006). MBIs are the drivers of the haline conveyor belt defined by Döös et al. (2004). MBIs are spurious phenomena of which the haline conveyor belt is the long-term result, MBIs and the haline conveyor belt in the Baltic Sea are two different visions of the same thing.

Many questions have arisen during the recent decades as the number of MBIs has decreased. After a stagnation period from 1983 to 1993, several MBIs have occurred but their frequency has been lower than during the 1960s and 1970s. Then MBIs occurred during three consecutive years (2014, 2015 and 2016), but it is yet too early to say if this latest series is part of a longer trend. The future of Baltic inflows is a subject of importance, and several studies have tried to identify whether changes of wind patterns related with a changing climate could be responsible for

✉ Robinson Hordoir
robinson.hordoir@smhi.se

[1] SMHI, 601 76 Norrköping, Sweden

Published online: 26 April 2017

their decrease. Lately, one can cite (Schimanke et al. 2014) who used a EOF decomposition of atmospheric pressure over Northern Europe to identify the atmospheric patterns that create MBIs. Based on this decomposition and using five different climate scenarios (Samuelsson et al. 2011), they have forecasted an increase of MBIs in the Baltic Sea towards the end of the 21st century. However, their study was only based on atmospheric patterns and did not include an ocean model. The Baltic Sea has complex reactions to changes in atmospheric patterns, such as changes in salinity, temperature or mixing, which affect its baroclinic dynamics. Thus, it is difficult to forecast if the number of MBIs will indeed increase. MBIs have for example a negative feedback on themselves: a too high salinity of the lower Baltic layers is a blocking factor. An increase of extreme wind strength is also a factor that influences vertical mixing, which is also a negative factor affecting MBIs and deep salinity (Meier 2005). However, the values of wind speed increase mentioned in Meier (2005) are far beyond the increases observed in our climate scenarios.

The purpose of this article is to provide a broader answer in terms of changes in the MBI process by combining the latest climate scenarios used by Schimanke et al. (2014) with the use of a Baltic Sea ocean model. In particular, we aim to understand what are the effect of changes in direct atmospheric forcing (wind forcing, temperature) on the Baltic Sea thermo-haline structure and how these changes affect the baroclinic circulation. Section 2 explains the methodology we use from a modeling point of view and how we analyzed these results. Results are presented in Sects. 3 and 4 we provide the analysis of the results and provide a theoretical relation between changes in climate change and changes in the overturning circulation in the Baltic Sea. A final section concludes this article.

2 Methodology

2.1 Ocean modeling strategy

We use the Nemo–Nordic configuration (Hordoir et al. 2013, 2015) in its most recent version, based on Nemo 3.6 (Madec 2015). Nemo–Nordic is a Nemo based ocean model for Baltic and North Seas that is able to reproduce the long term variability of the Baltic Sea haline structure (Hordoir et al. 2015). In addition, Nemo–Nordic abilities in reproducing the sea level and ice cover of Baltic and North Seas in operational mode have been asserted, and Nemo–Nordic is now SMHI's (Swedish Meteorological and Hydrological Institute) new forecast model in replacement of HIROMB (Funkquist and Kleine 2007).

In the present article, we use a restricted domain of Nemo–Nordic that includes only the Baltic Sea and the Kattegat region located between Denmark and Sweden. This restricted domain is chosen in order to save computing time as the purpose of this study is to focus on long term evolution of the Baltic Sea over time scales of almost 140 years. This restricted configuration has one open boundary along a zonal axis located between South of Skagen (Northern tip of Denmark) and Gothenburg (Swedish West Coast).

The vertical and horizontal grids of this Baltic only configuration are strictly identical to that of Nemo–Nordic, the only difference being that it has a restricted domain and a simplified open boundary condition. At this open boundary condition, sea level is imposed as well as temperature and salinity.

We set in total four simulations using the same atmospheric forcing that are used by Schimanke et al. (2014). Based on two global climate models (EC-EARTH and MPI) driving the RCA4 atmospheric configuration (Samuelsson et al. 2011), we have access to the simulated atmospheric circulation for the control period (1961–2005), and for two emission scenarios (RCP 4.5 and RCP 8.5) for the period 2005–2100.

All simulations start in 1961 from a rest state and with temperature and salinity fields taken from a climatology. Table 1 summarizes the simulations.

One crucial element to ensure a consistent haline circulation in the Baltic Sea is to set a proper sea level and sea level variability at the open boundary. We use the same method as described in Meier et al. (2012) to compute the sea level at the open boundary, using the atmospheric pressure simulated by RCA4 driven by an ERA-40 reanalysis on one side, and the sea level measurements at a tide gauge located in Gothenburg on the other. Just as in Meier et al. (2012), tides are neglected since they do not account for any significant contribution in the long term exchange between Baltic and North Seas. And as in Meier et al. (2012), temperature and salinity are set to climatological values: the exchange with the atmosphere between the open boundary condition and the Baltic Sea entrance is enough to ensure that water entering the Baltic Sea has a temperature trend that follows that of the atmospheric forcing. Runoff changes can dramatically affect the haline structure of the Baltic Sea (Meier et al. 2006), but in this set of experiments we want to concentrate on the Baltic Sea response to changes in atmospheric forcing. Therefore we use a climatological runoff and focus our research on the understanding of the changes in baroclinic circulation in the Baltic Sea related with the direct changes in atmospheric forcing.

2.2 Analysis protocol

The work done by Schimanke et al. (2014) identified atmospheric patterns related with MBIs. In their study,

they used observed salinities following the protocol defined by Matthäus (2006) in order to identify MBIs. Matthäus (2006) defined three criteria in order to identify an ongoing MBI based on Darss Sill salinity: The deep salinity at Darss Sill should be at least 17 PSU, with a low stratification, and last at least 5 days. However, this set of criteria is not easily transferable to an ocean model. Applying them to a hindcast simulation of Nemo–Nordic that has a good representation of the Baltic Sea deep salinity does not permit to identify many MBIs during the hindcast period used in Hordoir et al. (2015).

Modifying the criteria by either moving the observational point or the reference salinity (17 PSU) makes the criteria either over-sensitive to any inflow occurring in the ocean model, or on the contrary does not permit to identify many MBIs. Another solution in order to identify MBIs can be to analyze the deep salinity of the Baltic Sea at a station such as BY15 (Gotland Deep) which is often taken as a reference for its good representation of the mean Baltic Sea haline structure both in terms of salinity and stratification. But this strategy does not work either. First because there exists no criteria on how to identify a MBI based on deep Baltic Salinity. Second because even if there was such a criteria, as for the criteria defined for the Darss Sill by Matthäus (2006), applying measurement based criteria to a model does not take into account the inevitable biases of the model. A last method could have consisted in trying to measure the volume and salt flow variability to try to relate it to MBI occurency, but this method proved to be too sensitive to the salinity biases of the model as well. The definition of an MBI or of any Baltic Sea salt inflow is a very empirical concept, mostly based on observations, which makes it difficult to apply to an ocean model, especially when its resolution is rather low compared with the horizontal and vertical dimensions of the Danish Straits as it is the case in this study.

For these reasons we distance our analysis strategy from that taken by Matthäus (2006) or Schimanke et al. (2014): instead of analyzing MBIs, or any salt inflow that reaches the lower layers of the Baltic Sea, as discrete or quantified phenomena, we perform our analysis on the resulting circulation which is directly driven by MBIs, that is the Baltic Sea haline conveyor belt as defined by Döös et al. (2004).

2.2.1 *Meridional flux function*

Döös et al. (2004) define a meridional stream function in the Baltic Sea, which can be viewed along meridional and depth axis. We adopt a similar strategy but also use a meridional transport function. Figure 2 shows the meridional transport from the latitude of the Southern tip of Sweden towards the North of the Bothnian Bay. The Meridional Transport is computed by integrating meridional transport (in $m^3\ s^{-1}$) along the zonal axis, for every model grid cell of the integration box shown on Fig. 1, according to the following equation:

$$F(y,z) = \frac{1}{\lambda_{max} - \lambda_{min}} \int_{\lambda_{min}}^{\lambda_{max}} q(\lambda, y, z) d\lambda \quad (1)$$

in which λ is the longitude, with λ_{min} and λ_{max} being respectively the minimum and maximum values of λ along which integration is done. $q(\lambda, y, z)$ is the meridional transport (in $m^3\ s^{-1}$) at longitude λ and at position y (in nautical miles) along the latitude axis, and at depth z.

If computed based over a time period long enough to low-pass filter wind variability, $F(y, z)$ gives a representation of the overturning circulation of the Baltic Sea. $F(y, z)$ is positive from the bottom up to a level of about 30–40 m which is higher than that of the Baltic Sea pycnocline. Above this level, $F(y, z)$ is negative, reflecting the overturning circulation of the Baltic Sea.

The vertical variations of $F(y, z)$ are not only related with the transport, but also with the vertical resolution of the model. However, this does not affect the sign of the transport. In addition, we are interested in the variations of $F(y, z)$ between present and future climate more than in its value.

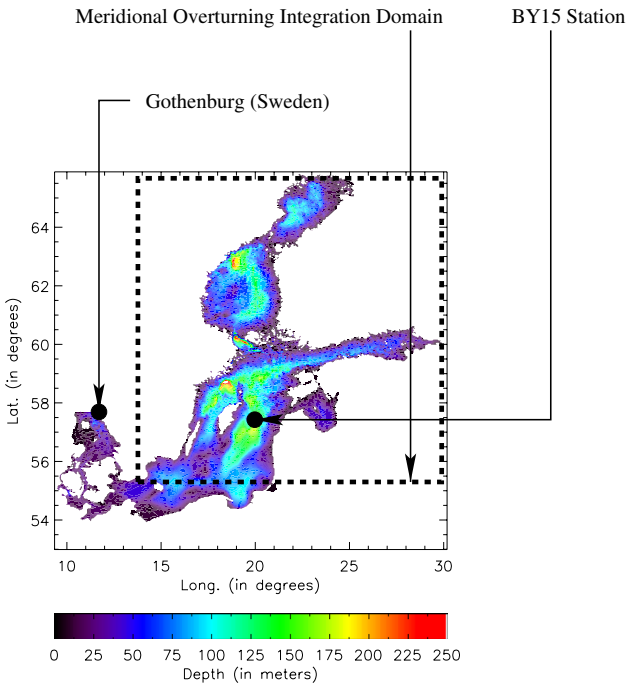

Fig. 1 Domain and bathymetry for the restricted Nemo–Nordic configuration used in the present study. The position of Gothenburg is shown as it is where the open boundary condition is located. The Gotland Deep (BY15) measurement station location is also shown

Table 1 Summary of simulations

Period and scenario/driving GCM	EC-Earth	MPI
1961–2005	EC-H	MPI-H
2006–2100 RCP 4.5	EC-4.5	MPI-4.5
2006–2100 RCP 8.5	EC-8.5	MPI-8.5

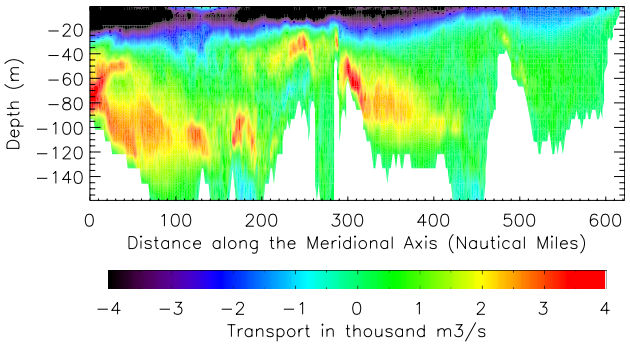

Fig. 2 Transport function $F(y, z)$ (in $m^3\ s^{-1}$), along the meridional axis of the Baltic Sea. Average value from 1975 to 2005 computed from the EC-H simulation. The values of transport in the *color scale* are bounded from −4000 to 4000 $m^3\ s^{-1}$ but can exceed these values

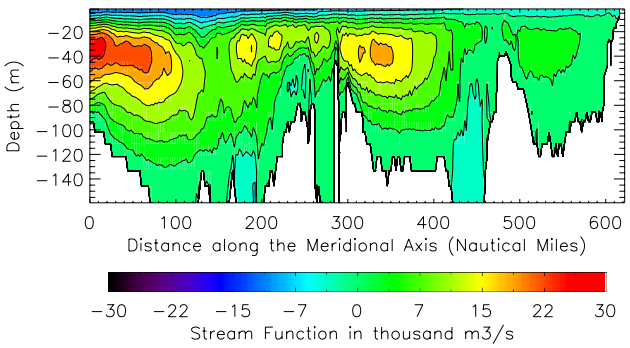

Fig. 3 Stream function $M_{st}(y, z)$ (in $m^3\ s^{-1}$), along the meridional axis of the Baltic Sea. Average value from 1975 to 2005 computed from the EC-H simulation

Based on $F(y, z)$, one can also compute a meridional stream function in the same manner as Döös et al. (2004) by depth integration from the bottom towards the surface:

$$M_{st}(y,z) = \frac{1}{H(y)-z}\int_{H(y)}^{z} F(y,z')dz' \tag{2}$$

Based on the same simulation as for Fig. 2, Fig. 3 shows the meridional stream function $M_{st}(y, z)$.

Figure 3 shows that there are four overturning cells from the Southern tip of Sweden towards the coast of the Bothnian Bay. From left towards right, the first cell corresponds

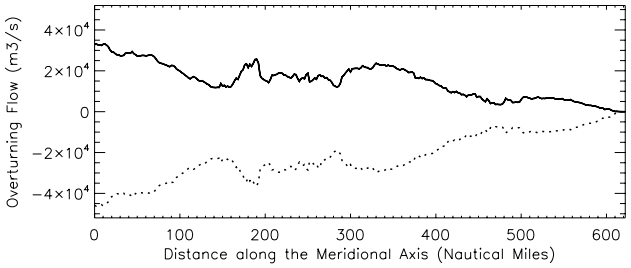

Fig. 4 Baltic overturning (*solid line*) extracted from the period 1975–2005 from the EC-H simulation (Table 1), and total resulting circulation eventually leaving the Baltic Sea (*dashed line*)

to the main Baltic Sea overturning circulation and ends approximately 30 nautical miles North of the latitude of Gotland Deep (BY15).

2.2.2 *Overturning circulation computation*

In the same manner as for the computation of function $F(y, z)$ defined in Sect. 2.2.1, we can compute the Baltic Sea Overturning. The Baltic Sea Overturning is the circulation which is generated by the input of vorticity through runoff combined with wind to the Baltic Sea, but which is not runoff. For any latitude, the value of this Baltic Sea Overturning $F_o(y)$ is therefore simply the total positive circulation:

$$F_o(y) = \int_{-H(y)}^{0}\int_{\lambda_{min}}^{\lambda_{max}} q^o(\lambda,y,z)d\lambda dz \tag{3}$$

with

$$\begin{aligned} q^o(\lambda,y,z) &= q(\lambda,y,z) \quad if\ q(\lambda,y,z) \geq 0 \\ q^o(\lambda,y,z) &= 0 \quad if\ q(\lambda,y,z) < 0 \end{aligned} \tag{4}$$

In the same manner, $F_t(y)$ which is the total resulting circulation heading towards the exit of the Baltic Sea can be defined as:

$$F_t(y) = \int_{-H(y)}^{0}\int_{\lambda_{min}}^{\lambda_{max}} q^t(\lambda,y,z)d\lambda dz \tag{5}$$

with

$$\begin{aligned} q^t(\lambda,y,z) &= q(\lambda,y,z) \quad if\ q(\lambda,y,z) \leq 0 \\ q^t(\lambda,y,z) &= 0 \quad if\ q(\lambda,y,z) > 0 \end{aligned} \tag{6}$$

Figure 4 shows the $F_o(y)$ and $F_t(y)$ overturning circulation extracted from simulation EC-H, and the resulting circulation leaving the Baltic Sea (negative dashed line). The symmetry between $F_o(y)$ and $F_t(y)$ is obvious and the difference of their absolute values reaches around more than 10,000

$m^3\ s^{-1}$ at the southernmost point, which corresponds to the cumulated amount of runoff released into the Baltic Sea above this latitude. The Baltic Overturning reaches almost 35,000 $m^3\ s^{-1}$ in the Southern Baltic Sea, which is almost triple the value of the cumulated runoff input. The resulting circulation leaving the Southern Baltic is of the order of 45,000 $m^3\ s^{-1}$.

3 Results

We can compute the differences in Baltic Sea Overturning circulation by computing the differences in Meridional Transport Function $F(y, z)$ and the differences in $F_o(y)$ and $F_t(y)$, between a control period that we define from 1975 to 2005, and a future climate period that we extract from 2069 to 2099. We do not use results of the control period located before 1975 in order to avoid spin-up effects inherent to the Nemo–Nordic configuration (Hordoir et al. 2015).

3.1 EC-Earth simulations

Figure 5a shows the transport function $F(y, z)$ for the control period of the EC-Earth Simulation. Below Fig. 5b, c show the transport functions between experiments EC-4.5 and EC-8.5 respectively. The pattern of differences is similar for EC-4.5 and EC-8.5 simulations, although it is more intense for the highest emission scenario. The analysis shows a significant decrease of flux at the level of the pycnocline, and to a lower extent of deep salt inflows. Since the ventilation at the level of the pycnocline is the dominant feature in terms of flux (Meier and Kauker 2002), this means basically that the decrease of meridional flux is highest at the vertical level where the meridional flux is itself highest. Further, the decrease in overturning is observable after each entrance to a sub-basin as the flux towards Northern latitudes below 40 m is decreased. Above 40 m, the value of $F(y, z)$ increases, meaning that the transport heading towards the exit of the Baltic Sea is also lower.

Figure 7 shows the integrated overturning flow difference between simulations EC-4.5/EC-8.5 and the EC-H simulation. The decrease in overturning reaches 4000 $m^3\ s^{-1}$ in the Southern Baltic Sea for the RCP 8.5 scenario, which corresponds to a decrease of more than 20% of the overturning circulation observed during the control period. The decrease in overturning circulation can be observed from South towards North. These results contradict the analysis done by Schimanke et al. (2014) which predicts a relatively important increase of salt inflows, and therefore in overturning circulation, when comparing the

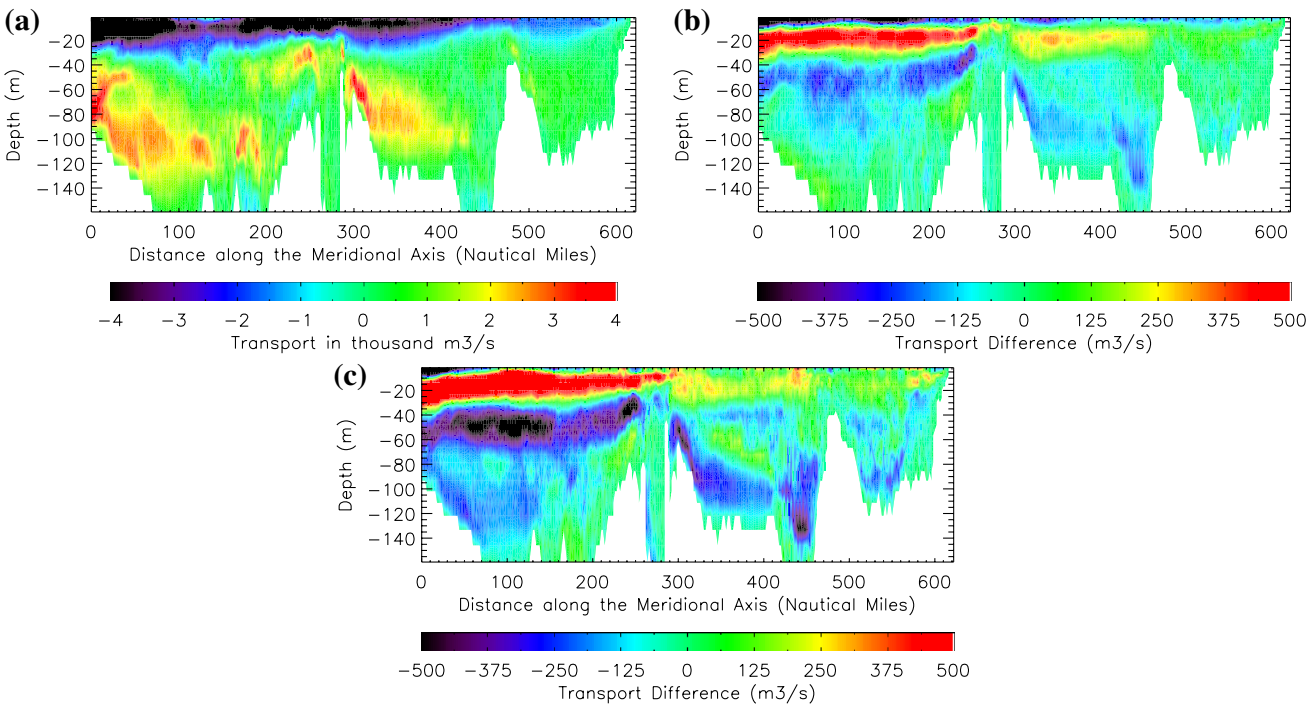

Fig. 5 **a** Transport function $F(y, z)$ along the meridional axis in the Baltic Sea in EC-H, same as Fig. 2. Average value from 1975 to 2005 computed from an EC-Earth forced simulation. The values of transport are bounded from −4000 to 4000 $m^3\ s^{-1}$ but can exceed these values. **b** Difference of transport function $F(y, z)$ between EC-4.5 and EC-H. **c** Difference of transport function $F(y, z)$ between EC-8.5 and EC-H

atmospheric patterns responsible for MBIs in the EC-Earth simulations, between the control period and the end of the 21st century. The Baltic Sea haline structure is affected by a mean salinity increase of about 0.5 PSU (Fig. 6). The haline stratification is slightly affected with a smoother halocline.

Figure 8 shows the salinity difference profile at BY15 station (Fig. 1), which is located East of Gotland Island. This station located on one of the deepest places of the Baltic Sea is the end of the pathway for salt water inflows. One notices a consistent salinity increase between the control period and the end of the 21st century, which appears to be surprising if one considers that the overturning circulation, or the probability of MBI occurency, is actually lower.

Figure 8 shows the differences in the mean stratification structure (Brunt-Vaisala Frequency changes) of the Baltic Sea at BY15 station. It shows that the stratification structure of the Baltic Sea central basin (The Baltic Proper) changes between present and future climate. The stratification structure does not change in the deepest part of the Baltic Sea, but diminishes between 35 and 55 m. Above 35 m there is a strong increase of stratification. Assuming that salinity or temperature changes are small enough to keep the equation of state linear around a point of equilibrium, we also construct the stratification structure assuming that only temperature or salinity changes between present and future climate. Using this approximation permits to show that salinity changes are responsible for the decrease of stratification previously mentioned, and that temperature changes are responsible for the increase of stratification. Salinity and temperature changes are also plotted and show a consistent salinity and temperature increases. However, temperature changes are higher close to the surface than deeper. This result is similar to that obtained by Hordoir and Meier (2011): temperature increase leads to a strong thermal stratification increase in the Baltic Sea, which increases with lower salinities. The increase of stratification observed in the present experiment fits with the values observed by Hordoir and Meier (2011), although they are lower compared with the summer values found by Hordoir and Meier (2011) as the present experiment is a long term mean including all seasons. Alongside the changes in stratification structure, Fig. 8 also shows the meridional transport at the latitude of BY15 and the temperature and salinity changes at BY15. The positive changes in stratification precisely match the area where we see a net increase of negative transport, meaning that the thermal stratification increase coincides with the decrease of the outgoing flux.

3.2 MPI simulations

The results of the MPI forced simulations are presented in a similar fashion. Figure 9 shows the transport function for the control period 1975–2005. One can also

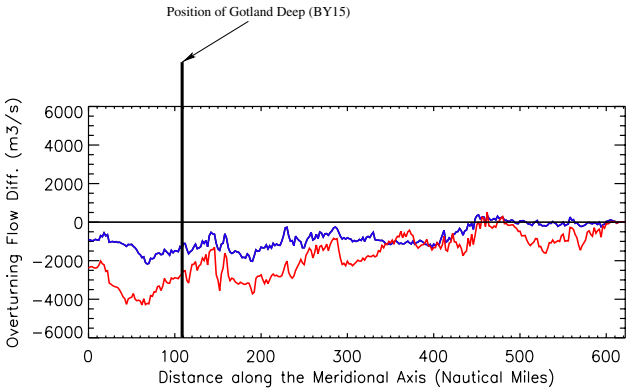

Fig. 7 Difference of overturning circulation, between experiments EC-4.5 and EC-H (*blue curve*), and between experiments EC-8.5 and EC-H (*red curve*). The relative difference of overturning circulation is −6.5 and −15% for EC-4.5 and EC-8.5 at Gotland Deep (BY15), respectively

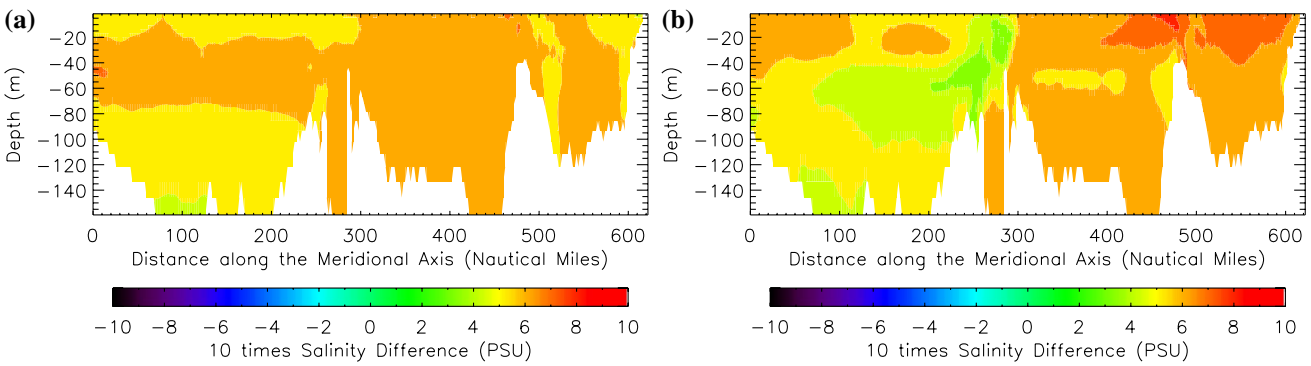

Fig. 6 **a** Difference of zonally integrated salinity between EC-4.5 and EC-H. **b** Difference of zonally integrated salinity between EC-8.5 and EC-H

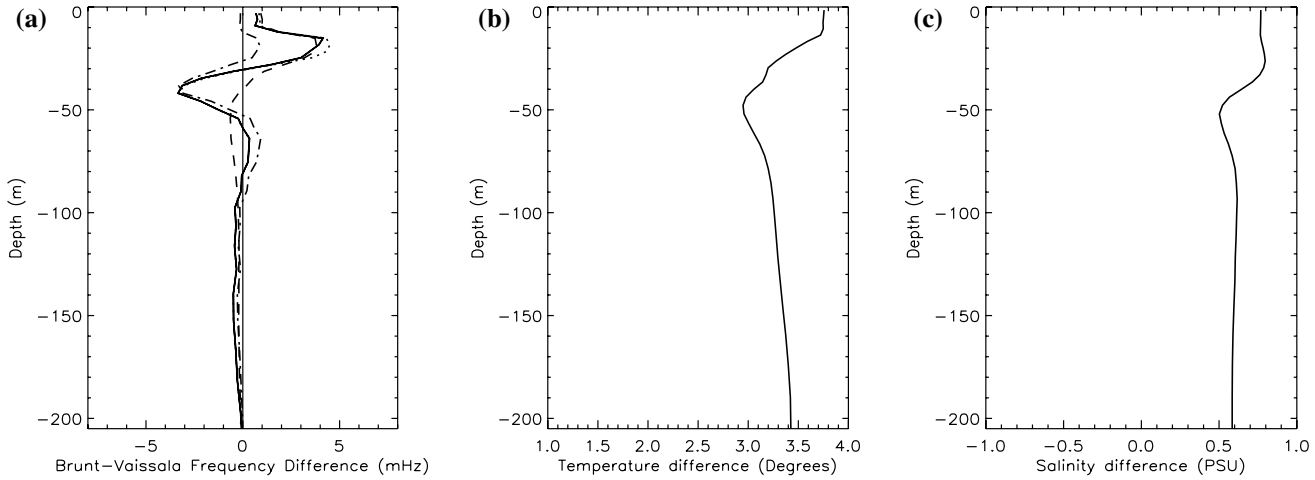

Fig. 8 **a** Difference of stratification (Brunt–Vaisala frequency, in mHz) between EC-8.5 and EC-H at BY15. *Plain line* stratification difference, computed from the difference of mean stratification between the two times periods. *Dotted line* stratification difference computed linearly from differences in mean temperature and salinity between the two time periods. *Dashed line* stratification difference computed from differences in temperature only between the two time periods. *Dashed-dotted line* stratification difference computed from differences in salinity only between the two time periods. **b** Temperature difference (in degrees) between EC-8.5 and EC-H time periods. **c** Salinity difference (in PSU) between EC-8.5 and EC-H time periods

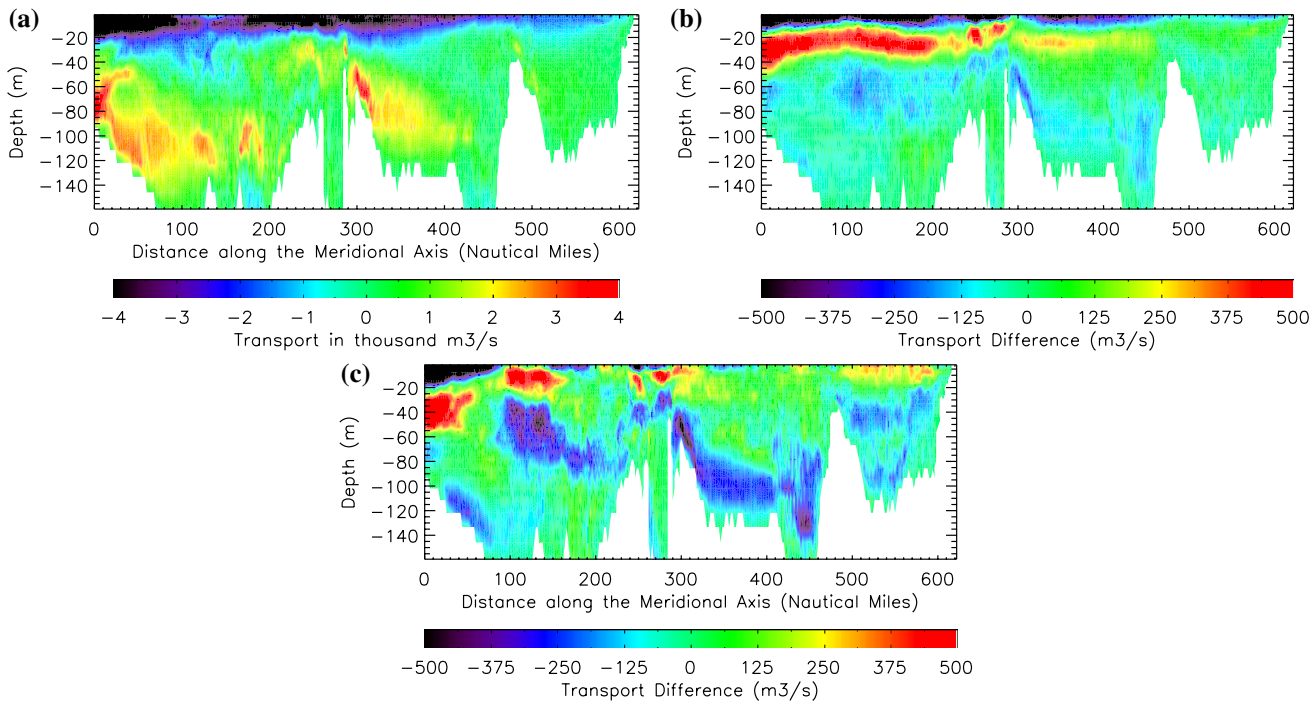

Fig. 9 **a** Transport function $F(y, z)$ along the meridional axis in the Baltic Sea in MPI-H, same as Fig. 2. Average value from 1975 to 2005 computed from an MPI-Earth forced simulation. The values of transport are bounded from −4000 to 4000 $m^3\ s^{-1}$ but can exceed these values. **b** Difference of transport function $F(y, z)$ between MPI-4.5 and MPI-H. **c** Difference of transport function $F(y, z)$ between MPI-8.5 and MPI-H

notice a decrease of the positive incoming circulation, and an increase of the outcoming negative circulation, which suggests a lower overturning circulation in this set of simulation. The decrease in overturning circulation is higher when Nemo–Nordic is forced by a scenario which has a highest greenhouse gas emission (RCP8.5).

The associated changes in overturning circulation are shown in Fig. 11. One can actually notice an increase of

overturning circulation in the Southern Baltic, which is consistent with the predictions made by Schimanke et al. (2014). However, as one moves further up there is a consistent decrease in overturning circulation in the Baltic Proper. The decrease becomes even higher in the Bothnian Sea and Bothnian Bay, which means that the relative decrease (in percent) for these areas is even higher than in the EC-EARTH forced simulations. The salinity structure is more affected by changes than in the EC-EARTH simulations (Fig. 10), with a moderate decrease of about 0.5 PSU for the MPI-8.5 simulation, but which is not distributed evenly. There is a haline stratification decrease above the level of the halocline in the Northern part of the Baltic Proper.

Changes in the stratification structure can also be observed (Fig. 12). The changes in stratification structure are similar although not identical. Temperature related stratification does increase close to the surface, although it does less, and does not extend as deep as in for the EC-Earth forced simulation. An increase in haline stratification also occurs below the level of the halocline, followed by a decrease of haline stratification.

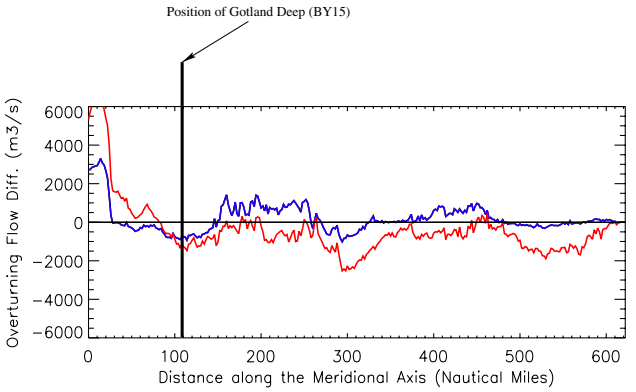

Fig. 11 Difference of overturning circulation between experiments MPI-4.5 and MPI-H (*blue curve*), and between experiments MPI-8.5 and MPI-H (*red curve*). The relative difference of overturning circulation is −5 and −9% for MPI-4.5 and MPI-8.5 at Gotland Deep (BY15), respectively

4 Analysis

As for the Atlantic Meridional Overturning Circulation (AMOC hereafter), any estuarine circulation is associated with an overturning circulation, and requires mixing between entering saltier water masses, and fresher water masses created by runoff. If estuarine mixing did not occur, then freshwater coming from rivers would just slide over saltier water masses like oil over water without creating any overturning circulation. Tides and internal tidal wave breaking is an essential process to allow water masses to mix and ensure the continuity of the AMOC in convection or upwelling areas. In many estuaries, tidal mixing is less important since the shear between incoming and outgoing water masses becomes so high at some point that the induced turbulence eventually mixes water masses together and ensures the overturning circulation. However, in the case of deep sill-bounded estuaries such a the Baltic and Black Seas, mixing of lower and upper water masses is a slower process that requires longer time scales and that requires a contact between the base of the thermal mixed layer and the halocline. For the specific case of the Baltic Sea, Stigebrandt (1985) explicitly states that "for a large part of the year the seasonal thermocline shields the main halocline in the Baltic Sea from direct contact with the well mixed surface layer". From a climate change perspective, this means that a change in the physical structure and seasonality of the thermally controlled mixed layer influences the mixing of heavy saltier masses with the mixed layer, controlled by the changes in "entrainment velocity" w_e (Stigebrandt 1985) (Eq. 4). When it comes to the Baltic Sea, this mixing occurs independently in different basins as the halocline in the Baltic Proper is located below the level

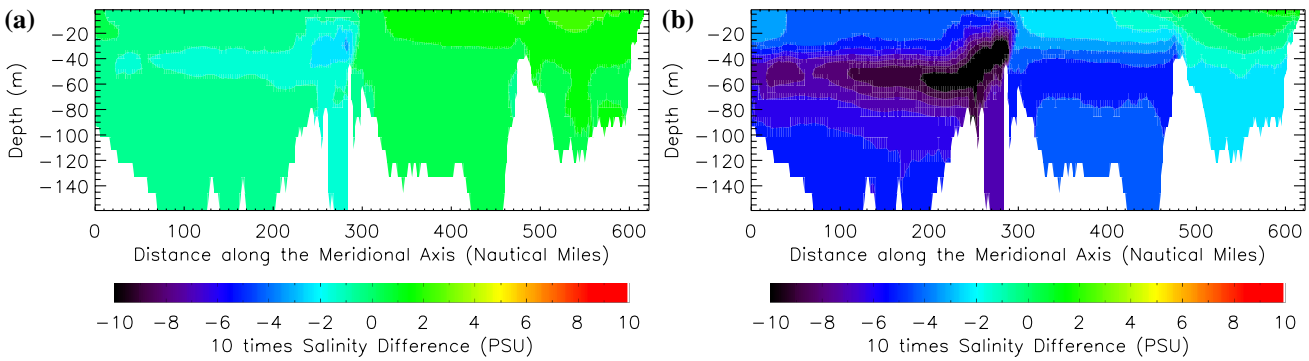

Fig. 10 **a** Difference of zonally integrated salinity between MPI-4.5 and MPI-H. **b** Difference of zonally integrated salinity between MPI-8.5 and MPI-H

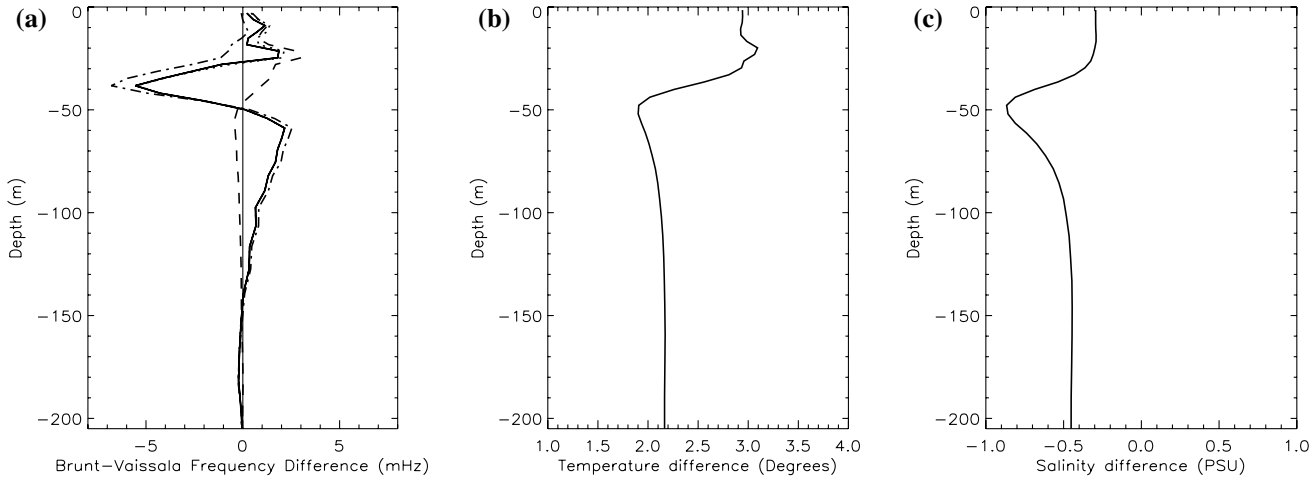

Fig. 12 **a** Difference of stratification (Brunt–Vaisala frequency, in mHz) between MPI-8.5 and MPI-H at BY15. *Plain line* stratification difference, computed from the difference of mean stratification between the two times periods. *Dotted line* stratification difference computed linearly from differences in mean temperature and salinity between the two time periods. *Dashed line* stratification difference computed from differences in temperature only between the two time periods. *Dashed-dotted line* stratification difference computed from differences in salinity only between the two time periods. **b** Temperature difference (in degrees) between MPI-8.5 and MPI-H time periods. **c** Salinity difference (in PSU) between MPI-8.5 and MPI-H time periods

of the sill located at the entrance of the Gulf of Bothnia. The baroclinic circulation of these sub-basins originates and finishes above the level of the Baltic Proper halocline. For the case of the Baltic Proper, the changes in stratification structure at its central point (Gotland Deep BY15, Figs. 8 and 12) exhibit an increase of thermal stratification in both EC-EARTH and MPI forced simulations in the mixed layer. From a haline point of view, there is always a decrease of saline stratification below, and for the case of the MPI forced runs an increase of saline stratification further down. However, changes in haline structure can only increase the salt flux further up either by easing its contact upwards (in the case of the decrease of haline stratification), or not changing the final erosion of the halocline into the surface mixed layer since the increase in haline stratification is below the level of the sharpest halocline, which is precisely the case in our study. Therefore, the new limiting factor of diffusion of saltier water masses towards the surface mixed layer is the increase of thermal stratification between the surface and approximately 35 m. It does not matter if there is a decrease of stratification that accelerates the migration of salt towards the surface at one place if a decrease occurs at another location on the water column, the increase of stratification acts as a bottleneck for the migration of salt from the depths of the Baltic Sea towards the surface.

Based on a balance of wind stress, buoyancy and stratification power fluxes, Stigebrandt (1985) provides a way to estimate the entrainment velocity w_e, which is detailed below:

$$w_e = \frac{2m_0 u_*^3}{gh\Delta\rho/\rho} - \frac{B}{g\Delta\rho/\rho} \tag{7}$$

in which m_0 is an empirical constant, u_* is the wind friction velocity, h is the thickness of the mixed layer, $\Delta\rho$ is the density gradient between the base of the thermal mixed layer and surface, ρ is a reference density and g is gravity. B is a buoyancy flux that accounts both for thermal and freshwater buoyancy fluxes. B latest can be written as:

$$B = g\left(\frac{\alpha}{\rho C_p} Q_{in} - \beta FS\right) \tag{8}$$

in which α and β are respectively the thermal and haline expansion coefficients in the mixed layer, C_p is a heat capacity, Q_{in} is the incoming heat flux, F is the net freshwater input through the surface, and S is the mixed layer salinity. The friction velocity u_* is computed based on the surface stress τ, which is extracted from the model:

$$u_* = \sqrt{\frac{\tau}{\rho}} \tag{9}$$

We have implemented this simple model of the entrainment velocity within the surface mixed layer, by taking Gotland Deep (BY15) as a reference. The net freshwater input comes directly from the simulation. The surface mixed layer density difference is also taken from the model and h is adjusted to the thickness on which one notices an increase of thermal stratification. The entrainment velocity is computed for the entire control period and its mean

value is taken. The same is done for the 2005–2099 period, during which we compute the annual mean value of the entrainment velocity. In both cases, we do not take into account the heat flux as its mean annual value is supposed to be close to zero, especially when integrated over long time scales.

We compute the relative change of entrainment velocity $w_e(y)$ between each year of the 2005–2099 period, in comparison with that of the control period w_{ref}. This is defined as:

$$Rw(y) = (w_e(y) - w_{ref})/w_{ref} \quad (10)$$

Equation 7 uses a ratio of wind stress power and stratification, and this formulation is used for the computation of $Rw(y)$. However it is also possible not to take the changes of wind stress power. $Rw_\rho(y)$ is a function similar to $Rw(y)$ where $w_e(y)$ is computed using only density changes for the period 2005–2099. Of course, the final stratification structure itself results from a balance between wind power and buoyancy fluxes, so both can not be separated, but the computation of $Rw_\rho(y)$ allows to see how $Rw(y)$ would have evolved if only stratification and buoyancy fluxes had changed in the equation. Figure 13 shows the evolution of $Rw(y)$ and $Rw_\rho(y)$ for the EC-4.5 and EC-8.5 simulations. Both functions are also plotted as their least-squared linear regressions.

The mean relative decrease of $Rw(y)$ and $Rw_\rho(y)$ for the period 2069–2099 compares with the relative decrease in overturning circulation at Gotland Deep (BY15) , even though it is higher: the decrease in overturning circulation extracted from Nemo–Nordic, reaches 6.5% for the EC-4.5 run, and 15% for the EC-8.5 run. Therefore the figures extracted from the model seem to agree better with the variation of $Rw_\rho(y)$ than with that of $Rw(y)$ which seems to over-estimate the changes.

The same approach has been made for the MPI-4.5 and MPI-8.5 based simulations. Changes observed in the Nemo–Nordic simulations show a decrease of 5 and 9% respectively.

If one considers the relative changes of $Rw_\rho(y)$ for the period 2069–2099, they also fit with the changes observed in the Nemo–Nordic simulations. The relative changes of

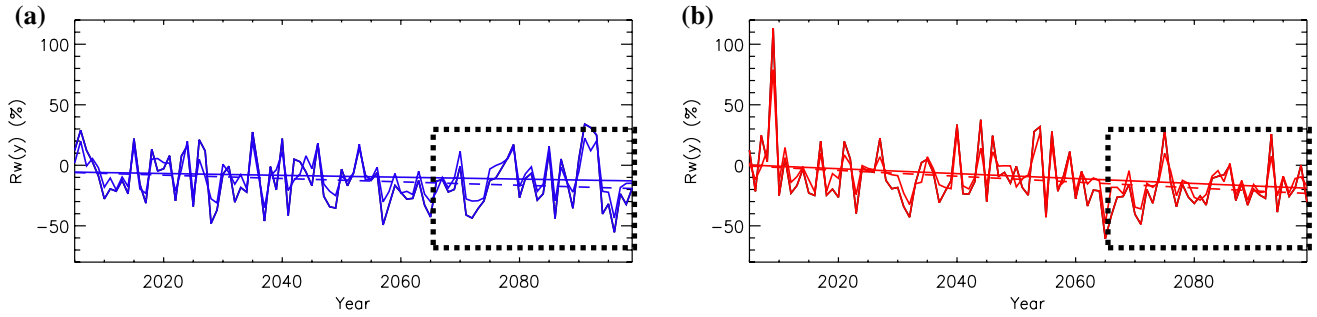

Fig. 13 Functions $Rw(y)$ (*solid line*) and $Rw_\rho(y)$ (*dashed line*) plotted with their least squared regressions. **a** EC-4.5 simulation, the linear variation coefficients of $Rw(y)$ and $Rw_\rho(y)$ are respectively −0.14 and −0.08 y^{-1}. The mean values of $Rw(y)$ and $Rw_\rho(y)$ for the period 2069–2099 (*dashed box*) are respectively −14 and −9%. **b** EC-8.5 simulation, the linear variation coefficients of $Rw(y)$ and $Rw_\rho(y)$ are respectively −0.24 and −0.20 y^{-1}. The mean values of $Rw(y)$ and $Rw_\rho(y)$ for the period 2069–2099 (*dashed box*) are respectively −19 and −15%

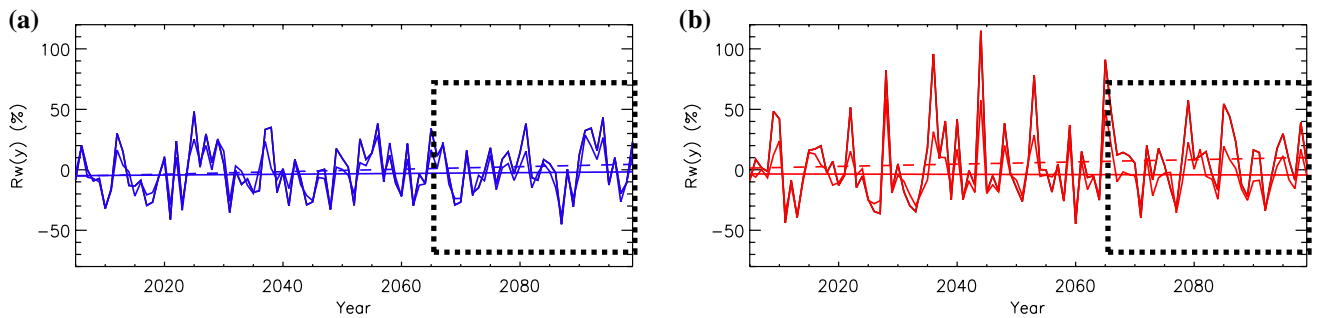

Fig. 14 Functions $Rw(y)$ (*solid line*) and $Rw_\rho(y)$ (*dashed line*) plotted with their least squared regressions. **a** MPI-4.5 simulation, the linear variation coefficients of $Rw(y)$ and $Rw_\rho(y)$ are respectively 0.10 and 0.03 y^{-1}. The mean values of $Rw(y)$ and $Rw_\rho(y)$ for the period 2069–2099 (*dashed box*) are respectively 1.68 and −3.23%. **b** MPI-8.5 simulation, the linear variation coefficients of $Rw(y)$ and $Rw_\rho(y)$ are respectively 0.07 and −0.05 y^{-1}. The mean values of $Rw(y)$ and $Rw_\rho(y)$ for the period 2069–2099 (*dashed box*) are respectively 7 and −5%

$Rw(y)$ suggest an increase in the overturning circulation (Fig. 14).

5 Discussion and conclusion

If one considers only changes in thermal stratification of the model, then the change estimate of entrainment velocity in the thermal mixed layer fits adequately with the changes in overturning circulation.

This occurs when Nemo–Nordic is forced by two climate models, each using two greenhouse gases emission scenarios.

The computation of the entrainment velocity takes into account the net freshwater flux, however this term appears to have a small impact in comparison with the changes of stratification. It is also important to notice that the net freshwater input to the Baltic Sea decreases in the EC-4.5 and EC-8.5 simulations (−2 and −3% respectively). A decrease of the net freshwater input to the Baltic Sea should on the contrary ease the occurency of salt water inflows from a barotropic point of view (Meier et al. 2006), and the overturning circulation. The net freshwater input to the Baltic Sea does not change in the MPI-4.5 simulations and increases by 4% in the MPI-8.5 simulations. However, in these simulations one can observe a strong increase of the overturning circulation in the Southern Baltic Sea, especially in the MPI-8.5 simulations, which shows that the increase in the freshwater budget (P-E increases) does not prevent potential salt inflows to enter the Southern Baltic Sea , but that these salt inflows do not penetrate further towards the center of the Baltic Proper and cannot fuel the overturning circulation of the Baltic Sea.

The study made by Schimanke et al. (2014) shows that the intensity of Major Baltic Inflows should increase towards the end of the 21st century. Their conclusions are based on the analysis of atmospheric patterns in two climate models, forced by two greenhouse gases emission scenarios. In the present study, we use the same atmospheric data as a forcing, but combine it with the use of an ocean model of the Baltic Sea. The concept of "overturning circulation" is a low-frequency perspective of salt water inflows. Salt water inflows are the driver fueling the overturning circulation. We analyze the changes of overturning circulation towards the end of the 21st century by comparing its intensity between two time periods, the first one being for years 1975–2005, the second one being for years 2069–2099. Our findings are opposite to that of Schimanke et al. (2014): we conclude that the overturning circulation of the Baltic Sea is going to decrease by up to 15% towards the end of the 21st century. This is true for the main basin of the Baltic Sea, the Baltic Proper. It is also true for the other basins such as the Bothnian Sea and the Bothnian Bay: although smaller in absolute value, this decrease is even higher in relative value (more than 20%).

The decrease of the overturning circulation follows a trend which strengthen with the greenhouse gases scenarios and the temperature increase: a higher decrease in overturning circulation can be observed when RCP 8.5 emission scenarios are used, regardless of the climate model that is used to provide the atmospheric forcing. In our simulations, the runoff data that is used is a climatological runoff, which does not change for any year of the simulation. Moreover, the net freshwater input to the Baltic Sea (Runoff plus Precipitation minus Evaporation) decreases in the EC-EARTH forced simulations, and does not increase significantly in the MPI forced simulations. Either the runoff changes should increase salt water inflows, or should at least not affect them significantly from a barotropic point of view. This means that the decrease of the overturning circulation is not related with the changes in net freshwater input to the Baltic Sea, nor is this decrease related with changes in wind patterns, which should increase the overturning circulation. Too much mixing in the Southern Baltic could also reduce deep salt inflows (Meier 2005), but we notice a slight decrease of wind speed for the EC-EARTH forced scenarios (−1.85 and −0.8% for EC-4.5 and EC-8.5 respectively). For the case of the MPI scenarios, a slight increase can be noticed (1.83 and 3.73% for MPI-4.5 and MPI-8.5 respectively), but which is far less than that required to impact deep salt inflows according to Meier (2005). The decrease of overturning circulation could be related with a change of wind strength or variability, especially if one considers upwelling dynamics as an important element of the overturning circulation. A decrease of wind strength and/or variability could affect Baltic Sea upwellings. A couple of studies investigated potential future changes of wind characteristics (average speed, gustiness, direction) over the Baltic Sea (NIKULIN et al. 2011; Gräwe et al. 2013; Junjie et al. 2015). All of these studies conclude either that wind characteristics do not change (Junjie et al. 2015) or they state very carefully that there might be a small increase in wind speed/gustiness (NIKULIN et al. 2011; Gräwe et al. 2013). To our knowledge, no study claims that the wind speed will decrease in the future. Hence, we did not investigate this possibility: we concluded that the documented changes of the overturning circulation are the result of a change in thermohaline circulation.

Our analysis based on the theory of Stigebrandt (1985) shows that the relative changes of entrainment velocity are close to that of overturning circulation as far as the Baltic Proper is considered. It also strongly suggests that the modeled changes in overturning circulation are related with an increase of thermal stratification at the level of the mixed layer. This increase contributes to a stronger shielding of the erosion of the permanent halocline of the Baltic Sea.

If wind effects are not directly considered in the theory of Stigebrandt (1985), then the trend of decrease of the entrainment velocity within the layer in which thermal stratification changes occur correlate with the changes of overturning circulation in the center of the Baltic Proper. For the EC-EARTH forced runs, using this theory at the center of the Baltic Proper predicts a change of −9 and −15% of the entrainment velocity caused by increased thermal stratification, for EC-4.5 and EC-8.5 scenarios respectively. The model itself predicts a change of respectively −6.5 and −15% respectively. In the case of the MPI forced runs, the theory predicts a change of −3 and −6% which is very close to what the model gives (−5 and −8% respectively). The theory contradicts with the model predictions if wind changes are used directly in the theory: the theory then overestimates the changes when it comes to the EC-EARTH forced simulations and predicts an increase of overturning circulation which is contrary to model predictions for the MPI forced simulations.

It should be noted that the model does predict an increase of overturning circulation in the Southern Baltic Sea for this latest case, but this could be related with an increase of wind-forced potential salt inflows, which however do not penetrate any further in the Baltic Proper.

However, neglecting the wind changes for the computation of friction velocity according to the theory of Stigebrandt (1985) does not mean that changes in wind stress are not taken into account: wind stress has an impact on mixed layer stratification within the model, which forms the basis of our computation. The discrepancy of results when changes in wind stress are directly taken into account in the theory. A possible explanation could reside into the fact that the theory of Stigebrandt (1985) uses a third power of the friction velocity which makes it extremely sensitive to any inaccuracy due to the approximation that the Gotland Deep (BY15) profile is used as a proxy for the entire Baltic Proper.

Our analysis predicts that the increase of thermal stratification in sill estuaries such as the Baltic Sea and the Black Sea, will decrease the overturning circulation, meaning the amount of the salty water masses that penetrate the deepest parts of the estuary and fuel what Döös et al. (2004) described as a “haline conveyor belt”. Since our approach provides a time integrated view of the problem, it is impossible to tell how the strength and variability of the Baltic Sea MBIs will be affected: will there be less MBIs with a smaller amplitude, or less MBIs with a larger amplitude, or more MBIs but with a much smaller amplitude. The question remains open. Since the ecosystem is usually more sensitive to extreme values more than changes in mean values (lower salinity or oxygen extremes for example), this question should also be answered but is left to further investigation.

Acknowledgements This work was part of the projects BONUS Stormwinds and BONUS BIO-C3, funded jointly by BONUS (Art 185) and the Swedish Research Council for Environment, Agriculture Sciences and Spatial Planning (FORMAS, grants no 292 985 and no 219-2013-2041). This work is also funded by the SmartSea project of the Strategic Research Council of Academy of Finland, grant No: 292 985. The authors wish to thank the editor and the anonymous reviewers who helped improve this manuscript.

References

Döös K, Meier M, Döscher R (2004) The baltic haline conveyor belt or the overturning circulation and mixing in the baltic. Ambio 33. doi:10.1357/002224006777606506

Fong D, Geyer W (2002) The alongshore transport of freshwater in a surface-trapped river plume. J Phys Oceanogr 32:957–972

Funkquist L, Kleine E (2007) Hiromb—an introduction to hiromb, an operational baroclinic model for the baltic sea. Tech. rep, SMHI

Garvine RW, Whitney MM (2006) An estuarine box model of freshwater delivery to the coastal ocean for use in climate models. J Mar Res 64(2):173–194. doi:10.1357/002224006777606506

Gräwe U, Friedland R, Burchard H (2013) The future of the western baltic sea: two possible scenarios. Ocean Dyn 63(8):901–921. doi:10.1007/s10236-013-0634-0

Hordoir R, Axell L, Löptien U, Dietze H, Kuznetsov I (2015) Influence of sea level rise on the dynamics of salt inflows in the baltic sea. J Geophys Res Oceans. doi:10.1002/2014JC010642

Hordoir R, Dieterich C, Basu C, Dietze H, Meier M (2013) Freshwater outflow of the baltic sea and transport in the norwegian current: A statistical correlation analysis based on a numerical experiment. Contin Shelf Res 64:1–9. doi:10.1016/j.csr.2013.05.006

Hordoir R, Meier M (2011) Effect of climate change on the thermal stratification of the baltic sea: a sensitivity experiment. Clim Dyn 38:1703–1713. doi:10.1007/s00382-011-1036-y

Hordoir R, Nguyen K, Polcher J (2006) Simulating tropical river plumes. A set of parametrizations based on macroscale data, a test case in the Mekong delta region. J Geophys Res 111:392. doi:10.1029/2005JC003

Hordoir R, Polcher J, Brun-Cottan JC, Madec G (2008) Towards a parametrization of river discharges into ocean general circulation models: a closure through energy conservation. Clim Dyn 31. doi:10.1007/s00382-008-0416-4

Junjie D, Jan H, Semjon S, Markus MHE (2015) ohs, vol. 44, chap. A method for assessing the coastline recession due to the sea level rise by assuming stationary wind-wave climate. doi:10.1515/ohs-2015-0035. http://www.degruyter.com/view/j/ohs.2015.44.issue-3/ohs-2015-0035/ohs-2015-0035.xml, p 362 3

Madec G (2015) The NEMO system team: Nemo ocean engine, version 3.6 stable. Tech. rep., IPSL. http://www.nemo-ocean.eu/. Note du Pôle de modélisation de l’Institut Pierre-Simon Laplace No. 27

Matthäus W (2006) The history of investigation of salt water inflows in the baltic sea—from the early beginning to recent results. Tech. rep, Baltic Sea Research Institute, IOW

Meier H, Hordoir R, Andersson H, Dieterich C, Eilola K, Gustafsson B, Höglund A, Schimanke S (2012) Modeling the combined impact of changing climate and changing nutrient loads on the baltic sea environment in an ensemble of transient simulations for 1961–2099. Clim Dyn 39(9–10):2421–2441. doi:10.1007/s00382-012-1339-7

Meier H, Kauker F (2002) Simulating Baltic sea climate for the period 1902–1998 with the rossby centre coupled ice-ocean model. Tech. rep., SMHI. Report Oceanography No. 30

Meier HEM (2005) Modeling the age of Baltic Sea water masses: quantification and steady state sensitivity experiments. J Geophys Res 110: C02,006. doi:10.1029/2004JC002 (607)

Meier HEM, Kjellström E, Graham LP (2006) Estimating uncertainties of projected baltic sea salinity in the late 21st century. Geophys Res Lett. doi:10.1029/2006GL026488

Nikulin G, Kjellstrm E, Hansson U, Strandberg G, Ullerstig A (2011) Evaluation and future projections of temperature, precipitation and wind extremes over europe in an ensemble of regional climate simulations. Tellus A 63(1):41–55. doi:10.1111/j.1600-0870.2010.00466.x

Samuelsson P, Jones CG, Willén U, Ullerstig A, Gollvik S, Hansson U, Jansson C, Kjellström E, Nikulin G, Wyser K (2011) The rossby centre regional climate model rca3: model description and performance. Tellus A 63(1):4–23. doi:10.1111/j.1600-0870.2010.00478.x

Schimanke S, Dieterich C, Meier HEM (2014) An algorithm based on sea-level pressure fluctuations to identify major baltic inflow events. Tellus A 66. http://www.tellusa.net/index.php/tellusa/article/view/23452

Stigebrandt A (1985) A model for the seasonal pycnocline in rotating systems with application to the baltic proper. J Phys Oceanogr 15(11):1392–1404

Potential habitat change in the Baltic Sea – implications of climate change and nutrient-load scenarios on the future marine environment

Iréne Wåhlström, Helén C. Andersson, Matthias Gröger, Kari Eilola, Anders Höglund, Brian R. MacKenzie, Elin Almroth-Rosell, Maris Plikshs

Embargoed until publication, for information contact Helén Andersson, email: helen.andersson@smhi.se